Establishment of anti-apoptotic brakes in human neurons during maturation

Dissertation

Zur Erlangung des Doktorgrades (Dr. rer. nat.) der Mathematisch-Naturwissenschaftlichen Fakultät der Rheinischen Friedrich-Wilhelms-Universität Bonn

Vorgelegt von

Karolina Kleinsimlinghaus

aus Essen

Bonn, 2019

Anfertigung mit Genehmigung der Mathematisch-Naturwissenschaftlichen Fakultät der
Rheinischen Friedrich-Wilhelms-Universität Bonn
am Institut für Rekonstruktive Neurobiologie

1. Gutachter: Prof. Dr. med. Philipp Koch
2. Gutachter: Prof. Dr. Walter Witke
Tag der mündlichen Prüfung 29.04.2019
Erscheinungsjahr, 2019

Table of contents

1 Introduction

1.1 Using human induced pluripotent stem (iPS) cell-derived neurons to assess maturation-dependent adoption of anti-apoptotic mechanisms

The majority of neurons have to persist the whole lifespan of an individual, since only in specific regions of the human brain, like the hippocampus and the subventricular zone, neurogenesis is observed (Eriksson et al., 1998). Hence for humans this can mean that neurons have to persist an entire century or more. It therefore seems plausible that there are mechanisms for human mature neurons that promote their long-term survival. To gain deeper insights into the mechanism established by mature human neurons to assure their persistence, human iPS cell-derived neurons were used in the experiments of the present study.

1.1.1 Human iPS cells and their neuronal offspring

In 2006, Takahashi and Yamanaka were able to show that somatic cells like embryonic or adult fibroblasts can be reprogrammed to an embryonic stem cell-like state. The reprogramming of the fibroblasts was achieved by the retroviral overexpression of the four transcription factors Oct3/4, Sox2, c-Myc and Klf4, in culture conditions identical to those of embryonic stem (ES) cells. The generated cells were designated as induced pluripotent stem (iPS) cells, exhibiting a similar gene expression profile as ES cells. The pluripotency of these cells was confirmed, as they differentiated into all three germ layers (Takahashi & Yamanaka, 2006). Reprogramming of cells can cause genetic alterations, including chromosomal aberrations, but apart from this they are similar to ES cells regarding the expression of pluripotency markers and the ability for long-term culture while maintaining genomic stability (Gore et al., 2011; Hussein et al., 2011; Mayshar et al., 2010; Wu & Izpisua Belmonte, 2016). Cultured ES cells and iPS cells can self-renew almost indefinitely and can differentiate into diverse linages similar to the in vivo development (Wu & Izpisua Belmonte, 2016). By using iPS cell technology ethical and legal issues regarding stem cell research and derivation of those cells can be overcome and hence pose a viable cell source for the scientific community in various different countries with different legislatives. In addition to this, the technology of generating iPS cells from any desired patient enables targeted assessment of disease-associated features in vitro while at the same time

maintaining the opportunity to get clinical feedback from the patient. This circumstance poses a viable and most valuable approach for modelling human diseases, perform personalised drug screenings and test the impact of gene corrections (Wu & Izpisua Belmonte, 2016).

For the neural linage, protocols for the targeted differentiation of long-term self-renewing rosette-type human ES cell-derived neural stem cells (lt-hESNSCs) also called long-term self-renewing neuroepithelial-like stem cells (lt-NES) cells were developed. These cells have long-term self-renewing potential and maintain their neuro-and gliogenic potential even after long-term proliferation (Koch et al., 2009). The precursors are cultivated in the presence of the growth factors, epidermal growth factor (EGF) and human fibroblast growth factor (FGF2) and B27. These neural precursors give rise to β-III tubulin expressing neurons, astrocytes positive for GFAP and O4-positive oligodendrocytes upon growth factor withdrawal and depending on the differentiation time. The obtained neurons are able to generate action potentials and the majority displays a GABAergic interneuron phenotype. In the presence of growth factors, lt-NES cells can be passaged more than a hundred times, which means that they are almost an unlimited source for the generation of neuronal cultures (Koch et al., 2009). The established protocol for the generation of lt-NES cells is also applicable for iPS cells (Falk et al., 2012).

Another protocol for iPS cell-derived derivates was established in 2013 Reinhardt and co-workers established a protocol for iPS cell-derived small molecule neural precursor (SM-NP) cells with immortal self-renewing properties. In contrast to lt-NES cells, they do not require splitting several times per week and can be split in high ratios and grow clonally, which makes their expansion more easily. SM-NP cells are induced from iPS cells, inhibition of BMP and TGFβ signalling through the small molecules dorsomorphin and SB43152, initiated neural induction. The small molecule CHIR99021 (CHIR) was used as GSK3b inhibitor to stimulate the WNT-pathway and prumorphamine was used to stimulate the SHH-pathway (Reinhardt et al., 2013). The differentiation potential of the SM-NP cells is upstream from lt-NES cells and the cultivation of SM-NP cells in the presence of FGF2 results in rosette-like structures and the transition into lt-NES cells. Neurons generated from SM-NP cells are electrical excitable and develop synaptic contacts (Reinhardt et al., 2013).

1.1.2 Mechanisms that promote long-term survival of neurons

Immature neurons have a built-in mechanism that allows them to perish. Since an excess of neurons is produced during the development of the nervous system, unnecessary neurons

undergo apoptosis to guarantee the correct number of neurons required for the formation of neuronal networks. In mature neurons, apoptosis is highly controlled. Studies on motor neurons indicate that several pathways: The FAS mediated pathway, the nitric oxide-dependent pathway and a p75 neurotrophin receptor ($p75^{NTR}$) mechanism need to be activated in order to induce neuronal death (Benn & Woolf, 2004). Similar studies on mature neurons of rodents reveal that those cells become more resistant to stress and injuries by using elaborate strategies that promote long-term survival. It has been shown that the pro-apoptotic proteins, apoptotic protease activating factor 1 (Apaf-1) and caspase3 are downregulated with maturation (Yakovlev et al., 2001). In addition, the levels of Bax, are decreased with maturation, while it is no longer localised to the mitochondria (Polster et al., 2003; Vogelbaum, Tong & Rich, 1998). In another experiment, a delayed dephosphorylation of tropomyosin receptor kinase A (TrkA) was observed after growth factor withdrawal when comparing mature neurons to immature neurons (Kole, Annis & Deshmukh, 2013). These findings point out that different strategies exist in mature neurons to overcome stress induction and apoptotic stimuli to ensure long-term survival. Some are related to the apoptosis pathway while others are related to pro-survival pathways.

1.2 The intrinsic apoptotic pathway

Apoptosis is a suicide program of cells, also called programmed cell death. It is important during development, for the immune regulation and for the homeostasis of the organism. Two pathways, the intrinsic- and the extrinsic pathway regulate apoptosis. The extrinsic pathway is also known as death receptor dependent pathway. This pathway is used to remove potentially harmful cells. The pathway is activated through binding of soluble or membrane attached ligands to death receptors, which are located on the cell surface, whereas the intrinsic pathway is dependent on the mitochondria (Park, 2012; Benn & Woolf, 2004). Here the mitochondrial membrane becomes permeable, which causes - among others - the release of cytochrome c (Benn & Woolf, 2004). Two major models are discussed to result in the permeabilisation of the mitochondrial membrane one model suggests a disruption of the outer mitochondrial membrane by opening the permeability transition pore, the other suggests, that members of the Bcl-2 family generate pores in the outer mitochondrial membrane (Degterev, Boyce & Yuan, 2001). Proteins of the Bcl-2 family are divided into three groups, one anti-apoptotic group and two pro-apoptotic groups. Bcl-2, Bcl-xl, Bcl-w

and myeloid cell leukemia-1 (MCL1) belong to the anti-apoptotic group, to the first pro-apoptotic group belong: Bax, Bak, Bok and Bcl-xs, the second pro-apoptotic group consists of BH3-only proteins like Bim, Bid, Bmf and Bad (Benn & Woolf, 2004). Binding of members of the anti-apoptotic Bcl-2 group to Bax and related proteins, prevents the induction of damage to mitochondria whereas, binding of Bcl-2 or Bcl-xl to BH3-only proteins sequesters the anti-apoptotic proteins away from Bax, favouring apoptosis (Downward, 1999). However, release of cytochrome c results in the formation of the caspase9 activating complex, apoptosome, consisting of seven Apaf-1, respectively bound to cytochrome c and caspase9, whose stoichiometry is unclear. Apaf-1 contains a CARD domain, which is interacting with CARD domain of caspase9 and responsible for its activation. The activation of caspase9 and thereby the induction of the caspase cascade, is achieved by autocatalytical cleavage, resulting in an activated form of the initiator caspase, containing two large and two small subunits. The active caspase9 can then cleave and activate effector caspases like caspase3, driving apoptosis. Caspase3 in turn can then cleave its downstream targets like poly (ADP-ribose) polymerase-1 (PARP-1) (Park, 2012; Benn & Woolf, 2004; Chaitanya, Alexander & Babu, 2010).

1.3 Cell survival-promoting attributes of the AKT-pathway

The AKT-pathway represents a cell survival pathway. Because mature neurons have developed mechanisms that promote their long-term survival, the cell survival-promoting attributes of the AKT-pathway are of interest. AKT is a serine/threonine protein kinase, also known as protein kinase B (PKB). It is composed of an N-terminal pleckstin homology (PH) domain and a C-terminal kinase catalytic domain. Since phosphatidylinositol 3-kinase (PI3K) is needed for the activation of AKT, the AKT-pathway is also termed PI3K-AKT-pathway. But also, a PI3K independent activation is discussed, for example by activation via protein kinase A (PKA) (Song, Ouyang & Bao, 2005). Following activation, AKT is able to transfer phosphate-residues to other proteins in the cytoplasm and the nucleus and thereby among others promotes cell survival (Song, Ouyang & Bao, 2005).
The binding of growth factors, like VEGFB, to receptor tyrosine kinases (RTKs) leads to the dimerization of the receptors and to their autophosphorylation, thereby generating binding sites for proteins containing an Src homology2 (SH2) domain like PI3K (Hale et al., 2008; Heldin, 1995). PI3K is a heterodimer of p110, the catalytic subunit, and p85 the regulatory

subunit. Following activation through binging to the phosphorylation sites (PI3K can also be activated by G-protein coupled receptors (GPCR)), it phosphorylates the 3'-OH position of phosphatidylinositols (PtdIns). The preferred substrate of PI3K is PtdIns(4,5)P_2 leading to the generation of PtdIns(3,4,5)P_3 (PIP_3) beside this, PI3K can also generate PtdIns(3,4)P_2 (PIP_2) (Franke et al., 1997; Vanhaesebroeck & Waterfield, 1999). These second messengers recruit AKT to the plasma membrane. AKT interacts with PIP_3 and PIP_2 through its PH domain. This causes a conformational change, resulting in the exposure of two phosphorylation sites Thr 308 in the kinase domain and Ser473 in the regulatory domain. Thr 308 is phosphorylated by 3-phosphoinositide-dependent protein kinase 1 (PDK1). The binding of mSin1 a component of the mammalian target of rapamycin complex 2 (mTORC2) to AKT is essential for the phosphorylation of Ser473 by mTORC2. PDK2 and integrin linked kinase (ILK) are also involved in the in the phosphorylation of AKT at Ser473. The phosphorylation of both residues is necessary for high levels of AKT activity (Lawlor & Alessi, 2001; Osaki, Oshimura & Ito, 2004; Lynch et al., 1999; Alessi et al., 1996; Yao et al., 2017). Succeeding the activation of AKT via the phosphorylation of Thr 308 and Ser473, AKT dissociates from the membrane and phosphorylates downstream targets in the nucleus and the cytoplasm, with a consensus sequence $RXRX_1X_1S/TH$, where X_1 represents small residues and H residues like leucine or phenylalanine. AKT is involved in proliferation and cell cycle progression (Lawlor & Alessi, 2001; Osaki, Oshimura & Ito, 2004). It can phosphorylate p21 and thereby inhibit the cell cycle arrest, since phosphorylated p21 is not able to enter the nucleus. Via this phosphorylation AKT promotes proliferation (Zhou et al., 2001). AKT is participating in metabolism, since its phosphorylation of glycogen synthase kinase 3 GSK-3 inhibiting GSK-3 allows the synthesis of glycogen (Cross et al., 1995). Furthermore, AKT is also involved in cell growth, via the activation of the mammalian target of rapamycin complex 1 (mTORC1). This is mainly achieved through the phosphorylation and inhibition of tuberous sclerosis complex 2 (TSC2), which is an inhibitor of mTORC1. Activation of mTORC1 promotes the synthesis of proteins, lipids and nucleotides, but also inhibits autophagy. In addition, it has a negative feedback loop on AKT, via priming IRS1 and IRS2, which are involved in IGF1 receptor signalling, by phosphorylations for degradation (Manning & Toker, 2017).

However, the main focus of this study is on the ability of AKT to promote cell survival. By phosphorylating pro-apoptotic proteins like Bad, AKT facilitates the cell survival. Bad is a BH3-only protein, interacting with Bcl-2 and Bcl-xl, which sequesters them from Bax, which, in turn can then induce damage to mitochondria. The phosphorylation of Bad by

AKT results in its interaction with 14-3-3 proteins and the release of Bcl-2 and Bcl-xl, counteracting the activity of Bax (Downward, 1999). Bax itself is also phosphorylated by AKT, maintaining its localisation in the cytoplasm and promoting heterodimerization with Bcl-2 family members, thereby promoting the integrity of the mitochondria (Gardai et al., 2004). p53 induces the expression of Bax, it is not directly regulated by AKT, but indirectly through its regulator, mouse double minute 2 homolog (Mdm2). After the phosphorylation via AKT, Mdm2 translocates to the nucleus, where it destabilises p53 (Miyashita & Reed, 1995; Mayo & Donner, 2001). AKT also phosphorylates caspase9 in humans, resulting in the inhibition of the protease activity of caspase9. However, as the phosphorylation site is not conserved in monkey or rodents, it is controversial whether phosphorylation of caspase9 is an anti-apoptotic key-mechanism (Cardone et al., 1998; Lawlor & Alessi, 2001). Furthermore, AKT phosphorylates the apoptosis signal-regulating kinase1 (ASK1), which is a MAP kinase kinase kinase, that activates c-Jun N-terminale Kinasen (JNK) and p38 MAP kinase, which are involved in apoptosis. The phosphorylation of ASK1 leads to a reduced activity of these kinases (Kim et al., 2001; Wada & Penninger, 2004). Other targets of AKT are forkhead transcription factors. The phosphorylation by AKT inhibits their ability to induce pro-apoptotic genes. When forkhead transcription factors are phosphorylated, they are sequestered in the cytoplasm, because they associate with 14-3-3 proteins. Through this interaction, the expression of cell death promoting genes, like Fas ligand gene or BIM-1 are prevented (Brunet et al., 1999; Brunet, Datta & Greenberg, 2001). AKT is also involved in the regulation of transcription factors that support the expression of anti-apoptotic genes. Nuclear factor kappa-light-chain-enhancer of activated B cells (NF-κB) is usually sequestered in the cytoplasm by an inhibitor protein, the IκB kinase (IKK), a complex consisting of IKKα and IKKβ. The phosphorylation of IKKα by AKT and NIK, a MAP kinase kinase kinase, results in the activation of NF-κB (Ozes et al., 1999). NF-κB can then enter the nucleus and induce the expression of Bcl-xl, A1/Bfl-1, which is a Bcl-2 homologue, which leads to reduced release of cytochrome c and reduced capase3 activation (Barkett & Gilmore, 1999; Wang et al., 1999). Additionally NF-κB induces the expression of inhibitor of apoptosis proteins (IAPs) and c-Myb (Lauder, Castellanos & Weston, 2001; Barkett & Gilmore, 1999). But NF-κB is also involved in the expression of pro-apoptotic genes like c-myc and p53 (Barkett & Gilmore, 1999). In addition, AKT is able to phosphorylate and activate the cyclic AMP response element-binding protein (CREB) and promote the recruitment of the co-activator CEB (Du & Montminy, 1998).

1.4 The diverse roles of heat shock proteins

Heat shock proteins (HSPs) are conserved in prokaryotes and eukaryotes and are ubiquitously expressed. Depending on their molecular mass, they are grouped into families, HSP100, HSP90, HSP70, HSP60, HSP40 and small heat shock proteins (sHSPs) (Bakthisaran, Tangirala & Rao, 2015). HSPs are transcriptionally activated after different stimuli. The most investigated transcription factor of heat shock proteins is the heat shock factor 1 (HSF1). Upon activation by stress conditions, it trimerizes, gets hyperphosphorylated at several serine residues, where Ser326 seems to be critical for the activation, and translocates to the nucleus, where it binds to DNA regions that contain heat shock elements (HSE) in the promoter region (Guettouche et al., 2005; Baler, Dahl & Voellmy, 1993). The transcription is diminished by an auto-regulated feedback loop. Under normal conditions HSP70 binds to HSF1, but dissociates under acute stress induction and then reassociates with HSF1 (Zheng et al., 2016).

Despite their molecular mass, HSPs can also be grouped into several classes, depending on their function. They act as molecular chaperones, as components of the proteolytic system and they cure covalent modifications of nucleic acids, e.g. heat-induced methylation of ribosomal RNA. Furthermore, they act as metabolic enzymes, which maybe needed for reorganising energy supply after heat stress, they are regulatory enzymes, e.g. they are involved in the biogenesis of ribosomes, they preserve the cytoskeleton and they are involved in transport, detoxification and membrane modulation (Richter, Haslbeck & Buchner, 2010).

HSP70 belongs to the molecular chaperones, under normal conditions it is responsible for the de novo folding of proteins, under stress conditions, it prevents aggregation and refolds aggregated proteins. Unfolded proteins are recognised by HSPs, because of their increased exposure of hydrophobic amino acids (Richter, Haslbeck & Buchner, 2010). A proper folding is achieved by different mechanisms, HSP70 binds hydrophobic patches and prevents aggregation. Through repetitive binding and release cycles HSP70 keeps the free concentration of substrate low, to prevent aggregation, so that it can fold into the active form. In addition, HSP70 in cooperation with HSP100 is able to solubilize protein aggregates (Mayer & Bukau, 2005). The chaperone activity of HSP70 is ATP-dependent, therefore HSP70 has an N-terminal ATPase domain and a C-terminal substrate-binding

domain. HSP70 exists in a low affinity ATP-bound state and a high affinity ADP-bound state (Mayer & Bukau, 2005).

HSPs are overexpressed in many human tumours, which contributes to their resistance towards therapy (Jäättelä, 1999). Moreover the inhibition of HSP70 in tumour cells results in cell death, which is independent of caspases (Nylandsted et al., 2000).

The resistance of tumour cells may also be due to the anti-apoptotic properties provided by HSPs. HSP70 protects against tumour necrosis factor (TNF), Staurosporine and doxorubicin induced apoptosis, the protective effect of HSP70 is mediated downstream of caspase3 (Jäättelä et al., 1998). But HSP70 has also anti-apoptotic properties upstream of caspase3 activation, via binding to Apaf-1, it thereby prevents the formation of the apoptosome and the recruitment of caspase9 to the apoptosome (Beere et al., 2000). The overexpression of HSPs is also protective against the toxicity of aggregation prone proteins causing neurodegenerative diseases like α-synuclein, because e.g. HSP70 reduces the amount of misfolded and aggregated α-synuclein (Klucken et al., 2004).

The constitutively expressed form of HSP70 is Hsc70, which targets proteins for degradation. In this process, it recognises a pentapeptide motive on target proteins, binds then to lysosomal-associated membrane protein 2 (LAMP2A), next the protein is unfolded and translocates into the lysosomal lumen and gets degraded (Dokladny, Myers & Moseley, 2015).

Another group of HSPs are sHSP, they are characterised by a conserved 80-100 amino acid stretch, the α-crystallin domain, in their C-terminus. HSP27 and α-crystallins belong to the family of sHSPs, they form large oligomeric species, and are general chaperones. αB-crystallin (Cryab) and αA-crystallin (Cryaa) can form homo- and heterooligomers with chaperone function. The phosphorylation of these sHSPs results in a decreased oligomeric size and influences the chaperone activity (Bakthisaran, Tangirala & Rao, 2015). As molecular chaperones HSP27 and Cryab prevent aggregation of unfolded proteins and promote functional refolding of proteins in an ATP-independent manner. But a binding of ATP and not its hydrolysis, can increase the chaperone activity. For the complete inhibition of aggregation, stoichiometric amounts of the sHSP are needed. (Jakob et al., 1993; Bakthisaran, Tangirala & Rao, 2015).

In addition to its chaperone activity, HSP27 is also involved in the stabilisation of the actin microfilament upon a p38-mediated phosphorylation (Guay et al., 1997).

Protective properties of HSP27 and Cryab have also been shown. HSP27 promotes the survival of sensory neurons after axotomy and growth factor withdrawal (Lewis et al.,

1999), it also blocks FAS/APO-1 and Staurosporine induced apoptosis, (Mehlen, Schulze-Osthoff & Arrigo, 1996). Phosphorylated, dimeric HSP27 interacts with Daxx and thereby inhibits its interaction with Fas and apoptosis signal regulation kinase1 (ASK1) (Charette et al., 2000). In addition, the overexpression of HSP27 has been shown to prevent the activation of procaspase9 (Garrido et al., 1999). HSP27 is also able to reduce caspase3 activation and the release of cytochrome c from mitochondria, it alters the activation of Bax and inhibits its oligomerisation and translocation to mitochondria, and it increases the pAKT level (Havasi et al., 2008). The reduced caspase3 activation is not limited to the inhibition of Bax by HSP27, because HSP27 also binds procaspase3 and cytochrome c, and inhibits thereby the activation of the caspase cascade (Concannon, Orrenius & Samali, 2001). Beside this, HSP27 binds to mRNA of Bim and thereby prevents its translation in neurons (Dávila et al., 2014).

Cryab has also anti–apoptotic properties, which differ from those of HSP27. It interacts with IκB kinase (IKK)β, resulting in the degradation of IKKα, a negative regulator of the transcription factor NF-κB, which upregulates Bcl-2 (Bakthisaran, Tangirala & Rao,2015). Cryab also reduces the number of apoptotic cells after treatment with TNF-α and etoposide. It leads to the accumulation of p24 a processing intermediate of caspase3 (prodomain plus large subunit of caspase3) and a reduction of p17 (large subunit containing the active site). Cryab blocks the autocatalytical maturation of caspase3 by binding to p24. Further, cleavage of caspase3 after cytochrome c and caspase8-dependent activation of caspase3 is inhibited by binding to p24 (Kamradt, Chen & Cryns, 2001). Binding of Cryab to procaspase3 to prevent its activation has also been observed (Mao et al., 2001). In addition, Cryab is able to prevent the upregulation of Bak, and it binds to Bax and Bcl-XS and inhibits their translocation to the mitochondria, this leads to decreased cytochrome c release into the cytosol, decreased activation of caspase3 and almost no cleavage of PARP (Mao et al., 2004).

The expression of HSP27 and Cryab result in a decrease of reactive oxygen species (ROS) levels, most probably by increasing glutathione levels (Mehlen et al., 1996).

The different anti-apoptotic mechanism used by Cryab and HSP27 seem to result from their different amino and/or carboxyl termini, since in the other regions they are quite homologue (Kamradt, Chen & Cryns, 2001).

2 Aim of the study

The majority of neurons in contrast to all other renewable cell types have to persist a whole lifetime. To be able to sustain viable over such a long time, neurons have certain survival strategies. So the first part of this study set out to investigate and demonstrate that iPS cell-derived neurons become more resistant towards stress induction and apoptotic stimuli during their differentiation. In case this is verifiable, the second aim was to identify different mechanisms established by mature neuronal cultures to overcome apoptotic stimuli. Therefore, on the one hand the study aimed to identify potential downregulation of death pathways and apoptosis promoting proteins in mature neuronal cultures, and on the other hand aimed to identify upregulations of survival pathways in these cultures. In addition to this, the third goal was to discover proteins with anti-apoptotic features to be upregulated in mature neuronal cultures. In case protective proteins are identified, the aim was to decipher their impact on stress resistance in mature neuronal cultures.

Due to the former inaccessibility of human neurons, post-mortem tissue, non-human models or immortalised cell lines were and are often used to investigate neuropathology. To this end the fourth aim was to uncover whether a neuroblastoma cell line is a suitable model to investigate neuronal properties.

3 Materials and solutions

3.1 Cell culture media

All cell culture media were stored at 4 °C.

MEF (mouse embryonic feeder) medium

Compound	Volume [%]	Volume [ml]
DMEM high glucose	86	500
FCS, heat inactivated	10	50
L-Glutamine	1	5
Non-essential amino acids	1	5
Sodium pyruvate	1	5
Penicillin Streptomycin (Pen/Strep)	1	5

Table 1: Composition of 500 ml MEF (mouse embryonic feeder) medium.

Basic neural stem cell (N2) medium

Compound	Volume [%]	Volume [ml]
DMEM/F12	97.6	500
N2 supplement	1	5
D-Glucose solution	0.4	2
Pen/Strep	1	5

Table 2: Composition of 500 ml basic neural stem cell (N2) medium.

Neural stem cell proliferation medium

Compound	Volume [%]	Volume [µl]
FGF2	0.1	50
EGF	0.1	50
B27 supplement	0.1	50

- ad. 50 ml N2 medium.

Table 3: Composition of 50 ml neural stem cell proliferation medium.

Neural generation (NGMC) medium

Compound	Volume [%]	Volume [ml]
DMEM/F12	96.3	500
N2 supplement	0.5	2.5
B27 supplement	1	5
D-Glucose solution	0.2	1
Non essential amino acids	1	5
Pen/Strep	1	5

Table 4: Composition of 500 ml neural generation (NGMC) medium.

Neural generation (NGMC) medium with DAPT

Compound	Volume [%]	Volume [µl]
DAPT solution	0.2	100

➢ *ad. 50 ml NGMC medium.*

Table 5: Composition of neural generation (NGMC) medium with DAPT.

Basic small molecule (BSM) medium

Compound	Volume [%]	Volume [ml]
DMEM/F12	98.3	500
N2 supplement	0.5	2.5
D-Glucose solution	0.2	1
Pen/Strep	1	5

Table 6: Composition of 500 ml basic small molecule (BSM) medium.

Small molecule (SM) medium

Compound	Volume [%]	Volume [µl]
B27 supplement	0.5	250
L-Ascorbic acid	0.05	25
CHIR99021 (CHIR)	0.03	15
Purmorphamin	0.01	5

➢ *ad. 50 ml Basic small molecule medium.*

Table 7: Composition of 50 ml Small molecule (SM) medium.

Washing medium

Compound	Volume [%]	Volume [ml]
DMEM low glucose	99	500
Pen/Strep	1	5

Table 8: Composition of 500 ml washing medium.

Lt-NES cell treatment medium

Compound	Volume [%]	Volume [µl]
FGF2	0.1	50
EGF	0.1	50

➢ ad. 50 ml N2 medium.

Table 9: Composition of 50 ml lt-NES cell treatment medium.

Neuron treatment medium (N2+)

Compound	Volume [%]	Volume [ml]
Non essential amino acids	1	0.5

➢ ad. 50 ml N2 medium.

Table 10: Composition of 50 ml neuron treatment medium (N2+).

3.1.1 Cell culture freezing media

All cell culture freezing media were stored at 4 °C.

FCS-based freezing medium

Compound	Volume [%]	Volume [ml]
FCS, heat inactivated	90	45
Dimethyl sulfoxide (DMSO)	10	5

Table 11: Composition of 50 ml FCS-based freezing medium.

Neural stem cell freezing medium

Compound	Volume [%]	Volume [ml]
KnockOut™ Serum Replacement	70	35
Cyto Buffer	20	10
DMSO	10	5

Table 12: Composition of 50 ml neural stem cell freezing medium.

3.2 Cell culture solutions

All cell culture solutions were stored at 4 °C or used directly after preparation.

Glucose solution (0.4 g/ml)

Compound	Volume [%]	Volume [ml]
H_2O	100	50
D-Glucose		20 g

Table 13: Composition of 50 ml Glucose solution.

DAPT solution (5 mM)

Compound	Volume [%]	Volume [µl]
DAPT stock solution in DMSO (25 mM)	20	20
Ethanol	80	80

Table 14: Composition of DAPT solution.

1x Trypsin EDTA

Compound	Volume [%]	Volume [ml]
PBS	90	45
10 x Trypsin EDTA	10	5

Table15: Composition of 1x Trypsin EDTA.

Trypsin inhibitor (TI)

Compound	Volume [%]	Volume [ml]
PBS	100	50
Trypsin inhibitor (>700 units/mg)		0.25 mg/ml

Table 16: Composition of Trypsin inhibitor (TI).

Poly-L-ornithine (PO) solution

Compound	Volume [%]	Volume [ml]
H_2O	99	990
Poly-L-ornithine stock solution	1	10

Table 17: Composition of Poly-L-ornithine solution.

Laminin (LN) coating solution

Compound	Volume [%]	Volume [ml]
PBS	99.9	50
Laminin	0.1	0.05

Table 18: Composition of Laminin (LN) coating solution.

Geltrex™ coating solution

Compound	Volume [%]	Volume [ml]
Washing medium	98	49
Geltrex™	2	1

➢ *Geltrex™ was thawed over night at 4 °C or on ice.*

Table 19: Composition of Geltrex™ coating solution.

Cyto buffer

Compound	Volume
Myo-Inositol (in 800ml distilled water)	43,25g
PBS	200 ml
Polyvinylalcohol	5g

Table 20: Composition of Cyto buffer for freezing cells.

3.3 Cell culture stock solutions

Solvents and concentrations

Compound	Concentration	Solvent
B27 supplement	50 x	Pure supplement mix
CHIR	10 mM	DMSO
D-Glucose	0.4 g/ml	H_2O
DAPT	25 mM (5mM)	DMSO (+ Ethanol)
DNase		H_2O
EDTA	0.5 M	H_2O
EGF	10 µg/ml	0.1 M Acetic acid + 0.1 % BSA
FGF2	10 µg/ml	PBS + 0.1 % BSA
L-Ascorbic acid	200 mM	H_2O
L-glutamine	100 x	
Laminin	1 mg/ml	
N2 supplement	100 x	Pure supplement
Non-essential amino acids	100 x	
Poly-L-ornithin	1.5 mg/ml	(Ampuwa) H_2O
Purmorphamin	5 mM	DMSO
Puromycin	1 mg/ml	H_2O
Rho-Kinase (ROCK) inhibitor	5 mM	
Sodium pyruvate	100 x	
Trypsin-EDTA	10 x	

Table 21: Concentrations and solvents of cell culture stock solutions.

3.4 Cell lines

Cell lines

Cell line	Source
SKNSH	
Lt-NES ctr line 1	Bonn, Germany (Koch et al. 2011)
Primary stem cell-derived lt-NES cells	
Cryab knockout #69; #45, #38	

Table 22: Utilised cell lines.

3.5 Cell culture and molecular biology consumables

Consumables and their manufacturer

Consumables	Manufacturer	Registered office
12-well culture dishes	FALCON, Corning	Corning, USA
24-well culture dishes	FALCON, Corning	Corning, USA
48-well culture dishes	FALCON, Corning	Corning, USA
6-well culture dishes	FALCON, Corning	Corning, USA
96-well culture dishes	FALCON, Corning	Corning, USA
cOmplete™, Mini, EDTA-free Protease Inhibitor Cocktail	Roche	Basel, Switzerland
Coverslips	Mänzel Gläser	Braunschweig, Germany
Cryovials 1 ml	Nunc	Wiesbaden, Germany
Cryovials 1.8 ml	Nunc	Wiesbaden, Germany
Cuvette		
PCR strip tubes 0.2 ml	PeqLab	Erlangen, Germany
Petri dishes ⌀ 10 cm	PAA	Pasching, Austria
PhosSTOP™ EASYpack	Roche	Basel, Switzerland
Polyvinylidenfluorid (PVDF) membrane (0.2 µm)	GE Healthcare	Little Chalfont,UK
qPCR plates	4titude	Wotton, UK

Consumables	Manufacturer	Registered office
qPCR seals	4titude	Wotton, UK
Serological pipettes 1 ml	Sarstedt	Nümbrecht, Germany
Serological pipettes 10 ml	Greiner Bio-One	Kremsmünster, Austria
Serological pipettes 2 ml	Corning Life Sciences	Schiphol-Rijk, The Netherlands
Serological pipettes 25 ml	Corning Life Sciences	Schiphol-Rijk, The Netherlands
Serological pipettes 5 ml	Corning Life Sciences	Schiphol-Rijk, The Netherlands
Syringe 20 ml	BD Biosciences	Heidelberg, Germany
Syringe 3 ml	BD Biosciences	Heidelberg, Germany
Syringe filter 0.2 µm	PALL	Dreieich, Germany
Syringes Omnifix Luer 50 ml	Braun	Melsungen, Germany
TC dishes Ø 10 cm	FALCON, Corning	Corning, USA
TC dishes Ø 3.5 cm	FALCON, Corning	Corning, USA
TC dishes Ø 6 cm	FALCON, Corning	Corning, USA
Tubes 0.5 ml	Greiner Bio-One	Solingen, Germany
Tubes 1.5 ml	Greiner Bio-One	Solingen, Germany
Tubes 15 ml	FALCON, Corning	Corning, USA
Tubes 50 ml	FALCON, Corning	Corning, USA
Whatman® Filter Paper	GE Healthcare	Little Chalfont, UK

Table 23: Consumables of cell culture and molecular biology.

3.6 Molecular biology reagents

50 x Tris-acetate-EDTA-buffer (TAE)

Reagent	Amount
Tris	242 g
EDTA (0.5 M) pH 8	100 ml
Water-free acetic acid	57.1 ml

➢ ad. 1 l H_2O. For use 50 x TAE was diluted 1:50 with H_2O.

Table 24: Composition of 50 x Tris-acetate-EDTA-buffer.

6 x DNA loading buffer

Reagent	Amount
EDTA (0.5 M) pH 8	2 ml
Sucrose	6 g
2 % Bromphenol-blue-solution	0.2 ml
2 % Xylene-cyanol-solution	0.2 ml
Ficoll	0.2 g
Aqua bidest.	3.8 ml

Table 25: Composition of 6 x DNA loading buffer. PFA

PFA fixation solution (4 %)

Reagent	Amount
Paraformaldehyde (PFA)	40 g
H_2O	100 ml

➢ The solution was heated until PFA dissolved. The pH was adjusted to 7.4.

Table 26: Composition of PFA fixation solution.

Blocking solution for Immunocytochemistry

Reagent	Amount
PBS	89.9 ml
FCS	10 ml
Triton™ X-100	0.1 ml

Table 27: Composition of Blocking solution for Immunocytochemistry.

Mowiol/DABCO

Reagent	Amount
Tris solution (0.2 M) pH 8.5	12 ml
H_2O	6 ml
Glycerol	6 g
Mowiol	2.6 g
DABCO	0.1 g

Table 28: Composition of Mowiol/DABCO.

RIPA buffer

Reagent	Amount
Tris HCl (1 M)	2.5 ml
NaCl (1.5 M)	5 ml
EDTA (0.5 M)	2.5 ml
Triton™ X-100	100 µl

➢ ad. 50 ml aqua bidest.; freshly per 10 ml 1 x complete, mini, EDTA free; 1x PhosSTOP™ tablets.

Table 29: Composition of RIPA buffer.

Protein loading buffer

Reagent	Amount
Tris solution (0.1 M) pH 6.8	75.75 %
Glycerol	20 %
Sodium dodecyl sulfate (SDS)	4 %
Bromphenol blue	0.25 %

Table 30: Composition of Protein loading buffer.

10 % SDS solution

Reagent	Amount
SDS, powder	100 g
Aqua bidest.	1 l

Table 31: Composition of 10 % SDS solution.

SDS-PAGE separation gel buffer (pH 8.8)

Reagent	Amount
Tris	90.8 g
SDS	2 g

➢ *ad. 500 ml H_2O*

Table 32: Composition of SDS-PAGE separation gel buffer.

SDS-PAGE stacking gel buffer (pH 6.8)

Reagent	Amount
Tris	15.1 g
SDS	2 g

➢ ad. 500 ml H_2O.

Table 33: Composition of SDS-PAGE stacking gel buffer.

10 x Tris buffer (T-buffer) (pH 8.0)

Reagent	Amount
Tris	30.3 g
Glycine	143 g

➢ ad. 1 l aqua bidest.

Table 34: Composition of 10 x Tris buffer.

SDS-PAGE running buffer

Reagent	Amount
SDS solution	10 ml
10 x T-buffer	100 ml

➢ ad. 1 l aqua bidest.

Table 35: Composition of SDS-PAGE running buffer.

Western blotting buffer (pH 8.8)

Reagent	Amount
10 x T-buffer	100 ml
Methanol	200 ml
SDS solution	10 ml

➢ ad. 1l aqua bidest.

Table 36: Composition of Western blotting buffer.

10 x TBS buffer

Reagent	Amount
NaCl	80 g
KCl	2 g
TrisBase	30 g

➢ *ad. 1 l aqua bidest.*

Table 37: Composition of 10 x TBS buffer.

TBS-T buffer (pH 8.0)

Reagent	Amount
10 x TBS buffer	100 ml
Tween-20	1 ml

➢ ad. 1 l aqua bidest.

Table 38: Composition of TBS-T buffer.

Membrane blocking solution

Reagent	Amount
TBS-T buffer	50 ml
Milk, powder	2 g

Table 39: Composition of Membrane blocking solution.

Chemo luminescence (CL) solution

Reagent	Amount
H_2O	4.5 ml
Tris HCl (1 M)	0.5 ml
Luminol	50 µl
p-Coumaric acid	20 µl
H_2O_2 (30 %)	1 µl

Table 40: Composition of Chemo luminescence solution.

PCR Master Mix (10 ml)

Reagent	Amount
10 x PCR buffer	20000 µl
$MgCl_2$ (50 mM)	600 µl
dNTPs	Each 40 µl (160)
H_2O (Ampuwa)	7240 µl

Table 41: Composition of PCR Master Mix.

Primer Master Mix

Reagent	Amount
H_2O (Ampuwa)	360 µl
Forward Primer (100 µM)	20 µl
Reverse Primer (100 µM)	20 µl

Table 42: Composition of Primer Master Mix.

PCR Reaction Mix (25 µl)

Reagent	Amount
PCR Master Mix	12.5 µl
H_2O (Ampuwa)	8.3 µl
Primer Master Mix	3 µl
cDNA (200 ng/µl)	1 µl
Taq	0.2 µl

Table 43: Composition of PCR Reaction Mix.

qPCR Master Mix (5 ml)

Reagent	Amount
5 x GoTaq® Flix buffer	2000 µl
$MgCl_2$ (25 mM)	1000 µl
dNTPs	Each 20 µl
1000 x SYBR-green	7.5 µl
Fluorescein	1 µl
DMSO	400 µl
H_2O (Ampuwa)	1511.5 µl

Table 44: Composition of PCR qPCR Master Mix.

qPCR Reaction Mix (25 µl)

Reagent	Amount
qPCR Master Mix	12.5 µl
cDNA (200 ng/µl)	1 µl
Primer Master Mix	1 µl
GoTaq®	0.15 µl
H_2O (Ampuwa)	10.35 µl

Table 45: Composition of qPCR Reaction Mix.

3.7 Antibodies

Antibodies

Antibody	Manufacturer	Dilution
AKT (rb)	Cell Signaling	1:2000
Caspase3 (rb)	Cell Signaling	1:2000
Caspase9 (rb)	Cell Signaling	1:1000
Cleaved Caspase3 (rb)	Promega	1:250
Cleaved PARP (rb)	Cell Signaling	1:2000
Cryab (ms)	Developmental Studies Hybridoma Bank	0.7 µg/ml
DACH1 (rb)	ProteinTech	1:100

Antibody	Manufacturer	Dilution
HSP27/HSPB1 (ms)	Developmental Studies Hybridoma Bank	0.7 µg/ml
HSP70/72 (rb)	Cell Signaling	1:2000
MAP2ab	Sigma Aldrich	1:250
Nestin (ms)	R&D Systems	1:600
pAKT (rb)	Cell Signaling	1:2000
Pax6 (ms)	Developmental Studies Hybridoma Bank	1:500
SOX2 (ms)	R&D Systems	1:300
β-Actin (ms)	Millipore	1:5000
βIII tubulin (ms)	BioLedgend	1:1000
βIII tubulin (rb)	Sigma Aldrich	1:2000
Alexa488 gt-anti-ms	Life technologies	1:1000
Alexa488 gt-anti-rb	Life technologies	1:1000
Alexa555gt-anti-ms	Life technologies	1:1000
Alexa555gt-anti-rb	Life technologies	1:1000
HRP-gt-anti-ms	GE Healthcare Life Sciences	1:1000
HRP-gt-anti-rb	Jackson ImmunoResearch	1:20000

Table 46: Utilised enzymes, their manufacturers and dilutions.

3.8 Enzymes

Enzymes

Enzyme	Manufacturer	Registered office
DNase I (cell culture)	Roche	Basel, Switzerland
DNase I (mol. Bio.)	Invitrogen	Karlsruhe, Germany
Taq DNA polymerase	Invitrogen	Karlsruhe, Germany

Table 47: Utilised enzymes and their manufacturers.

3.9 Kits

Kits

Name	Manufacturer	Registered office
iScript cDNA Synthesis Kit	Bio-Rad	Munich, Germany
peqGold Gel Extraction Kit	Peqlab Biotechnologie	Erlangen, Germany
peqGOLD TriFast™	VWR	Radnor, USA
GoTaq® DNA Polymerase	Promega	Madison, USA
Pierce™ BCA Protein Assay Kit	Thermo Fisher Scientific	Waltham, USA
PrestoBlue® Cell Viability Reagent	Thermo Fisher Scientific	Waltham, USA
CellTiter-Glo® Luminescent Cell Viability Assay	Promega	Madison, USA
Nuclefection	Lonza	Basel, Switzerland

Table 48: Employed kits and source.

3.10 Plasmids

Plasmids

Plasmid	Manufacturer	Registered office
αB-crystallin HDR Plasmid (h)	Santa Cruz Biotechnology	Dallas, USA
αB-crystallin CRISPR/Cas9 KO Plasmid (h)	Santa Cruz Biotechnology	Dallas, USA

Table 49: Utilised plasmids and their manufacturer.

3.11 Primer

Primer

Gene	Name	Primer sequence (5'- 3')
Cryab	Cr3 left	TCTGATGGGGTCCTCACTGT
Cryab	Cr3 right	ACAGCAGGCTTCTCTTCACG
p62	SQSTM1 2 left	AGAACGTTGGGGAGAGTGTG
p62	SQSTM1 2 right	TTCTTTTCCCTCCGTGCTCC
18s	18s for	TTCCTTGGACCGGCGCAAG
18s	18s rev	GCCGCATCGCCGGTCGG
VEGFB	VEGFB2 left	GAGATGTCCCTGGAAGAACACA
VEGFB	VEGFB2 right	GAGTGGGATGGGTGATGTCA
SCG2	SCG2 left	GCAGTGGCCAGAAAGAAAGC
SCG2	SCG2 right	GGTCCTGTCAGTTTCCCCAG
GCLM	GCLM left	TCCTTGGAGCATTTACAGCCT
GCLM	GCLM right	TGGCATCACACAGCAGGAG
Rab31	Rab31 right	ACACTGGGGTTGGGAAATCA
Rab31	Rab31 left	CCACAAGGCACAGTTTTGGT
SRXN1	SRXN1 2 left	AGGAGGAACGCTGGGC
SRXN1	SRXN1 2 right	CACGTTGTGCACCGCG
RPLPO	RPLPO F	AGCCCAGAACACTGGTCTC
RPLPO	RPLPO R	ACTCAGGATTTCAATGGTGCC
Cryab	Cryab_g1-hom_fw	GGCATACGGGTTAAGGTCATC
Cryab	Cryab_g1_rev	ACGGGTGATGGGAATGGT
Cryab	Cryab_g2-hom_fw	TAGCTGTGCAAGAATCCGTG
Cryab	Cryab_g2_rev	TCTACATCAGCTGGGATCCG
Cryab	Cryab_g3-hom_fw	TTTTCTCCTCTTCGGTGGCA
Cryab	Cryab_g3_rev	AACAGGTGCTCTCCGAAGAA
Cryab	Cryab_g3_rev_2	GCTTGATAATTTGGGCCTGC

Table 50: Employed primers.

3.12 Chemicals and reagents

Substance	Manufacturer	Registered office
30%Bis/Acrylamid	Carl Roth	Karlsruhe, Germany
3-Methyladenine	Merck	Darmstadt, Germany
4,6-Diamidino-2-phenylindole, dihydrochloride (DAPI)	Sigma Aldrich	Deisenhofen, Germany
Agarose	PeqLab	Erlangen, Germany
Ammonium persulfate	Sigma Aldrich	Deisenhofen, Germany
Ascorbis acid	Sigma Aldrich	Deisenhofen, Germany
Azide	Sigma Aldrich	Deisenhofen, Germany
B27 supplement	Invitrogen	Karlsruhe, Germany
Bafilomycin		
Bromphenol blue	Sigma Aldrich	Deisenhofen, Germany
BSA solution (7.5%)	Sigma Aldrich	Deisenhofen, Germany
$CaCl_2$	Sigma Aldrich	Deisenhofen, Germany
complete, mini, EDTA free	Roche Diagnostics	Mannheim, Germany
DABCO	Sigma Aldrich	Deisenhofen, Germany
DAPT	Axon Medchem	Groningen, The Netherlands
DMEM high glucose	Invitrogen	Karlsruhe, Germany
DMEM/F12	Invitrogen	Karlsruhe, Germany
DMSO	Sigma Aldrich	Deisenhofen, Germany
dNTPs	PeqLab	Erlangen, Germany
EGF	R&D Systems	Minneapolis, USA
Ethanol	Sigma Aldrich	Deisenhofen, Germany
Ethidium bromide	Sigma Aldrich	Deisenhofen, Germany
FCS	Invitrogen	Karlsruhe, Germany
FGF2	R&D Systems	Minneapolis, USA
Geltrex	Gibco by Life Technologies	Waltham, USA
Glucose	Sigma Aldrich	Deisenhofen, Germany

Substance	Manufacturer	Registered office
Glycerol	Sigma Aldrich	Deisenhofen, Germany
Glycin	Sigma Aldrich	Deisenhofen, Germany
H_2O_2	Sigma Aldrich	Deisenhofen, Germany
HCl	Sigma Aldrich	Deisenhofen, Germany
Isopropanol	Sigma Aldrich	Deisenhofen, Germany
L-glutamine (100x)	Gibco by Life Technologies	Karlsruhe, Germany
Laminin	Thermo Fisher Scientific	Waltham, USA
Methanol ROTIPURAN	Carl Roth	Karlsruhe, Germany
MG-132		
Mowiol	Carl Roth	Karlsruhe, Germany
Myo-Inositol	Sigma Aldrich	Deisenhofen, Germany
N2 supplement (100x)	Gibco by Life Technologies	Karlsruhe, Germany
NaCl	Sigma Aldrich	Deisenhofen, Germany
Non-essential amino acids (100x)	Gibco by Life Technologies	Karlsruhe, Germany
p-Coumaric acid	Sigma Aldrich	Deisenhofen, Germany
PBS	Invitrogen	Karlsruhe, Germany
Penicillin-Streptomycin	Gibco by Life Technologies	Karlsruhe, Germany
PFA	Sigma Aldrich	Deisenhofen, Germany
PhosSTOP™ tablets	Roche Diagnostics	Basel, Swizerland
Polyvinylalcohol	Sigma Aldrich	Deisenhofen, Germany
Powdered milk	Carl Roth	Karlsruhe, Germany
Puromycin	PAA	Pasching, Austria
Rotenone	Merck	Darmstadt, Germany

Substance	Manufacturer	Registered office
SDS	Sigma Aldrich	Deisenhofen, Germany
Serum Replacement	Invitrogen	Karlsruhe, Germany
Sodium pyruvate (100x)	Invitrogen	Karlsruhe, Germany
Staurosporine		
TEMED	Sigma Aldrich	Deisenhofen, Germany
Thapsigargin	Merck	Darmstadt, Germany
Tris	Sigma Aldrich	Deisenhofen, Germany
Triton-X-100	Sigma Aldrich	Deisenhofen, Germany
Trypane Blue	Invitrogen	Karlsruhe, Germany
Trypsin inhibitor (TI)	Gibco by Life Technologies	Waltham, USA
Trypsin-EDTA (10x)	Gibco by Life Technologies	Waltham, USA
Tunicamycin	Sigma Aldrich	Deisenhofen, Germany

Table 51: Utilised chemicals and reagents.

3.13 Technical equipment

Technical equipment

Device	Name	Manufacturer	Registered office
Autoclave	D-105	Systec	Wettenberg, Germany
Balance	Bl610	Satorius	Göttingen, Germany
Balance	LA310S	Satorius	Göttingen Germany
Block heater	Thermomixer compact	Eppendorf	Hamburg, Germany
Centrifuge (cell culture)	Megafuge 1.0R	Sorvall	Hanau, Germany

Device	Name	Manufacturer	Registered office
Centrifuge (table top)	5415D	Eppendorf	Hamburg, Germany
Counting chamber	Neubauer improved	Laboroptik	Lancing, United Kingdom
Digital camera	C 5050 Zoom	Olympus Optical	Hamburg, Germany
Digital camera	Canon Power Shot G5	Canon	Krefeld, Germany
Fluorescence lamp	HAL100	Carl Zeiss	Jena, Germany
Fluorescence microscope	Axioskope 2	Carl Zeiss	Jena, Germany
Freezer -80 °C	HERAfreeze	Kendro	Hanau, Germany
Gel electrophoresis chamber	Agagel	Biometra	Göttingen, Germany
Imaging system	Chemidoc 2000	Bio-Rad	Munich, Germany
Imaging system	Geldoc EZ	Bio-Rad	Munich, Germany
Incubator	HERAcell	Kendro	Hanau, Germany
Liquid nitrogen store	MVE 611	Chart Industries	Burnsville, USA
Micro-Spectrophotometer	Nanodrop ND-1000	Thermo Fisher Scientific	Wilmington, USA
Microscope	Axiovert 200M	Carl Zeiss	Jena, Germany
Microscope (cell culture)	Axiovert 40 CLF	Carl Zeiss	Jena, Germany
Microscope camera	Axiocam MRM	Carl Zeiss	Jena, Germany
Microscope laser	Laser Mells Griot	Griot Lasergroup	Carlsbad, Germany
Microscope slides	Superfrost plus	Menzel-Gläser	Braunschweig, Germany
Nucleofector	Nucleofactor 2b	Lonza	Basel, Switzerland

Device	Name	Manufacturer	Registered office
PAGE gel power supply	PowerPac 200	BioRad	Hercules, USA
PAGE/Blot equipment	Mini-PROTEAN 3	Bio-Rad	München, Germany
PCR cycler	T300 Termocycler	Biometra	Göttingen, Germany
pH-meter	CG840	Schott	Mainz, Germany
Pipette-boy	Accu-Jet	Brand	Wertheim, Germany
Pipettes (1000, 100, 10 and 2 µl)		Eppendorf	Hamburg, Germany
Plate reader	Infinite® 200 PRO	Tecan	Männedorf, Switzerland
Plate reader	EnVison™Multilabel Reader	Perkin Elmer Inc	Baesweiler, Germany
Power supply for Electrophoresis	Standard Power Pack P25	Biometra	Göttingen, Germany
Power supply for electrophoresis	Standard Power Pack P25	Biometra	Göttingen, Germany
Real-time qPRC machine	Mastercycler realplex	Eppendorf	Hamburg, Germany
Refrigerators 4°C /-20°C	G 2013 Comfort	Liebherr	Lindau, Germany
Secure horizontal flow hood	HERAsafe	Kendro	Hanau, Germany
Shaker	Bühler WS10	Johanna Otto	Hechingen, Germany
Sterile laminar flow hood	HERAsafe	Kendro	Hanau, Germany
Table centrifuge	Centrifuge 5415R	Eppendorf	Hamburg, Germany
Thermocycler	T3 Thermocycler	Biometra	Göttingen, Germany

Device	Name	Manufacturer	Registered office
Vacuum pump	Vacuubrand	Brand	Wertheim, Germany
Vortex mixer	Vortex Genie 2	Scientific Industries	New York, USA
Water bath	1008	GFL	Burgwedel, Germany
Water filter	Milipak 40	Millipore	Eschborn, Germany

Table 52: Manufacturer of technical equipment.

3.14 Software

Software

Computer program	Manufacturer
ApE – A plasmid editor	M. Wayne Davis
AxioVision 40 4.5.0.0	Carl Zeiss
Enricher	Avi Ma'ayan
Excel 2011	Microsoft
GenomeStudio 2011	Illumina
Image J 1.42q	NIH
Primer3web 4.0.0	
Prism 6	GraphPad
Quantity One 4.6.8	Bio Rad
Word 2011	Microsoft

Table 53: Utilised software.

4 Methods

4.1 Cell culture

Handling of media and cells was performed under a sterile lamina flow hood using sterile glass and plastic ware.

4.1.1 Coating of tissue culture dishes

Depending on the cell population used, different coatings of the tissue culture (TC) dishes were used.

4.1.2 Poly-L-ornithine and Laminin coating of TC dishes

TC dishes were covered with Poly-L-ornithine (PO) solution. The dishes were incubated at 37 °C for >= 1 h. Subsequently, the PO solution was removed and the dishes were washed twice with PBS to eliminate remaining PO, which is toxic to cells. Then the TC dishes were coated with laminin, a component of the extracellular matrix (ECM) to which cells can bind. The dishes were incubated overnight at 4 °C. To avoid contaminations, the dishes were sealed with Parafilm. Before use, the laminin solution was removed. This type of coating is used to improve the binding of lt-NES cells to the culture dish.

4.1.3 Geltrex™ coating of TC dishes

TC dishes were coated with Geltrex™ solution (40 µl-5 ml) according to their size. The incubation lasts at least overnight at 4 °C. To avoid contaminations, the dishes were sealed with Parafilm. Geltrex™ supplies basal membrane matrix to which cells can bind. Before the use of the dishes, the Geltrex™ solution had to be removed. The collected Geltrex™ solution was reused at least three times. This type of coating was used to improve the binding of neurons, differentiating lt-NES cells, SM cells and tumour cell lines.

4.1.4 Preparation of glass coverslips

Glass coverslips were incubated with 37 % HCl for at least one hour under a laboratory hood. The acid was removed and coverslips were washed twice with H_2O and subsequently washed twice with PBS. Afterwards, they were incubated with 70 % ethanol for approximately 10 min. Next, the glass coverslips were incubated with 10 x PO overnight at

37 °C. The following day coverslips were washed twice with PBS and then incubated with laminin in PBS (1:500) for two hours at 37 °C. Laminin was aspirated and the glass coverslips were covered with Geltrex™ and incubated for 1 h at 37 °C for direct use or stored at 4 °C. Cells were plated on glass coverslips for immunocytochemical analysis.

4.2 Cell line cultivation

4.2.1 Cultivation of tumour cell lines

The cells of the neuroblastoma cell line, SKNSH, were plated on Geltrex™ coated tissue culture dishes. They were seeded in low densities and kept on the dishes until the cultures were confluent. The SKNSH cells were cultivated in MEF (mouse embryonic feeder) medium. The medium was changed daily, or every other day.

4.2.2 Passaging, freezing and thawing of tumour cell lines

After the SKNSH cells became confluent, they were split in a ratio of up to 1:20. Therefor the medium was aspirated and the cells were washed once with PBS to remove remaining medium. Subsequently, the cells were incubated for 5 min at 37 °C and 5 % CO_2 with Trypsin EDTA. When starting to detach, the cells were washed from the plate with MEF medium. Afterwards the cells were centrifuged at 1200 rcf for 5 min. The supernatant was removed and the pellet resuspended with MEF medium. The cells were then plated on new Geltrex™ coated dishes. For freezing, the SKNSH cells were treated as described above, but after the centrifugation step, the cells were resuspended in 1 ml fetal calf serum (FCS)-based freezing medium and transferred into a cryovial. Then the cells were frozen at -80 °C.
For thawing the SKNSH cells, the cryovials were placed in a water bath (39 °C) until only a little ice was left, then the cells were transferred in a 15 ml tube with Wash medium. Afterwards the cells were centrifuged as described above and plated on new Geltrex™ coated dishes.

4.2.3 Cultivation of small molecule (SM) neural precursor (NP) cells

SM-NP cells can be generated from iPS cells and be converted into lt-NES cells by changing from SM medium to neural stem cell proliferation medium (Reinhardt et al., 2013). The SM-NP cells were cultured on Geltrex™ coated tissue culture dishes. The cell densities

varied from clonal to confluent. SM medium, containing CHIR, purmorphomine and ascorbic acid was used to cultivate SM-NP cells. CHIR is added to inhibit glycogen synthase kinase 3 (GSK-3), thereby accumulating β-catenin and inducing Wnt-target genes (Jope & Johnson, 2004). Purmorphamine activates the Hedgehog signalling pathway (Wu et al., 2004). Ascorbic acid serves as an antioxidant (Arrigoni & De Tullio, 2002). The SM medium was exchanged every day. The cells were cultivated on the dish until they were confluent.

4.2.4 Passaging, freezing and thawing of SM-NP cells

As soon as the SM-NP cells became confluent, the cells were split in a ratio of between clonal and 1:2. The cells were incubated with Typsin EDTA for 5 min at 37 °C and 5 % CO_2. The cells were washed from the plate using trypsin inhibitor and wash medium. Subsequeltly, the cells were centrifuged at 1200 rcf for 5 min. Next, the supernatant was removed and the SM-NP cells were resuspended in SM medium and seeded on new Geltrex™ coated dishes. For freezing the SM-NP cells, the cells were treated as described above, but after the centrifugation step, the cells were resuspended in 1 ml neural stem cell freezing medium and transferred to a cryovial. They were then immediately stored at -80 °C. For thawing SM cells, the cryovials were placed in a waterbath of 39 °C until only a little ice was left. Then the cells were transferred into a 15 ml tube and centrifuged as described above and plated on Geltrex™ coated dishes.

4.2.5 Cultivation of lt-NES cells

Lt-NES cells are a homogenous cell population, which can be passaged over more than 100 passages. These cells can give rise to neurons, astrocytes and oligodendrocytes depending on the culture conditions (Koch et al., 2009). Lt-NES cells were cultivated on PO/LN coated dishes. The cells were plated to a confluence of approximately 40 %, so that cells have cell-cell contact, which is important for their proliferation and survival. The cells were cultivated in neural stem cell proliferation medium, containing FGF2, EGF (each10 ng/ml) and B27 (1 µl/ml) to promote their proliferation. A media change was performed every day. The cells were kept on the dish until they were confluent.

4.2.6 Passaging, freezing and thawing of lt-NES cells

Upon reaching confluency, the lt-NES cells were split in a ratio of 1:2 or 1:3. For splitting the lt-NES cells were incubated with Trypsin EDTA at 37 °C and 5 % CO_2 until they start to detach (ca. 5 min). The cells were washed from the plate using trypsin inhibitor and wash medium. Following, the lt-NES cells were centrifuged at 1200 rcf for 5 min. Afterwards, the supernatant was removed and the cells were resuspended in neural stem cell proliferation medium and seeded on new PO/LN coated dishes. For freezing, the lt-NES cells were treated in the same manner as described above, but after the centrifugation step, the cells were resuspended in 1 ml neural stem cell freezing medium and transferred to a cryovial. They were then immediately stored at -80 °C. To thaw lt-NES cells, the cryovials were placed in a waterbath of 39 °C until only a little ice was left. Then, the cells were transferred into a 15 ml tube and centrifuged as described above and plated on PO/LN coated dishes.

4.2.7 Differentiation of lt-NES cells to neuronal cultures

For differentiation of lt-NES cells to neuronal cultures, lt-NES cells, the cells were transferred to a Geltrex™ coated tissue culture dish and upon reaching confluency, differentiation was induced by withdrawal of growth factors. For that, the medium was changed to NGMC medium containing DAPT for 3 days. DAPT inhibits Notch signalling via the inhibition of γ-sectretase. The inhibition of Notch signalling promotes neuronal differentiation (Ben-Shushan, Feldman & Reubinoff, 2015). DAPT was added to enrich the amount of neurons in the culture and to avoid the formation of astrocytes. After 3 days of differentiation, the cultures were split onto new dishes. For this, the cells were dissociated by the application of TrypLE for 20 min at 37 °C. Then the cells were transferred to a 15 ml tube by diluting TrypLE with washing buffer (1:1). Next, the neurons were centrifuged at 1200 rcf for 5 min. The supernatant was removed and the cell pellet was resuspended in NGMC medium, supplemented with ROCK Inhibitor (1:1000). The cells were plated directly on new Geltrex™ coated culture dishes and cultivated in NGMC medium. The medium change was performed every second day. Depending on the experiment, neurons were harvested or used for experiments 2-5 days after splitting – either as immature neurons or they were cultured for another 4-9 weeks and then harvested or utilised as mature neurons.

4.3 Treatments for modelling cellular stress

In order to investigate the cellular stress response of diverse types of different cell populations, their response to various stress inducing factors was analysed: I) Staurosporine was used as a protein kinase inhibitor, II) MG-132 served as proteasome inhibitor, III) Bafilomycin (Baf) and 3-Methyladenine (3-MA) in combination were employed to model autophagy stress, IV) Tunicamycin and Thapsigargin were applied to induce endoplasmic reticulum (ER) stress, while Rotenone was used to simulate oxidative stress. Treatment medium plus Dimethyl sulfoxide (DMSO) or treatment medium was used as control. The concentrations used are listed in the following table.

Treatment concentrations of cellular stressors

Compound	Final concentration
Staurosporine	5 nM
Rotenone	5 µM
MG-132	7.5 µM
Baf/3-MA	15 nM/2 mM
Thapsigargin	2 µM
Tunicamycin	1.5 µM
DMSO	2 µl/ml

Table 54: Treatment concentrations of employed cellular stressors.

The cells were treated with the different stressors in the absence of B27 to avoid redox protection by the supplement. Ribonucleic acid (RNA) was collected after 8 h of treatment, protein was harvested 16 h after incubation with stressors. For cell viability assays, the cells were treated for 0 h, 16 h, 32 h, and 48 h with the respective stressors.

4.4 Immunocytochemistry

4.4.1 Principal of the immunocytochemical analysis

The immunocytochemical analysis represents a method to make proteins and cell compartments visible, by utilizing fluorescent dye marked antibodies. In a first step, specific antibodies (primary antibodies) are applied that bind to a unique antigen. By using

fluorescence marked antibodies (secondary antibodies) that bind specifically to the primary antibodies, the presence or absence of an antigen can be investigated. If the secondary antibody binds to the primary antibody, the binding can be monitored via fluorescence microscopy. The fluorescent dye is stimulated by the light of a certain wavelength and a photon will be absorbed. The absorbed energy is released by emitting light of a longer wavelength. The immunocytochemical workflow is shown in Figure 4.1.

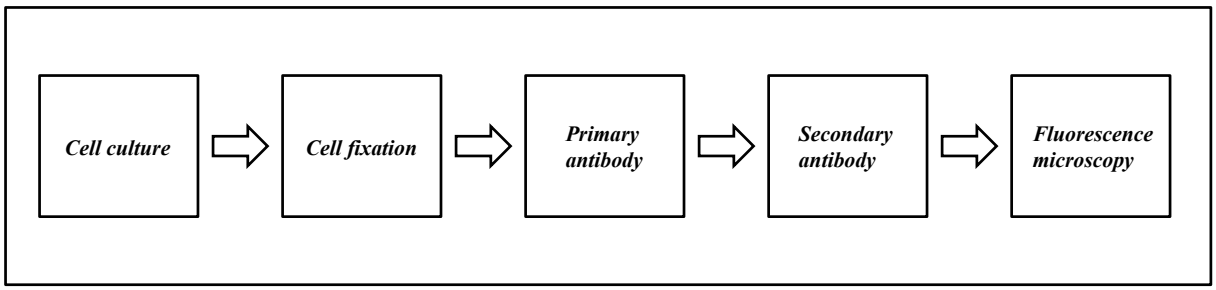

Figure 4.1: Immunocytochemical workflow.

4.4.2 Immunocytochemical analysis

First, the cells were fixed with 4 % paraformaldehyde (PFA) for 10 min at room temperature (RT), washed twice with PBS and blocked with blocking solution (PBS with 10 % FCS) for one hour at RT. For staining of intracellular antigens, 0.1 % Triton™ X-100 was added to the blocking solution. Subsequently, the cells were incubated with respective primary antibodies (listed) in blocking solution over night at 4 °C. Before the secondary antibody was applied, the cells were rinsed twice with PBS to eliminate the surplus of primary antibody. The secondary antibody (listed) was applied for two hours at RT. The cell nuclei were counterstained with 4,6-Diamidino-2-phenylindole, dihydrochloride (DAPI) for 5 min at RT. Finally, the cells were washed twice with PBS, mounted with Moviol/DABCO and covered with a glass coverslip.

4.5 Cell viability assays

To investigate the viability of different cell populations (SKNSH cells, lt-NES cells, immature and mature neurons after the application of different cellular stressors), cell viability assays were performed. For all viability assays the cells were cultivated on Geltrex™ coated 96-well culture dishes. Depending on the respective cell population, the cells were seeded in different densities (SKNSH cells 15000 cells/well, lt-NES cells 30000 cells/well and neurons 50000 cells/well). Mature neurons were cultured for 4 or 9 weeks

before they were examined. To assess their viability, the cells were cultivated in 50 µl medium per well. The cell viability was evaluated 20 h after treatment for concentration-dependent experiments and measured 0 h, 16 h, 32 h and 48 h after treatment for time-dependent experiments.

4.5.1 PrestoBlue® assay

The detection of cell viability via PrestoBlue® is based on the irreversible reduction of resazurin (blue) to resorufin (pink) by viable, metabolically active cells. The colour change is proportional to the number of viable cells and can be investigated by measuring changes in absorbance using a plate reader.

To examine the cell viability, 5 µl of PrestoBlue® reagent per well were added. Medium and reagent were carefully mixed. The cultures were incubated for 30 min at 37 °C and 5 % CO_2. The plate reader (Infinite® 200 PRO) was used to detect the colour change with an excitation wavelength of 540 nm and an emission wavelength of 590 nm.

4.5.2 CellTiter-Glo® Luminescent Cell Viability Assay

The determination of cell viability via CellTiter-Glo® is based on adenosine triphosphate (ATP) quantification. The presence of ATP marks metabolically active cells. The CellTiter-Glo® reagent lyses cells and generates a luminescence signal that is proportional to the amount of ATP, which can be used to approximate the number of viable cells in culture.

To investigate the metabolic activity of the cultures, 50 µl of CellTiter-Glo® reagent were applied per well. To promote cell lysis and to mix the contents, the plates were placed on an orbital shaker for 5 min. The plates were incubated for 10 min at RT to stabilize the luminescence signal. The luminescence was measured using a plate reader (EnVison™Multilabel Reader).

4.6 Western Blotting

4.6.1 Principal of Western Blotting

Western Blotting is a method to detect and estimate the amount of different proteins in cell lysates. Total protein solutions are loaded on a sodium dodecyl sulfate (SDS)-Gel. The proteins are separated via electrophoresis according to their molecular mass, whereby small proteins migrate faster through the acrylamide mesh than big proteins. The SDS-loaded negatively charged proteins are then transferred from the gel to a membrane by electroblotting. Before incubation with primary antibody, the membrane is blocked to prevent unspecific antibody binding. Then, a horseradish peroxidase (HRP)-conjugated secondary antibody is applied. Its binding can be detected by a chemoluminescence signal. The signal is based on the HRP-catalysed oxidation of luminol. The generated signal is proportional to the amount of protein.

4.6.2 Sample preparation

For the protein samples for Western Blotting, the cultures were treated with MG-132 and DMSO for 16 hours. The cultures were harvested in RIPA buffer to lyse the cells and solubilize the proteins. The RIPA buffer contains protease and phosphatase inhibitors to prevent protein digestion and dephosphorylation. The samples were incubated in RIPA buffer for 1 h on ice. They were then centrifuged for 30 min at 4 °C and 16,000 rcf. The supernatant was transferred to a new tube. Lysates were stored at -20 °C.

4.6.3 Pierce™ BCA protein assay

The total protein concentration was estimated using Pierce™ BCA Protein assay. The assay is based on the reduction of Cu^{+2} to Cu^{+1} by proteins in alkaline medium. Cu^{+1} is chelated by bicinchoninic acid (BCA), which leads to a purple coloured reaction product exhibiting a strong absorbance at 562 nm. The signal is linear proportional to the amount of protein.

The assay was performed in a 96-well format. Bovine serum albumin (BSA) was utilised as a standard. To determine the protein concentration, 25 µl of each standard (25-2000 µg/ml) were pipetted as well as 25 µl of 1:5 dilutions of the protein samples. 200 µl of BCA reagent were added per well. The plate was mixed and incubated for 30 min at 37 °C. The absorbance at 595 nm was measured using a plate reader (Infinite® 200 PRO).

4.6.4 SDS-gel electrophoresis and Western Blotting

Lysates containing 25-30 µg of protein were supplemented with 6 x protein loading buffer. The samples and a protein ladder were loaded in wells on a 12 % SDS-gel. First, the proteins were concentrated in the stacking gel and then separated in the separation gel via electrophoresis at 110 V up to 1.5 hrs. The proteins were then transferred to a polyvinylidenfluorid (PVDF) membrane (0.2 µm) for 1 h at 0.5 A 15 V in a semi-dry blotting chamber. Prior to the protein transfer, the PVDF membrane had to be incubated for at least 1 min with 100 % methanol to reduce its hydrophobia. After the protein transfer the membrane was incubated for one hour with membrane blocking solution (4 % milk powder in TBS-T).

Composition of 5 ml stacking gel

Component	Volume [ml]
H_2O	3.4
30 % Acrylamide mix	0.83
Stacking gel buffer (pH 6.8)	0.63
10 % SDS	0.05
10 % Ammonium persulfate	0.05
TEMED	0.005

Table 55: Formulation of stacking gel.

Composition of 20 ml 12 % separation gel

Component	Volume [ml]
H_2O	6.6
30 % Acrylamide mix	8.0
Separation gel buffer (pH 8.8)	5.0
10 % SDS	0.2
10 % Ammonium persulfate	0.2
TEMED	0.008

Table 56: Formulation of separation gel.

4.6.5 Protein detection

For protein detection, the PVDF membrane was incubated on a rotation device with primary antibody (listed) diluted in membrane blocking solution overnight at 4 °C. The membrane was washed thrice with TBS-T and incubated with an HRP-conjugated secondary antibody (listed) diluted in TBS-T at RT for one hour under rotation. Following three washing steps with TBS-T. Chemoluminescence (CL) solution was applied and the chemoluminescence was detected using the Chemidoc 2000 imaging system.

4.7 RNA isolation and complementary deoxyribonucleic acid (cDNA) generation

4.7.1 RNA isolation with TriFast™

RNA was isolated using TriFast™, a reagent suitable to isolate RNA, DNA and proteins in one sample. TriFast™ includes phenol and guanidinium thiocyanate. A separation into three phases is achieved after adding chloroform and centrifuging the sample. The upper aqueous phase contains the RNA, the interphase the DNA and the organic phase contains the proteins.

The cultures were treated with MG-132 and DMSO for 8 h. The samples were harvested and homogenized in 0.5 or 1 ml (12 well or Ø 3.5 cm TC dish) Trifast™. To induce phase separation, 0.1 or 0.2 ml of chloroform was added. The samples were shaken by hand for 30 sec, followed by incubation at RT for 15 min. The samples were then centrifuged at RT at 12.000 rcf, resulting in a phase separation, the colourless aqueous phase, the interphase and the red phenol-chloroform phase. The aqueous phase containing the RNA was transferred to a new tube without contaminations of the inter- or organic phase. To reduce the hydrophilicity of the RNA, isopropanol was used. For the precipitation, 0.25 or 0.5 ml isopropanol were added respectively. The samples were shaken by hand for 15 sec and incubated on ice for at least one hour. Thereafter, the samples were centrifuged for 10 min at 4 °C and 12.000 rcf. The resulting RNA-pellet was washed twice with 75 % ethanol and air-dried. The RNA was resuspended in 20 µl of RNase-free water under shaking for 30 min.

4.7.2 RNA purification using DNase I

20 µl of the RNA sample were mixed with 2.5 µl of 10 x DNase I reaction buffer and 2.5 µl of DNase I and incubated at RT for 15 min. To inactivate DNase I, 2.5 µl EDTA (25 mM) were added, the samples were incubated for 10 min at 65 °C.

4.7.3 Reverse Transcription (cDNA synthesis)

cDNA is synthetized from a RNA template. Reverse transcriptase uses the RNA template and a short primer, complementary to the 3' end of the template, to synthesize cDNA.
For reverse transcription, the quantitative PCR iScript™ cDNA Synthesis kit was used. The iScript Reaction Mix contains RNase H+, oligo(dT) and random hexamer primers. Per 20 µl reaction, 1 µg RNA, 4 µl 5 x iScript Reaction Mix and 1 µl iScript reverse transcriptase were applied, missing volume was refilled with nuclease-free water.

Reaction protocol

Step	Time and temperature
Priming	5 min at 25 °C
Reverse Transcription	30 min at 42 °C
Inactivation	5 min at 85 °C
Optional step	Hold at 4 °C

Table 57: Reaction protocol of reverse transcription.

4.8 Polymerase chain reaction and quantitative Polymerase chain reaction

4.8.1 Polymerase chain reaction

Polymerase chain reaction (PCR) is used to multiply few copies of DNA to thousands of copies. PCR amplifies a specific region of DNA, depending on the primers used. Several components are needed for a PCR: A DNA-template, a heat stable DNA polymerase (Taq polymerase), two primers (complementary to the 3'ends), nucleotides, buffer solution and Mg. Typically, a PCR has 30-40 cycles. The first step of a cycle is the denaturation, a 95 °C short heating step, that causes melting of the DNA. The next step is the annealing, here primers bind to the single stranded DNA, followed by the elongation, whereby DNA

polymerase synthetizes a new DNA strand complementary to the template DNA. The final step is a hold step at 4 °C for short-term storage.

PCR program

Step	Time and temperature
Initial denaturation	5 min at 95 °C
Denaturation	30 sec 95 °C
Annealing	30 sec 60 °C
Elongation	60 sec 72 °C
Final elongation	10 min 72 °C
Hold	4 °C

Table 58: Typical PCR program.

4.8.2 Quantitative PCR or real-time PCR

Quantitative PCR (qPCR) is based on the same principal as normal PCR, but the amplification can be monitored in real-time and it can be used quantitatively. Quantitative PCR can be used to investigate gene expression levels on the basis of the amount of messenger RNA (mRNA) transcripts. Messenger RNA is transcribed into cDNA as described in 4.7.3. Quantitative PCR was performed in triplets in a realplex mastercycler and SYBR-green was used as detection method. Melting curves prove the specifity of the amplified DNA. The obtained data were normalized to 18S or RPLPO mRNA levels respectively. $\Delta\Delta C_t$-method, whereby C_t represents the number of cycles after which the fluorescence signal exceeds the threshold, was used to analyse the data.

qPCR program

Step	Time and temperature
Taq activation	2 min at 95 °C
Denaturation	15 sec at 95 °C
Annealing	15 sec at 60 °C
Elongation	20 sec at 72 °C

Table 59: Utilised qPCR program.

Melting curve program

Time and temperature
15 sec at 60 °C
20 min 95 °C
15 sec 95 °C
Hold 4 °C

Table 60: Program employed for melting curves.

4.9 Genome expression analysis

The genome expression analysis was outsourced to the group of Prof. Nöthen and based on the HumanHT-12 v4 Expression BeadChip kit (Illumina).
RNA samples were prepared as described under 4.7.1 and 4.7.2. and 200 ng RNA were submitted for analysis. The GenomeStudio V2010.3 Gene Expression Module was used to process the data. Quantile-normalized raw data of the Sample Probe Profile, with a P value < 0.01 in mature neuronal cultures were extracted without background subtraction. The data was further analysed utilising Excel 2011.

4.10 Generation and validation of an isogenic knockout line

4.10.1 CRISPR-Cas9 genome editing

The CRISPR-Cas9 system is an adaptive immune system in bacteria against viruses and plasmids. Clustered regularly interspaced short palindromic repeats (CRISPRs) are short repetitive sequences of host DNA, followed by short sequences of foreign DNA, which are expressed. Next to CRISPR sequences, CRISP-associated (Cas) genes are located. Cas9 contains two nuclease domains, HNH and RuvC-like (Doudna and Charpentier, 2014).
A guide sequence, which binds in a base-pair specific manner to DNA sequences, guides Cas9 to this site where it induces site-specific double strand brakes. By changing the guide sequence, it is possible to induce double strand brakes at virtually any desired position that exhibits a PAM sequence (Doudna and Charpentier, 2014).

The cells were nucleofected with a CRISPR/Cas9 knockout plasmid and a homology-directed repair plasmid carrying a puromycin resistance gene (Santa Cruz).

4.10.2 SM-NP cell nucleofection

Nucleofection is a special form of electroporation with proprietary buffers and pulse protocols and is used to transfect RNA, DNA and proteins into the cell. The nucleofection of cells is achieved by electroporation, which creates small pores in cell membranes.
For nucleofection, 2-3 x 10^6 cells were resuspended in a mixture of 2 µl of DNA (mixture of αB-crystallin HDR Plasmid (h) and αB-crystallin CRISPR/Cas9 KO Plasmid (h)) and 100 µl of nucleofection solution (Lonza). The cell solution was transferred to a cuvette for electroporation. Nucleofector 2b (Lonza) using program B23 was utilised for electroporation. Thereafter, the cell suspension was mixed with SM-NP cells split from two Ø 3.5 cm dishes and plated on new Geltrex™ coated dishes.

4.10.3 Clone selection and identification

After the electroporation of the SM-NP cells, they were cultivated for 2 days until they were almost confluent. Then the selection was initiated by application of puromycin. Selection was stopped when only clonal growing cells were left. The clones were picked and transferred to Geltrex™ coated 96-well plates. The clones were passaged and frozen as backups (see 4.2.4). The clones carrying the knockout were identified via qPCR and Western Blotting.

4.11 Statistical analysis

Quantitative data was acquired at least in biological triplicates and technical duplicates (qPCR and cell viability assays) and at least in biological replicates for the other experiments, (unless stated otherwise). Means and standard error of the mean (SEM) were calculated using Microsoft Excel 2011. GraphPad Prism 6 was utilised for statistical analysis. A student's t-test was performed for two samples. For group analysis, a one-way ANOVA with a post hoc analysis (Tukey´s multiple comparisons test) was performed. Levels of significance are mentioned in table 61.

Levels of significance

Level of significance	Code
> 5 %	Not significant
≤ 5 %	*
≤ 1 %	**
≤ 0.1 %	***
≤ 0.01 %	****

Table 61: Utilised levels of significance.

5 Results

5.1 Human neuronal cultures, their progenitors and tumour cell lines for investigating maturation-dependent anti-apoptotic brakes

The first section of the current study is focused on the generation of neuronal cultures from lt-NES cells, in order to explore anti-apoptotic mechanisms developed by mature neurons as well as to address differences of neural precursor cells and neuronal cultures. The human neuroblastoma line SKNSH was implemented as well in this study, because it was used to explore neuronal disorders like Parkinson's or Alzheimer's disease (Dang et al., 2010; Singsai et al., 2015; Zhang et al., 2017). Cell lines used in this study are shown in Fig. 5.1.

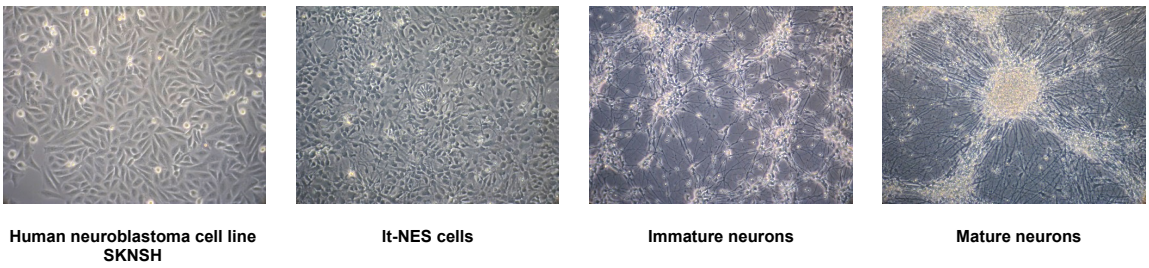

Figure 5.1: Cell lines used to uncover neuronal anti-apoptotic brakes. *The human neuroblastoma cell line SKNSH, lt-NES cells, immature and mature neurons were used to investigate maturation-dependent anti-apoptotic mechanisms.*

5.1.1 Characterisation of SM-NP cells and neuronal cultures to decipher stress adaption and resistance to cell death

Since SM-NP, cells can be split in high ratios and grow clonally (Reinhardt et al., 2013), the cells were kept as SM-NP cells and used to generate lt-NES cells for the experiments when needed. SM-NP cells can be identified by their expression of Pax6, SOX2 and DACH1 in the nucleus and Nestin as intermediate filament (Fig. 5.2b). Lt-NES cells were generated from SM-NP cells by changing their growth conditions using a medium change from SM medium to neural stem cell proliferation medium, containing the two growth factors FGF2, EGF and the supplement B27. Neuronal differentiation then was induced by withdrawal of the growth factors in the cultivation medium with a majority of cells expressing β-III tubulin and MAP2ab (Fig. 5.2c). In addition to the growth factor removal, the cells were treated with DAPT, which inhibits γ-sectretase and thereby Notch signalling. The inhibition of Notch signalling promotes neuronal differentiation (Ben-Shushan, Feldman & Reubinoff, 2015). This treatment aimed at the generation of synchronized neuronal cultures to keep the content of astrocytes as low as possible. The differentiation procedure from SM-NP cells to

lt-NES cells and to human neurons is shown in Fig. 5.2a. Previous studies showed that the precursors have a ventral anterior hindbrain identity and that the majority of neurons obtained from this protocol, display a GABAergic phenotype (Koch et al., 2009; Falk et al., 2012).

In the present study, SKNSH cells, lt-NES cells, immature neurons, differentiated for 1 week and mature neurons, differentiated for 4-9 weeks, were analysed and compared to each other.

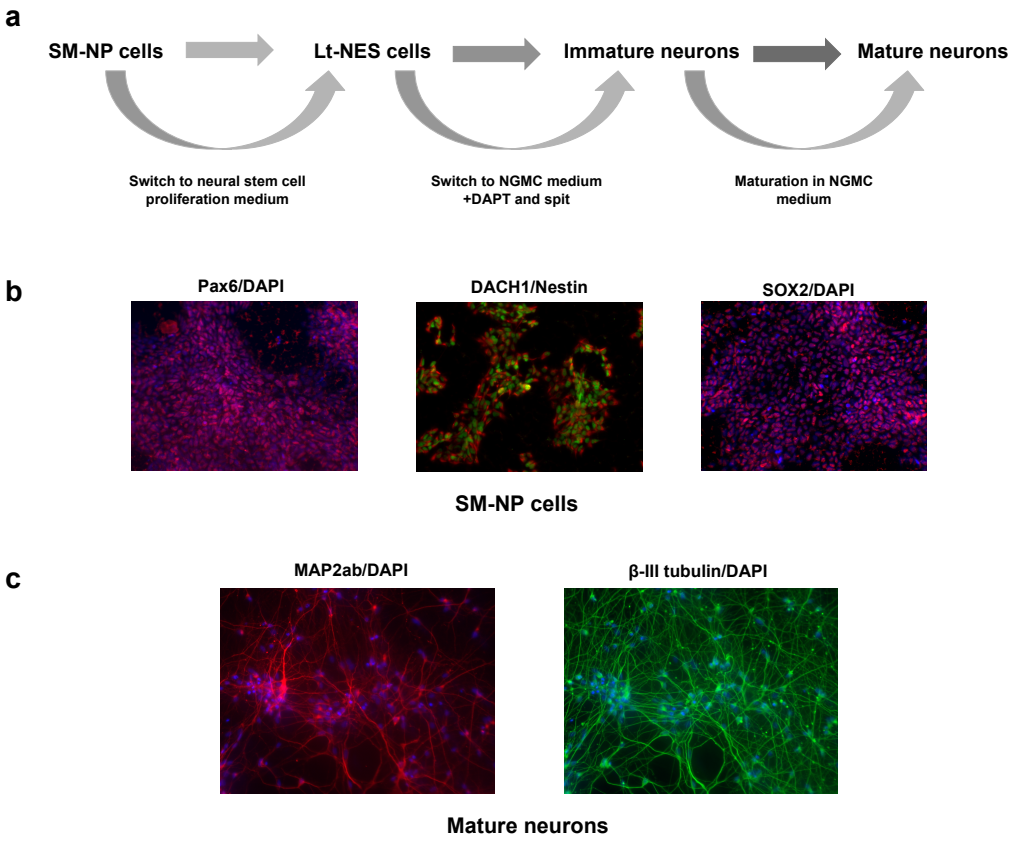

Figure 5.2: Generation and culture of mature neuronal cultures. ***a:*** *Schematic overview showing the differentiation protocol form SM-NP cells to mature neuronal cultures.* ***b:*** *Immunofluorescence staining for Pax6 (red), DACH1(green), Nestin (red) and Sox2 (red) of iPS cell-derived SM-NP cells.* ***c:*** *Immunofluorescence staining of 4 weeks differentiated mature neuronal cultures for the markers Map2ab (red) and β-III (green) tubulin.*

5.2 Increased tolerance to cellular stress in mature human neuronal cultures

Since neurogenesis is limited in the mammalian central nervous system, most neurons have to persist a whole lifetime. So is seems reasonable that they have elaborated maturation-dependent anti-apoptotic strategies, making them less vulnerable towards stress, which is

observed in neurons of rodents (Kole, Annis & Deshmukh, 2013). The first question was whether in vitro generated iPS cell-derived mature human neurons are more resistant to stress than immature neurons. In order to decipher stress tolerance and anti-apoptotic brakes in human mature neuronal cultures, the first step was, to investigate the cell viability of the different cell populations, including SKNSH cells, lt-NES cells, immature and mature neurons, after stress induction. Lt-NES cells, immature and mature neuronal cultures were used to decipher differentiation and maturation-dependent differences between the cultures. SKNSH cells were also used in these experiments to explore their suitability as a model cell line. The different cell populations were exposed to various cellular stressors. The condition of the cells was assessed by cell viability assays. The cellular stressors included Staurosporine as protein kinase inhibitor, Rotenone as inducer of oxidative stress, Tunicamycin and Thapsigargin as ER stressors, MG-132 as proteasome inhibitor and Baf/3-MA as autophagy inhibitors. For all experiments B27 was removed from the culture medium to avoid protection against oxidative stress.

5.2.1 Maturation-dependent alterations regarding stress resistance

Concentrations used were adopted from literature and pretested on SKNSH cells and immature neurons to find an optimal and active working concentration (data not shown). The following experiments were performed to address the impact of these stressors regarding cell viability of the four different cell populations, SKNSH cells, lt-NES cells, immature neurons and mature neurons in a time-dependent manner. To induce stress, the cultures were treated with the stressors Staurosporine (5 nM), Rotenone (5 µM), Thapsigargin (2 µM), Tunicamycin (1.5 µM), Baf/3-MA (15 nM/2 mM) and MG-132 (7.5 µM). The cell viability was assessed by the PrestoBlue® assay every 16 hours over a total period of 48 h. Cultures treated with DMSO 2 µl/ml or with the respective treatment medium, were used as control to which results were normalized. The assay is based on the metabolisation of a dye, which leads to a change of colour that can be measured by a plate reader.

In SKNSH cultures the exposure to cellular stressors resulted in massive reduction in cell viability. Already after 16 h of treatment with Rotenone, MG-132 and Thapsigargin, a significant reduction of cell viability was observed (Fig. 5.3). After 48 hours, the cell viability was strongly reduced in all treated neuroblastoma cultures. The application of Rotenone, MG-132 and Thapsigargin for 48 hours almost led to a complete decay of the SKNSH cultures (Fig. 5.3). Lt-NES cells also displayed severe reduction in metabolically

active cells after stress induction. In this population, the first significant impairments of viability were detected after 16 hours of exposure. At this time point a predominant reaction to Tunicamycin, MG-132, Thapsigargin and Baf/3-MA was observed. At the end of the experiments all applied stressors resulted in a significant reduction of the cell viability of the lt-NES cells. In contrast to the neuroblastoma cells, the lt-NES cells did not react that strong to the induction of oxidative stress and protein kinase stress, but they showed a more pronounced response to autophagy stress than the SKNSH cells. The tolerance of immature neurons to stress was investigated as well. Neurons differentiated for 1 week were affected by stress induction. A drop of cell viability over time was observed (Fig. 5.3, column 3). Significant reductions in cell viability were detectable after 48 hours of exposure to the stressors, with the exception of Baf/3-MA, which led to significant loss of cell viability after 16 hours. No significant reductions at all were detected for 4 weeks differentiated neurons. As well as for the 9 week differentiated neuronal cultures only minor alterations were observed, but importantly for both mature cultures no significant reductions in cell viability were detected after 48 hours of treatment (Fig. 5.3, column 4 and 5). Together the results pointed out that mature neurons were less vulnerable to stress induction compared to the other cell populations.

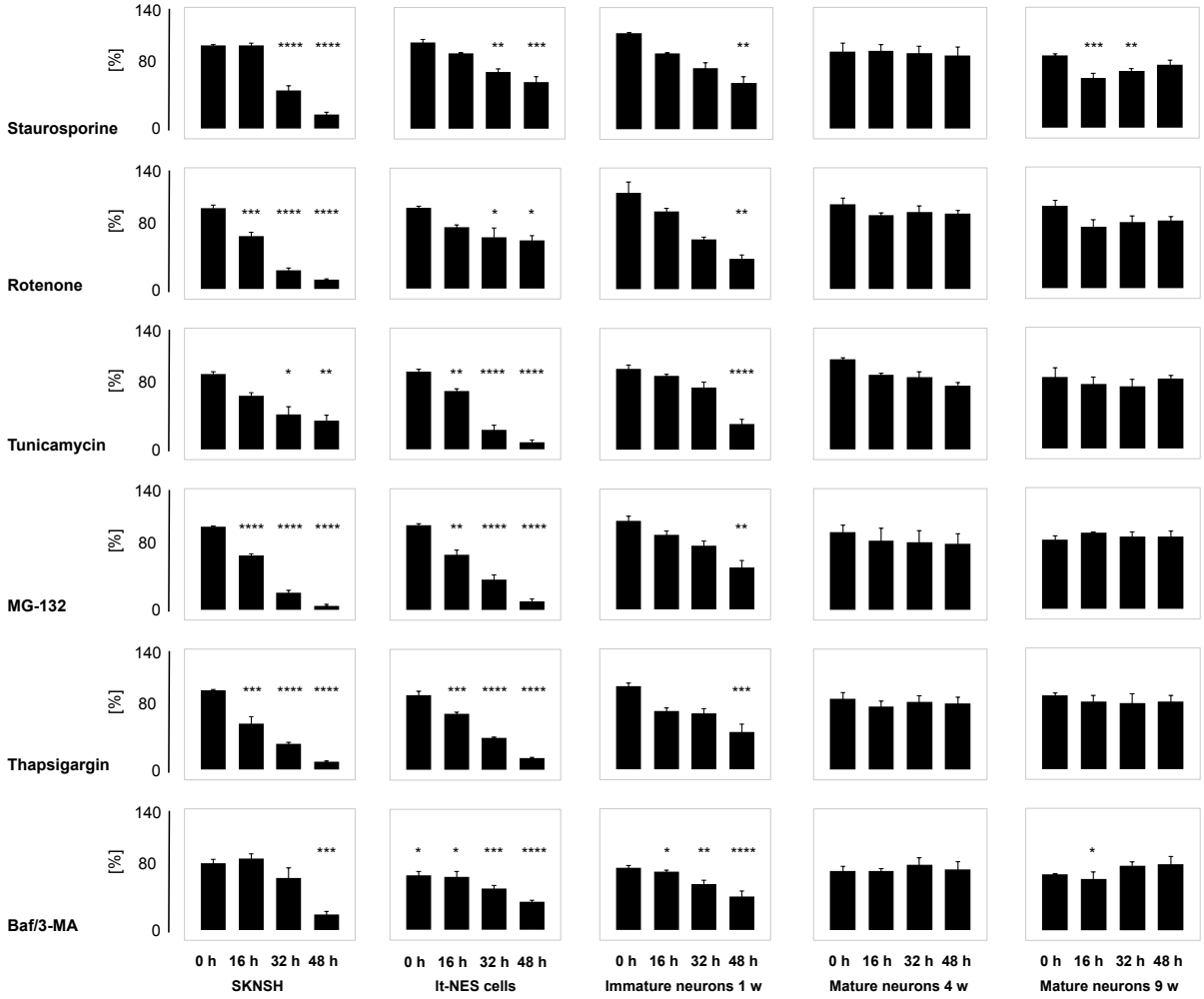

Figure 5.3: The cellular stressors used in the present study have no impact on the cell viability in mature human neuronal cultures, assessed by PrestoBlue® assay. *SKNSH cells, lt-NES cells, immature neurons and mature neurons, differentiated for 4 or 9 weeks were exposed to the cellular stressors Staurosporine, Rotenone, Tunicamycin. MG-132, Thapsigargin and Baf/3-MA over a time period of 48 hours. Results were normalized to the respective controls. The cell viability was investigated every 16 hours via PrestoBlue® assay. In contrast to the other cell populations no decrease in cell viability after 48 hours can be detected in mature neuronal cultures. Bar graphs display mean ± SEM; (n=3) (*p < 0.05; **p < 0.01; ***p < 0.001; ****p < 0.0001). The controls are not depicted.*

In addition to the PrestoBlue® assays, CellTiter-Glo® assays were performed to confirm the viability results of the respective cultures. In contrast to the PrestoBlue® assay, the CellTiter-Glo® assay is not based on the digestion of a dye by metabolically active cells, but on the content of ATP in the cultures. The assays performed with CellTiter-Glo® showed comparable results (Fig. 5.4).

The application of every stressor resulted in a massive reduction of cell viability in neuroblastoma cultures. The strongest effects were detected after 48 hours of exposure to MG-132 and Thapsigargin. Also the cell viability of lt-NES cultures was strongly reduced

after stress induction. The application of some stressors, like Baf/3-MA, Thapsigargin and MG-132, had the same outcome as in SKNSH cultures. Others, like Staurosporine and Rotenone were less effective in lt-NES cultures compared to the neuroblastoma cultures. The exposure to Tunicamycin led to a higher decrease in cell viability compared to SKNSH cells. Immature neurons as well displayed significant reductions in cell viability after treatment with the cellular stressors. The loss of viable cells in immature neuronal cultures was significant after 48 hours but not as strong as in cultures of neuroblastoma cells and lt-NES cells (Fig. 5.4, column 3).

In contrast to the other three populations, the cell viability of the mature neuronal cultures was not influenced by stress induction over a time period of 48 hours. One exception was the result obtained after the application of Staurosporine for 48 hours in 4 weeks differentiated cultures (Fig. 5.4).

In summary, the results pointed out that the cell viability of SKNSH cells, lt-NES cells and immature neurons was massively affected after stress induction, whereas mature neuronal cultures showed no or non-significant effects.

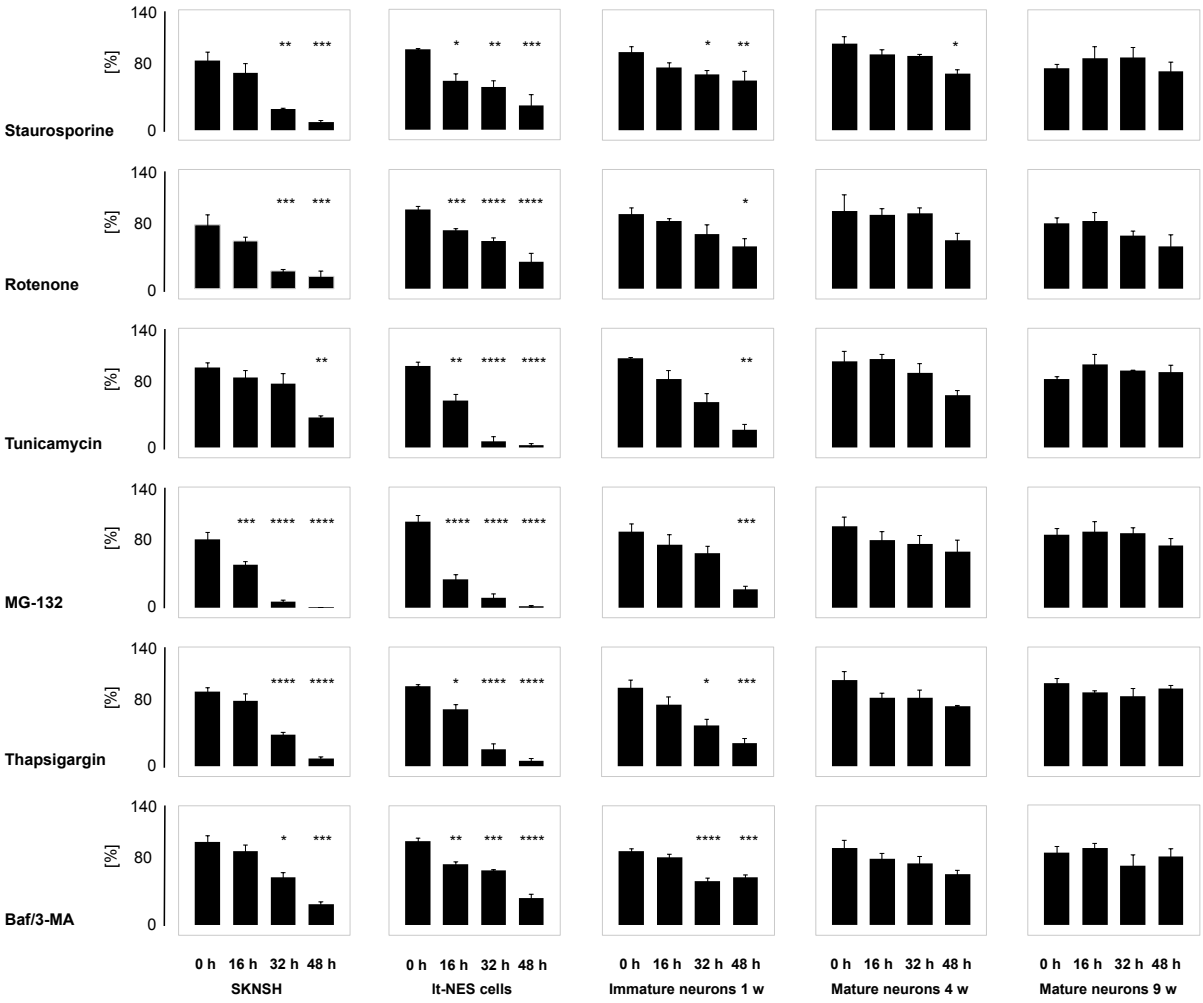

Figure 5.4: The cellular stressors used in the present study have no impact on the cell viability in mature human neuronal cultures, assessed by CellTiter-Glo® assay. *For 48 hours the cell populations, SKNSH cells, lt-NES cells, immature and mature neurons (4 and 9 weeks differentiated), were treated with the stressors Staurosporine, Rotenone, Tunicamycin, MG-132, Thapsigargin and Baf/3-MA. The CellTiter-Glo® assay was utilised to determine the cells' viability. The viability was monitored every 16 hours. Results were normalized to the respective controls. In mature neuronal cultures no significant alterations regarding viability can be observed after 48 hours of exposure, whereas the other populations are strongly affected. Bar graphs display mean ± SEM; (n=3) (*p < 0.05; **p < 0.01; ***p < 0.001; ****p < 0.0001). The controls are not shown.*

In order to verify that those findings were independent of the used cell line, the cell viability experiments were also preformed on human primary stem cell-derived immature and mature neuronal cultures.

Human primary stem cell-derived immature neuronal cultures displayed significant alterations in cell viability after exposure to all stressors used when investigated by PrestoBlue® assay and identical conditions used above. The decrease in viability in the immature primary stem cell-derived neuronal cultures was comparable to the reduction observed in the iPS cell-derived immature neuronal cultures (Fig. 5.5). For the mature

neuronal cultures derived from a primary line no significant reductions regarding cell viability were detected after the application of the stressors for 48 hours, with the exception of Baf/3-MA.

In conclusion, these results showed that mature neuronal stress resistance was also reproducible in other neuronal cultures derived directly from a human embryo with a different genetic background (Fig. 5.5). Summarising, the results pointed out that stress induction had no impact on the viability of mature neuronal cultures, whereas the other cell populations were strongly affected (Fig. 5.3, 5.4 and 5.5).

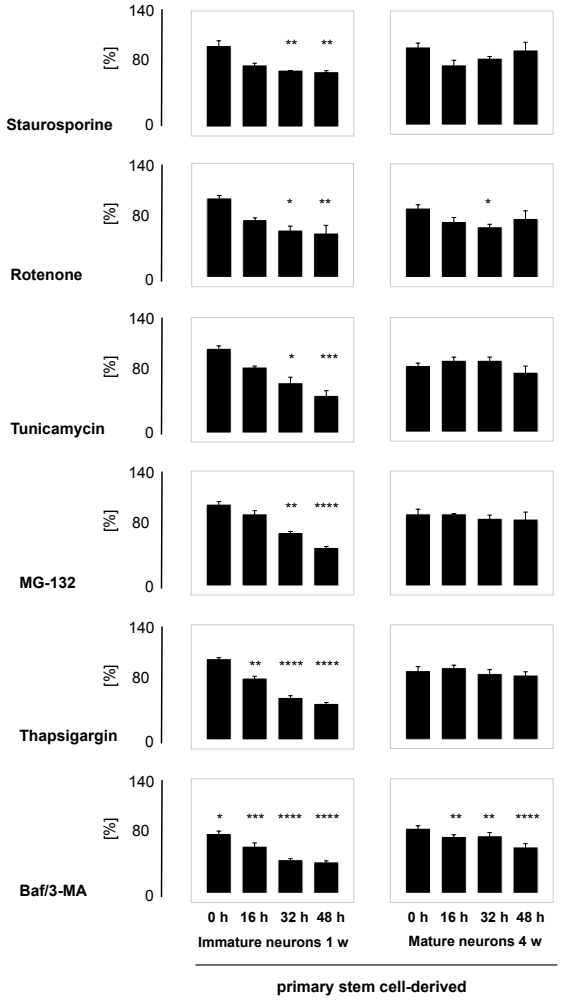

Figure 5.5: The stress resistance of iPS cell-derived mature neurons is reproducible in primary stem cell-derived neurons. *Primary stem cell-derived immature and mature neuronal cultures were treated with the same stressors for 48 hours as the cultures in the previous experiments. The obtained results were normalized to the respective controls. The cell viability was investigated via PrestoBlue® assay every 16 hours. iPS cell-derived and primary stem cell-derived mature neuronal cultures are less vulnerable to stress induction than their immature counterparts. Bar graphs show mean ± SEM; (n=3) (*p < 0.05; **p < 0.01; ***p < 0.001; ****p < 0.0001). The controls are not depicted.*

5.2.2 Alterations of caspase3 and its downstream targets after stress induction in mature neuronal cultures

Caspase3 is an effector caspase. Under apoptotic conditions the inactive proenzyme is cleaved by one of the initiator caspases such as caspase9, resulting in a large subunit, containing the active site and a small subunit (Clarke & Tyler, 2009). Upon activation, cleaved caspase3 cleaves its downstream targets like PARP or the scaffold protein α-fodrin (Porter and Jänicke, 1999; Chaitanya, Alexander & Babu, 2010). The cell viability assays revealed differences between mature neurons and the other cell populations regarding stress resistance. The loss of cell viability indicated that some cells in the culture underwent apoptosis.

To test for apoptosis, protein levels of caspase3 or cleaved caspase3 and poly (ADP-ribose) polymerase (PARP) are commonly analysed. Because of the strong reduction of cell viability that was observed in cultures of SKNSH cells, lt-NES cells and immature neurons, additional experiments were performed to identify whether the decreased cell viability is due to caspase3 activation. To determine, whether there were differences in apoptosis induction between SKNSH cells, lt-NES cells, immature and mature neuronal cultures, the protein amount of cleaved PARP (cPARP) and caspase3 was investigated via Western blot analysis. cPARP was detected for all applied stressors in SKNSH cultures (Fig. 5.6a). The highest protein levels were obtained after the exposure to Staurosporine and MG-132. For the DMSO control no cPARP was detected. In the lt-NES cell samples for all conditions cPARP was detectable. Most intense bands were observed following treatment with MG-132 and Tunicamycin. The blots of immature neuronal cultures displayed no cleaved PARP, also no cPARP protein was observed in blots of mature neurons (Fig. 5.6c,d). The absolute protein levels of the effector caspase3 were comparable in all cell lines under control conditions.

In summary, the results indicated that the decrease in cell viability is due to activation of caspase3 and apoptosis. The results also revealed that apoptosis in neuroblastoma and in neural precursor cells was observable as early as 16 hours of treatment. These results were in line with the results of the cell viability experiments as the SKNSH and lt-NES cultures showed a reduction in cell viability already at early time points, whereas neurons displayed no or only slight reductions of cell viability at early time points (16 hours).

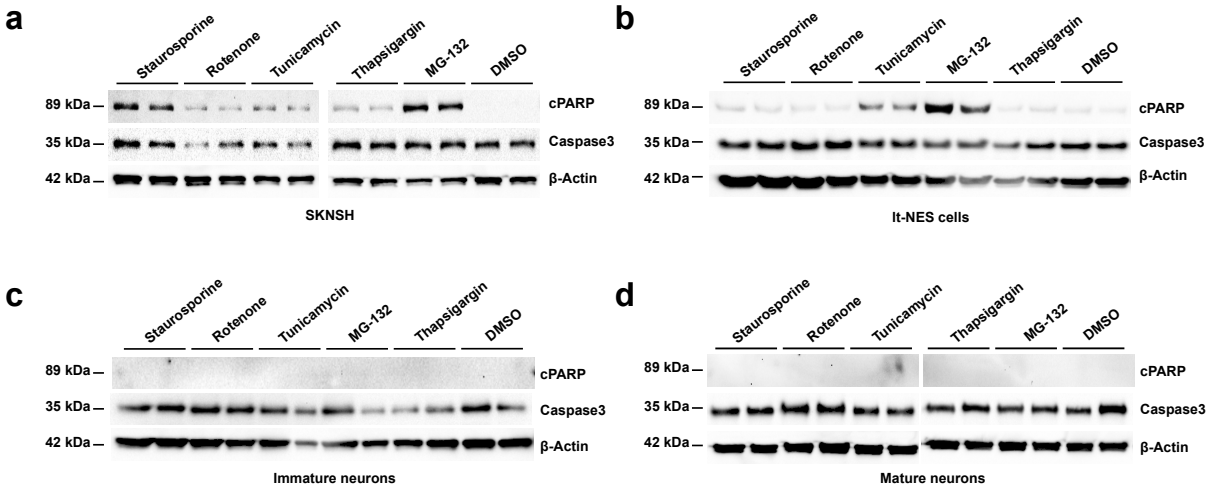

Figure 5.6: PARP cleavage indicated activation of apoptosis in stressor-treated cultures. ***a:*** *SKNSH cells (n=1),* ***b:*** *lt-NES cells (n=1),* ***c:*** *immature (n=1) and* ***d:*** *mature neurons (9 weeks differentiated) (n=2) were treated with Staurosporine, Rotenone, Tunicamycin, MG-132 and Thapsigargin for 16 h. Depicted are technical duplicates. The Western blot analysis shows cleavage products of PARP in SKNSH and lt-NES cultures, but not in immature and mature neuronal cultures, suggesting a lack of caspase3 activation in neuronal cultures.*

In order to validate activation of caspase3 on cellular level, immunocytochemical analysis was performed. Figure 5.7 shows that in SKNSH cultures, treated with Staurosporine and MG-132, for 16 hours, the number of cleaved caspase3 positive cells, compared to the control and to the other stressors, is increased. Additionally, the cell density in the cultures exposed to Rotenone and MG-132 was reduced, indicating dead cells that detached from the dish before staining. In lt-NES cultures elevated numbers of cleaved caspase3 positive cells were visible after treatment with all stressors (Fig. 5.7). Immature neuronal cultures showed slightly increased numbers of cleaved caspase3 positive cells after the application of MG-132 and Thapsigargin. The treatment with Baf/3-MA resulted in even higher numbers of cleaved caspase3 positive cells. In contrast to the other cell populations, after stress induction, in mature neuronal cultures no increase of cleaved caspase3 positive cells, compared to the control was observable.

Furthermore and as depicted in Figure 5.7b, treatment with Rotenone led to β-III tubulin disruption in immature neurons, visible by the dotted staining of their processes. For mature neurons such effects were not observed. In summary, results from cleaved caspase3 stainings were in line with the cell viability assay results and the results of the Western blot analysis and confirmed an increased stress resistance and the decrease of caspase3 activation in maturing neuronal cultures.

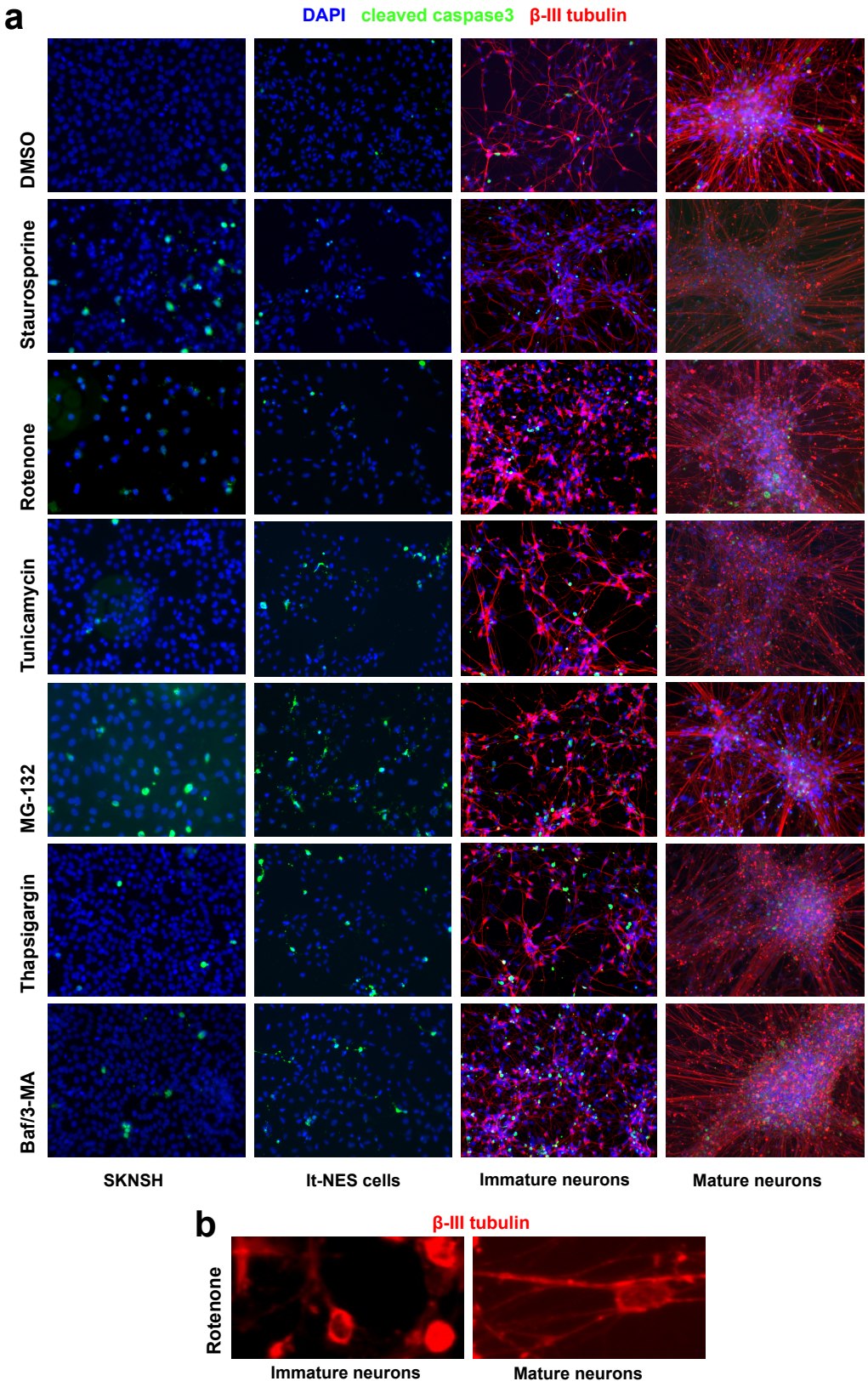

Figure 5.7: Increased numbers of cleaved caspase3 positive cells in all populations except for mature neuronal cultures. ***a:*** *Immunocytochemical analysis of cleaved caspase3 in SKNSH, lt-NES cells, immature and mature neurons under normal and stress conditions. (n=1)* ***b:*** *Investigation of immature and mature neurons reveals disruption of βIII tubulin in immature neurons under redox stress (n=1).*

5.3 Downregulation of caspase9 in mature neuronal cultures

Caspase9 is an initiator caspase of apoptosis. Upon release of cytochrome c from the mitochondria, caspase9 together with Apaf-1 and cytochrome c forms the apoptosome. Autocatalytical cleavage of caspase9 leads to the induction of the caspase-cascade, which results in cell death (Park, 2012). Since the caspase-cascade is important for the induction of apoptosis, the status of caspase9 was investigated in the different cell populations.

In order to test for differences in protein levels of caspase9 between immature and mature cultures and the other cell populations, Western blots were analysed for caspase9. As suggested by bands visible for a blot against caspase9, the caspase9 protein levels of immature and mature neurons were lower than in lt-NES and neuroblastoma cells (Fig. 5.8a). Additionally, Figure 5.8b suggested that the reduction of caspase9 on protein level seemed to be dependent on maturation time, since a continuous reduction was observable over a time when investigated between 1 to 4 weeks of maturation. To test whether the observed maturation-dependent differences were significant, Western blots comparing immature and mature neurons were performed. The Western Blots indicated that caspase9 levels of immature neurons were significantly higher than caspase9 levels of mature neurons as, seen in Figure 5.8c,d. Taken together, these results suggested that caspase9 was downregulated during the time course of maturation.

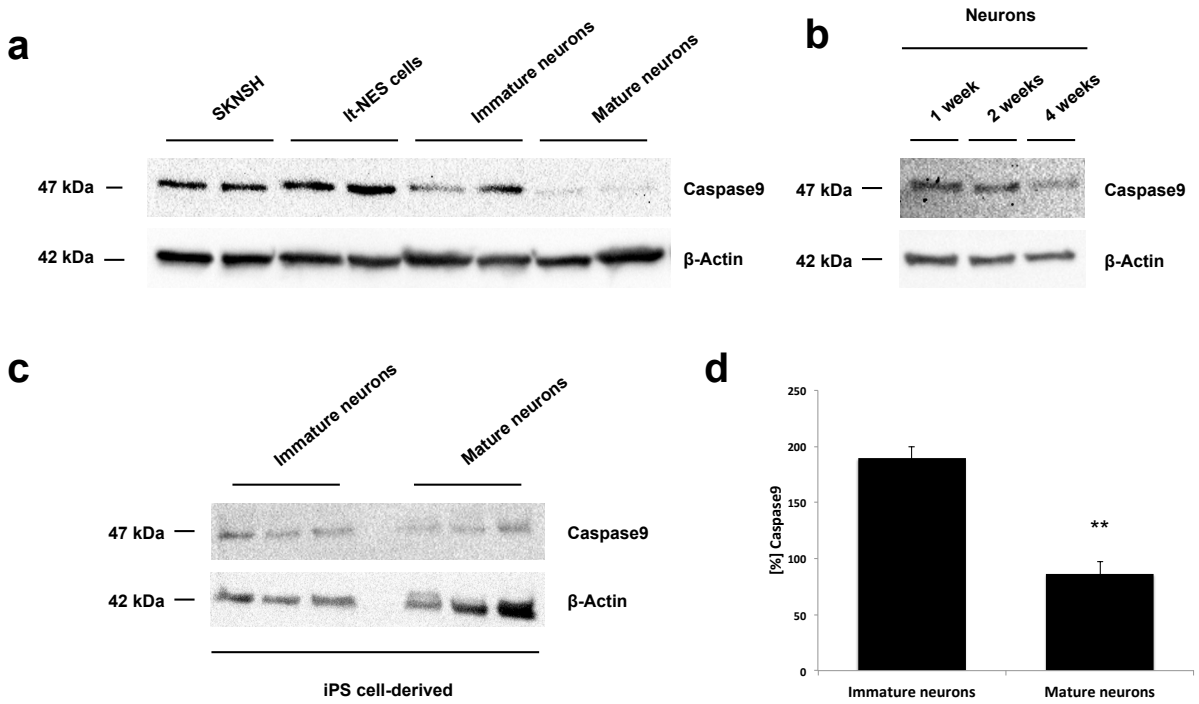

Figure 5.8: Caspase9 is differentially regulated in iPS cell-derived immature and mature neuronal cultures. ***a:*** *Caspase9 Western Blot of SKNSH cells, lt-NES cells, immature and mature neurons, showing reduced Caspase9 levels in mature neurons under normal conditions (n=1). Depicted are technical duplicates* ***b:*** *Caspase9 is downregulated in neuronal cultures over a time period of 4 weeks (n=1).* ***c:*** *In iPS cell-derived mature neurons caspase9 is decreased compared to immature neurons. Depicted are biological triplicates. Mature neurons were differentiated for 6 weeks, 6 weeks and 5 weeks.* ***d:*** *The diagram shows the amount of caspase9 in iPS cell-derived immature and mature cultures, pointing out significant differences. Bar graphs show mean ± SEM; (n=3) (**p < 0.01).*

5.4 Gene expression analysis revealed differential expression profiles in immature and mature neuronal cultures under normal conditions

The previous results indicated that neurons increase their resistance towards cellular stress induction during maturation, which was in line with the decreased activation of caspase3 and cleavage of its downstream targets observed in the chapters before. In order to shed light on a prospective mechanism for the maturity-dependent stress resistance, comparative gene expression analysis was performed. RNA samples of immature and mature neurons were used to investigate the gene expression. The results were processed using GenomeStudio V2010.3 Gene Expression Module and Excel 2011.

As depicted in Figure 5.9a, many genes were differentially expressed in immature and mature neuronal cultures by default. The most interesting group of genes were those upregulated in mature neurons compared to immature neurons (under control conditions), as

it was suggested, that protective proteins were elevated in mature neuronal cultures. Figure 5.9b displayed the 6 highest upregulated genes in mature neurons: I) αB-crystallin (Cryab) was massively upregulated in mature neurons. It is a small heat shock protein (sHSP) with known anti-apoptotic properties (Kamradt, Chen & Cryns, 2001). II) Spock2 encodes a proteoglycan of unknown function, but it is suspected to be part of a specialised extracellular matrix (ECM) of the brain (Marr et al., 2000). III) Another gene associated with the ECM is Sparkl1, a non-structural component of the ECM, which is involved in the regulation of cell migration and differentiation (Lloyd-Burton & Roskams, 2012). IV) CD44, a transmembrane receptor for hyaluronan that among others regulates signal transduction and synaptic plasticity (Roszkowska et al., 2016). V) C1orf61 is a gene, which was also upregulated in mature neurons and suggested to be involved in development and remodelling of neurons as a signalling molecule (Jeffrey et al., 2000). VI) GABBR2 encodes for a subunit of the $GABA_B$ receptor, which mirrors the GABAergic phenotype of the neurons (Freyd et al., 2017). To summarise, the top 6 upregulated were associated with the phenotype of the neurons, were suspected to have protective effects, or were associated with the ECM. The results indicated, that there were protective genes elevated in mature neuronal cultures, but that further investigation of the results is needed to uncover possible protective mechanisms. It is also important to note that also a minor fraction of astrocytes (Mertens, 2012; Poppe, 2015) which occur during the differentiation process, were present in mature cultures and that the elevated expression of the genes has to be validated on a cellular resolution level.

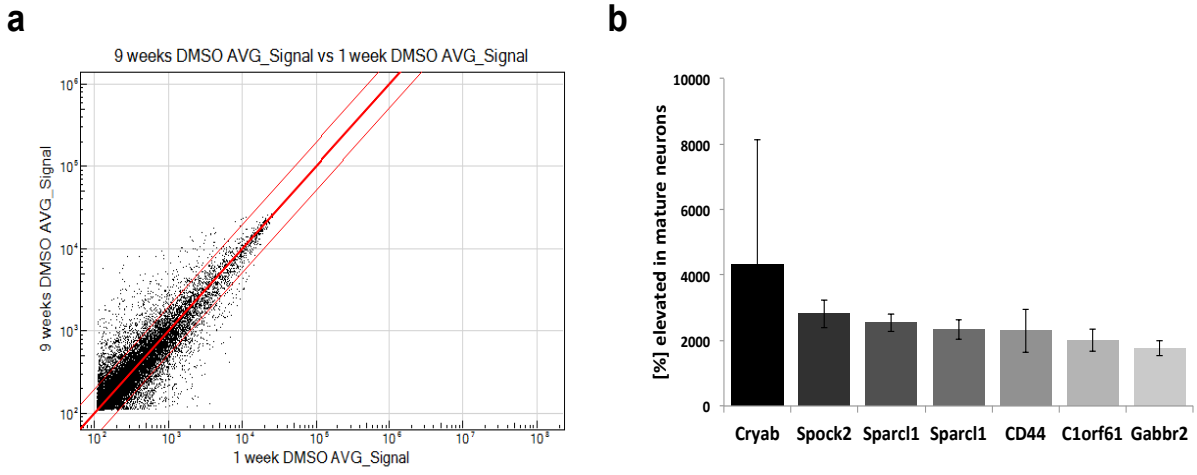

Figure 5.9: Differentially expressed genes in immature and mature neurons. ***a:*** *Scatter plot of neurons, differentiated for 1 week and 9 weeks, shows a lot of differentially expressed genes in the two populations.* ***b:*** *The diagram displays the 6 highest upregulated genes in mature neuronal cultures. Bar graphs show mean ± SEM.*

5.5 Increased activity of the AKT-pathway in mature neurons

The AKT-pathway is one of the major survival pathways within the cell. It promotes growth and cell survival upon extracellular stimulations. Here the binding of extracellular ligands to receptor tyrosine kinases (RTKs) causes activation of the receptor by autophosphorylation, and this generates binding sites for Src-homology 2 (SH2)-domain containing proteins like phosphatidylinositol 3-kinase (PI3K) (Hoeben et al., 2004; Heldin, 1995; Hale et al., 2008). Activated PI3K then generates the second messengers phosphatidylinositol(3,4,5)-trisphosphate (PIP_3) and phosphatidylinositol(3,4)-bisphosphate (PIP_2), which are anchored in the plasma membrane (Vanhaesebroeck & Waterfield, 1999; Franke et al., 1997). The serine/threonine kinase AKT is binding to the second messenger, resulting in conformational changes and exposure of Thr308 and Ser473, whose phosphorylation is required for full activation of AKT, (Lawlor & Alessi, 2001; Osaki, Oshimura & Ito, 2004). The cell survival is then achieved by the phosphorylation of AKT downstream targets (Cardone et al., 1998; Brunet et al., 1999; Downward, 1999; Kim et al., 2001). As the AKT-pathway has an important role with respect to cell survival, its activity was investigated in the different cell populations.

5.5.1 Protective proteins that stimulate the AKT-pathway and protective proteins regulated by the AKT-pathway are upregulated in mature neuronal cultures

The comparative gene expression data was used to generate further insight into the increased stress resistance of mature neurons. Of interest was, if protective proteins are upregulated in mature neuronal cultures and if some of them might belong to one cell survival pathway. The further investigation of the gene expression results and literature search revealed, that some of the most dominantly upregulated genes in mature neuronal cultures compared to immature neuronal cultures under normal conditions have previously reported neuroprotective roles and that these candidate genes converge into the AKT-pathway.

Three of these upregulated genes activate the AKT-pathway, namely VEGFB, Rab31 and p62. p62 prolongs the phosphorylation of AKT and plays an important role in autophagy (Heo et al., 2009; Joung, Kim & Kwon, 2005; Rusten & Stenmark, 2010). Vascular endothelial growth factor B (VEGFB) also activates the AKT-pathway and has positive effects on neuronal survival and neurogenesis in mice (Poesen et al., 2008; Sun et al., 2004; Sun et al., 2006). Protection by Rab31 is achieved by increasing AKT phosphorylation and the thereby gained upregulation of the Bcl-2/Bax ratio (Sui, Zheng & Zhao, 2015; Pan et al.,

2016). Additionally, autophagy is inhibited when Rab31 is downregulated (Liu et al., 2015). Three other genes identified as elevated in mature neuronal cultures are regulated by the AKT-pathway. The modulatory subunit of the glutamate-cysteine ligase (GCLM) is involved in the synthesis of glutathione; its overexpression in drosophila can extent their lifespan to more than 24% (Orr et al., 2005; Huang et al., 2013). Sulfiredoxin (SRXN1) is protective against oxidative stress (Wu et al., 2017; Kim et al., 2016). Secretogranin II (SCG2) counteracts nitric oxide (NO) toxicity, it is protective during oxygen and glucose deprivation and induces the expression of anti-apoptotic Bcl-2 (Li, Hung & Porter, 2008; Shyu et al., 2008). The increased expression of those candidate genes was validated by quantitative real time PCR (qPCR) analysis (Fig. 5.10a, with exception of non detectable SRXN1 in immature neuronal cultures). Figure 5.10b shows how the identified genes interact with AKT.

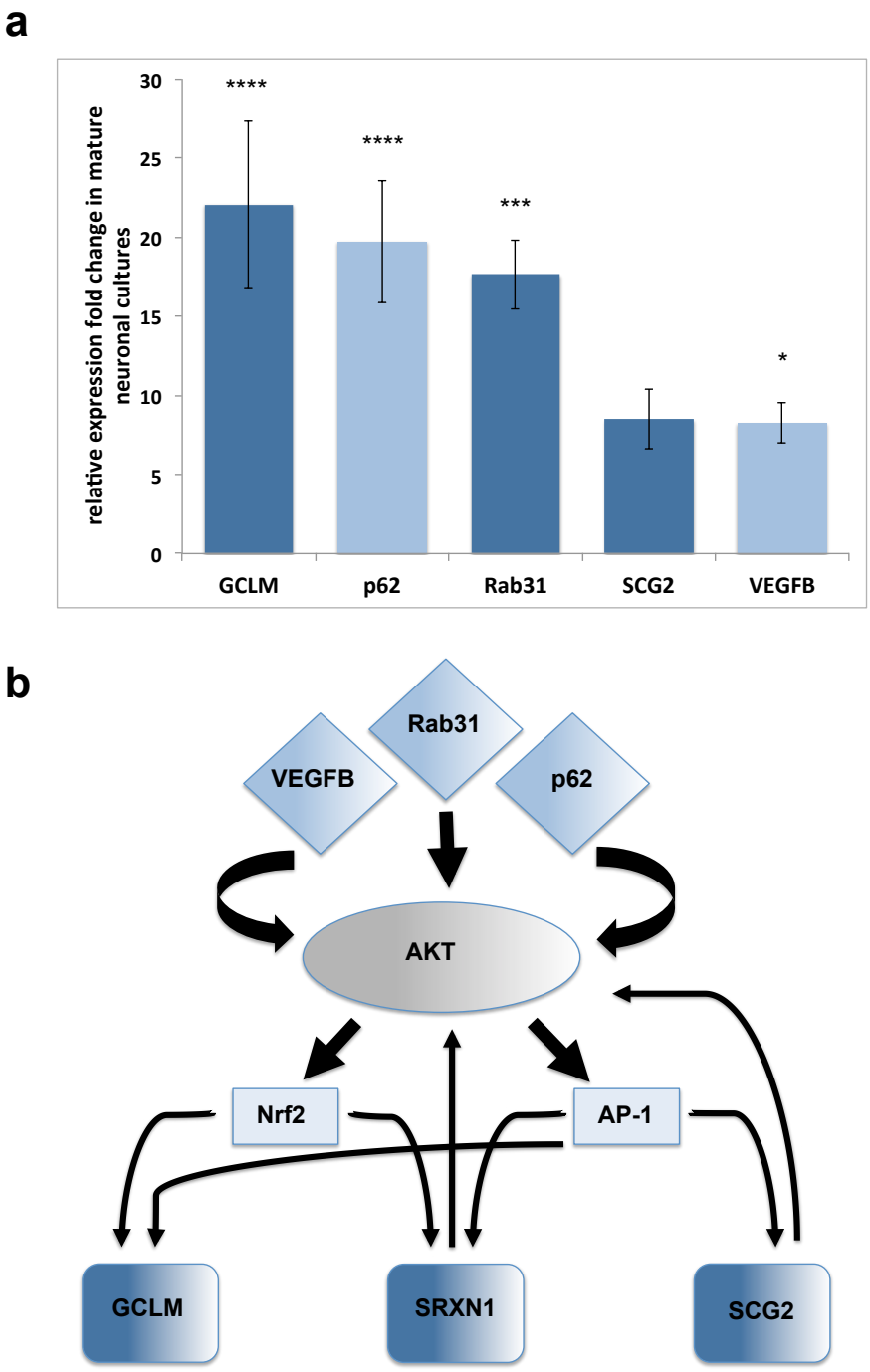

Figure 5.10: Neuroprotective genes converging into the AKT-pathway are upregulated in mature neurons. ***a:*** *The comparative gene expression analysis of immature and mature neurons identifies multiple candidates upregulated in mature neurons with a described neuroprotective role. Interestingly, several of these genes converge into the AKT signaling pathway, they are validated by quantitative real-time PCR. qPCR acknowledges the significant upregulation of protective genes in mature neurons compared to immature neurons. Bar graphs show mean ± SEM; n=3 (*p < 0.05; **p < 0.01; ***p < 0.001; ****p < 0.0001).* ***b:*** *Schematic representation of how these genes converge into the AKT signaling pathway.*

5.5.2 Elevated AKT activity in mature neuronal cultures

The results of the expression analysis and its validation via qPCR, indicated that the AKT-pathway is more active in mature neuronal cultures under control conditions, than in immature neuronal cultures. To explore, whether the AKT-pathway is more active in mature neurons, the activity of AKT was assessed by Western blot analysis of AKT and AKT, phosphorylated at Ser473 (pAKT) – representing the activated form. The other cell populations were also analysed regarding the activity of the AKT-pathway to explore the differences between the populations in activating protective pathways.

Figure 5.11a displayed the different levels of pAKT in SKNSH cells, lt-NES cells and immature and mature neuronal cultures. The observed phosphorylation levels of AKT were low in SKNSH cells (Fig 5.11a). For lt-NES cells and immature neurons higher amounts of pAKT were found, but the highest levels were detected in mature neurons. The phosphorylation level of AKT in neurons increased with time of maturation (Fig.5.11b), from lower levels at 1 week of differentiation, to higher levels after 4 weeks of differentiation. Further analysis of the AKT-pathway revealed, that the amount of active, phosphorylated AKT was significantly higher in mature neuronal cultures compared to immature neuronal cultures (Fig. 5.11c,d). Elevated protein levels of pAKT were also present in primary stem cell-derived mature neuronal cultures (Fig. 5.11e). In summary, the results indicated, that the AKT-pathway was more active in mature neurons than in immature neurons, which seemed to be dependent on maturation-time. Proteins upstream of AKT like p62, Rab31 and VEGFB stimulating the activation, which were upregulated in mature neurons, may have caused the elevated protein levels of pAKT. The results also indicated that the AKT-pathway in the neuroblastoma cells is hardly active.

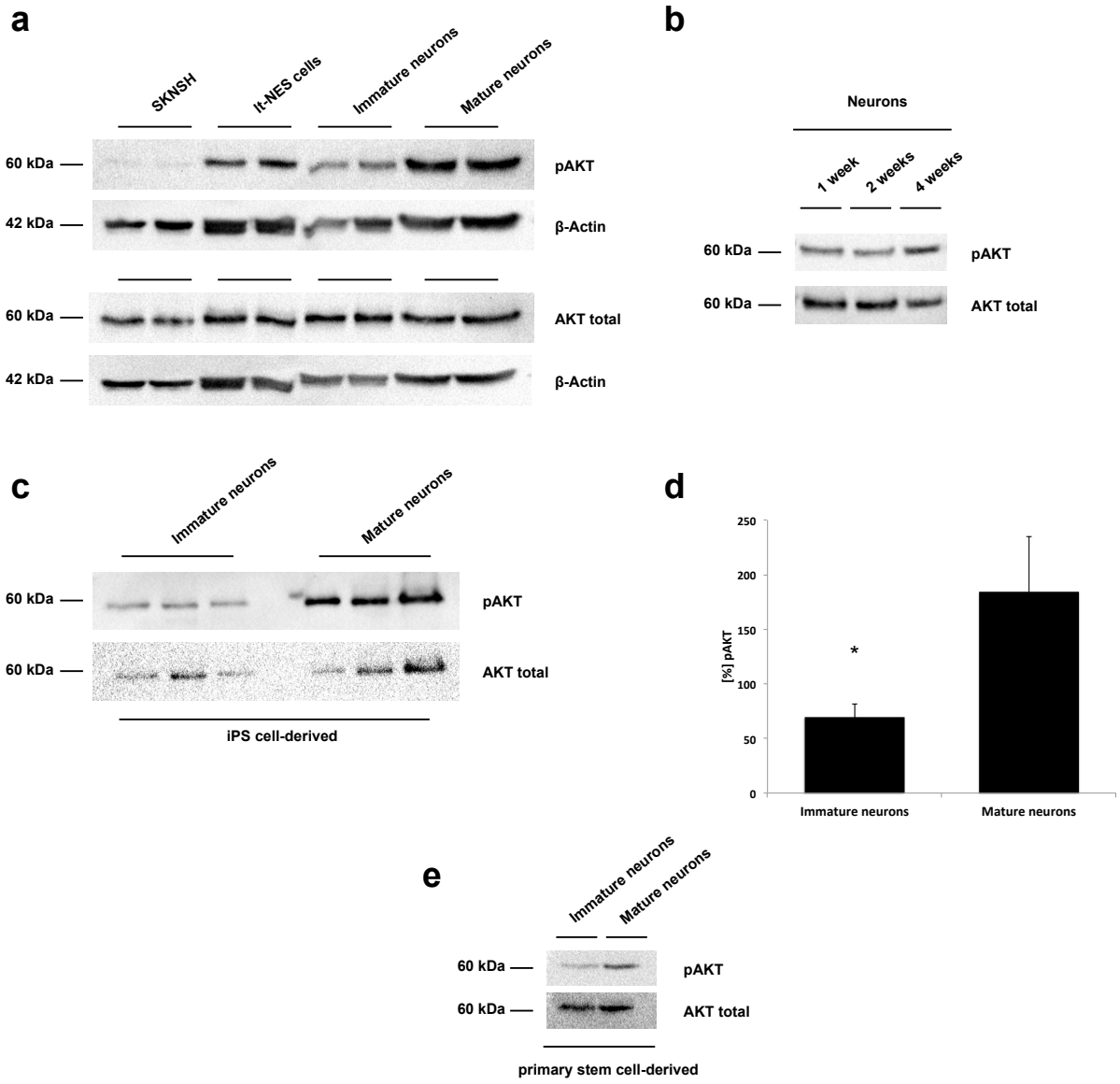

Figure 5.11: Elevated activity of the AKT-pathway in mature neurons. ***a:*** *The Western blot analysis of phosphorylated, active AKT (pAKT) and total AKT on SKNSH cells, lt-NES cells, immature and mature neuronal cultures shows elevated levels of pAKT in mature neuronal cultures. Depicted are technical duplicates (n=2).* ***b:*** *pAKT is increased when neurons mature (n=3).* ***c:*** *The protein levels of activated AKT are much lower in immature cultures compared to their mature counterparts. Depicted are biological triplicates. Mature neurons were differentiated for 5 weeks, 4 weeks and 5 weeks.* ***d:*** *The quantity of pAKT compared to total AKT in immature and mature neurons. The diagram shows mean ± SEM; n=3 (*p < 0.05).* ***e:*** *Increased activity of the AKT-pathway in primary stem cell-derived mature neurons. Mature neurons were differentiated for 4 weeks (n=3).*

5.6 The common heat shock response is attenuated in mature neuronal cultures but the small heat shock protein Cryab might compensate it

The heat shock response in neurons is attenuated (Marcuccilli et al., 1996). Reduced levels of SIRT1 promote the neuronal differentiation and the alleviated heat shock response (Liu et al., 2014; Westerheide et al., 2009). We tested, if these observations could be transferred to our cultures, because downregulation of the heat shock response is thought to result in a higher susceptibility for stress and age-related neurodegenerative diseases (San Gil et al., 2017; Marcuccilli et al., 1996)

To investigate the levels of the prominent heat shock protein, HSP70, Western blot analysis of HSP70 on SKNSH cells, lt-NES cells immature and mature neurons, was performed under control conditions and MG-132 treatment, which was shown, to induce a heat shock response (Westerheide et al., 2009). As depicted in Figure 5.12a, the amount of HSP70 under control conditions was relatively low in lt-NES cell cultures and immature and mature neurons, but elevated in neuroblastoma cultures. The application of MG-132 led to a strong upregulation of HSP70 in all cultures, despite the mature neuronal cultures. Highest levels were observed in the SKNSH cultures. Protein levels of the small heat shock protein (sHSP), HSP27 were analysed as well. HSP27 levels under control conditions were most prominent in neuroblastoma cultures, while the other cell lines analysed showed lower levels of HSP27. Stress induction resulted in a minor upregulation of HSP27 in all populations (Fig. 5.12b). Analysis of the comparative gene expression analysis revealed, that also the amount of SIRT1 was decreased in mature neuronal cultures, compared to their immature counterparts (Fig. 5.12c). The gene expression analysis also indicated, that another sHSP, Cryab, was increased in mature neuronal cultures compared to immature neuronal cultures under normal conditions. Stress induction led to an upregulation of Cryab in immature and mature neuronal cultures, whereas the amount of Cryab after the upregulation in immature neuronal cultures was still lower than in mature cultures under control conditions (Fig. 5.12d). The results of the gene expression analysis for Cryab were also confirmed by qPCR (data not shown). The protein levels of Cryab were elevated under normal and stress conditions in mature neuronal cultures when compared to the other cell populations, which displayed low levels of Cryab (Fig. 5.12e). The protein levels of HSP27 and Cryab were also analysed for primary stem cell-derived immature and mature neuronal cultures. The protein levels of HSP27 were reduced in mature neurons compared to immature neurons (Fig. 5.12f). The elevated levels of Cryab in mature neuronal cultures under control and

stress conditions were also detectable in primary stem cell-derived cultures (Fig. 5.12g). In summary, the results displayed a common attenuated heat shock response in mature neurons, together with a massive upregulation of the sHSP Cryab, which might compensate for the alleviated response of HSP70. However, a strong common heat shock response was observed for the SKNSH cells, lt-NES cells and immature neurons, while Cryab was only slightly increased in these cultures after induction.

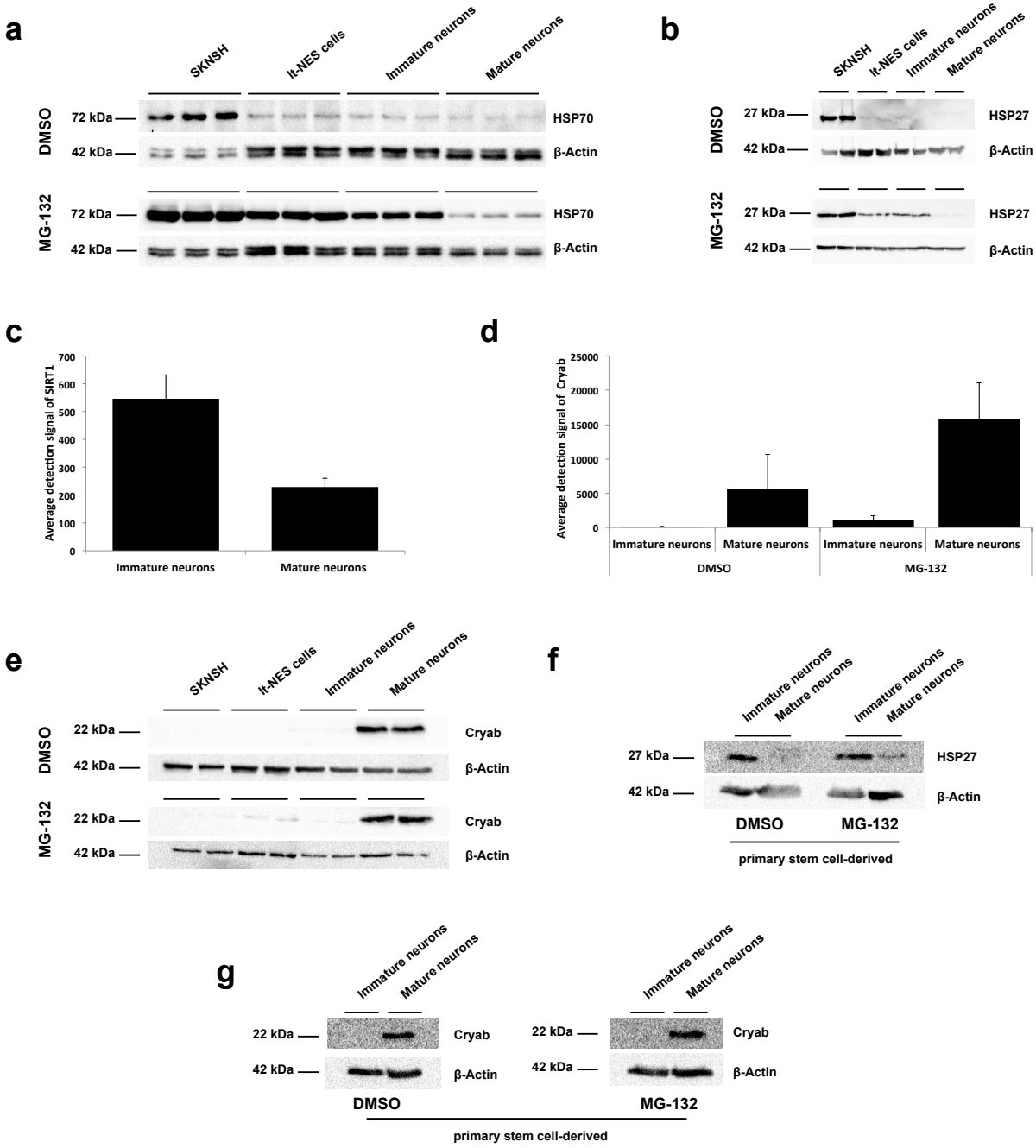

Figure 5.12: The common heat shock response of mature neurons is downregulated, but a small heat shock protein, Cryab is increased. ***a, b and e:*** *Western blot analysis on SKNSH cells, lt-NES cells, immature and mature neurons. Depicted are technical triplicates/duplicates.* ***f and g:*** *Western blot analysis on primary stem cell-derived neuronal cultures. Mature neurons were differentiated for 4 weeks.* ***a.*** *The protein levels of HSP70 under normal and under stress conditions are low in mature neuronal cultures (n=3).* ***b:*** *Slight increase of HSP27 in all cell cultures under stress conditions (n=3).* ***c:*** *The gene expression analysis reveals a decrease of SIRT1 in mature neurons (n=3).* ***d:*** *The gene expression analysis uncovers the upregulation of Cryab in mature neuronal cultures under control conditions and further upregulation after stress induction (n=3).* ***e:*** *The Western blot analysis of Cryab confirms elevated levels of Cryab under normal and stress conditions in mature neuronal cultures and induction in the other cell populations (n=3).* ***f:*** *Under stress conditions HSP27 is slightly increased in primary stem cell-derived neuronal cultures (n=3).* ***g:*** *The protein levels of Cryab are raised under control and stress conditions in primary stem cell-derived mature neurons. (n=3)*

5.7 Generation of CRISPR/Cas9 Cryab knockout cell lines to investigate the impact of Cryab on neuronal cell survival

The previous chapters showed that Cryab expression was detected in mature neuronal cultures and upregulated upon stress induction (Figure 5.12). Since one of its functions is to suppress apoptosis, it was of interest to investigate whether Cryab also showed these protective capacities in human neuronal cultures. In order to reliably show this effect, with the least background possible the CRISPR/Cas9 system was employed to generate an isogenic knockout line that could be compared to its parental line while only the Cryab gene is disrupted.

5.7.1 Generation and characterisation of Cryab knockout neural stem cells

IPS cell-derived SM-NP cells were nucleofected with a mixture of αB-crystallin CRISPR/Cas9 KO Plasmid (h) and αB-crystallin HDR Plasmid (h), which contained a puromycin resistance gene. The αB-crystallin CRISPR/Cas9 KO Plasmid (h) was provided as a mixture of three vector plasmids, each coding for a different guide RNA (gRNA), resulting in three putative cutting sites (Fig. 5.13a). Clones were selected by the administration of puromycin. Prospective Cryab knockout clones were screened by qPCR and Western blot (data not shown). Sequencing of genomic DNA of SM-NP cells was performed by Ruven Wilkens to validate the knockout of Cryab. Each reverse primer of the three primer pairs used for sequencing was based on one of the gRNAs of the CRISPR/Cas9 system (Fig. 5.13a). The application of the CRISPR/Cas9 system resulted in deletions of different length and regions in the Cryab gene (Fig. 5.13a,b). For clone #45 and #69 deletions in exon 4, coding for the alpha-crystallin domain (NCBI Reference Sequence: NP_001276737.1) were observed. Clone #69 showed an additional deletion in exon 2. A deletion of 10 base pairs (bp) in the C-terminus, in exon 4 was detected for clone #38 (Fig. 5.13a) (clones later also referred to as Cryab knockout clones). PCR on genomic DNA of wild type and Cryab knockout clones utilising primers shown in Figure 5.13a, revealed deletions in the Cryab gene (Fig. 5.13b). The deletion in the Cryab C-terminus of clone #38 resulted in a frame shift and an extension of the C-terminus (Fig 5.13c). A study investigating the impact of the C-terminus on the chaperone-like activity, via a substitution of the last two residues pointed out that the mutant αB-crystallins showed no significant chaperone-like activity (Plater et al., 1996). In order to validate the unchanged developmental identity of Cryab knockout clones, Cryab knockout SM-NP cells were

stained for the neural precursor markers Pax6, DACH1 and Nestin. These markers were investigated to show that the knockout had no impact on the typical precursor phenotype (Fig. 5.13d). Neuronal knockout cultures were stained for β-III tubulin and MAP2ab, to elucidate if the knockout had an effect on the precursor's ability to give rise to neuronal cultures. The staining results indicated that the knockout cells were still able to give rise to neurons (Fig. 5.13e). In summary, the results showed that CRISPR/Cas9 gene editing resulted in different deletions within the Cryab gene. The results also indicated, that the SM-NP knockout lines still express the neural precursor markers and are able to give rise to neuronal cultures.

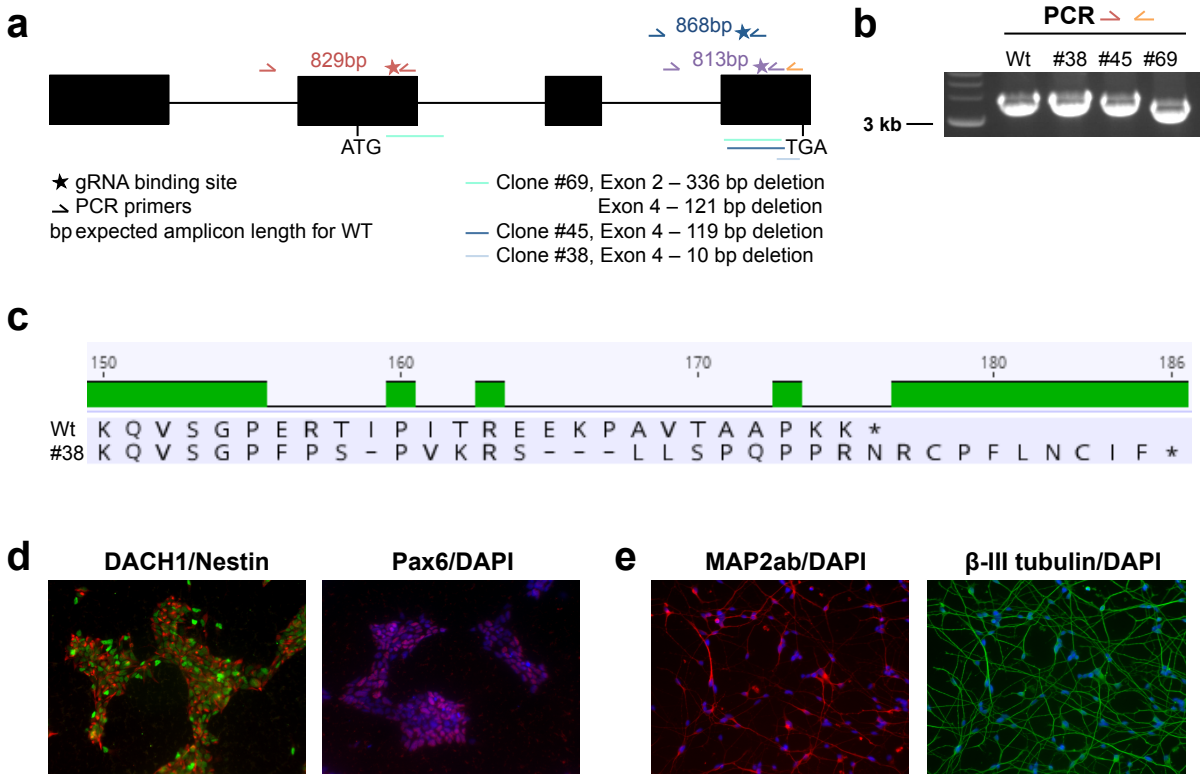

Figure 5.13: Characterisation of the Cryab knockout line. ***a:*** *Exon/intron structure of Cryab, displaying primer pairs (red, blue and purple) used for sequencing. Deleted areas for the different clones are also marked.* ***b:*** *PCR on genomic DNA of wild type and knockout SM-NP cells.* ***c:*** *Protein sequence of wild type (Wt) Cryab and Cryab of clone #38 (from amino acid 150 to 185)* ***d:*** *Immuncytochemical analysis of DACH1 (green), Nestin (red) and Pax6 (red) on Cryab knockout SM-NP cells.* ***e:*** *β-III tubulin (green) and MAP2ab (red) staining of neuronal Cryab knockout cultures (1 week).* ***a,b*** *and* ***c*** *adopted from Ruven Wilkens.*

5.7.2 Knockout of Cryab results in significant reduction of cell survival after stress induction in mature neuronal cultures

After the validation of the knockout clones, it was of interest, to investigate whether the lack of Cryab had any effect on the stress resistance in neuronal cultures. For this, cell viability

assays were performed on immature and mature neuronal knockout cultures. Three clones were used for these experiments, #69, #45 and #38. The cultures were treated with the stressors, Staurosporine (5 nM), Rotenone (5 µM), Thapsigargin (2 µM), Tunicamycin (1.5 µM), Baf/3-MA (15 nM/2 mM) and MG-132 (7.5 µM). The viability of the cells was assessed by the PrestoBlue® assay for 48 h, every 16 h.

First, the reaction of immature neurons towards stress induction was explored. Here the application of all stressors, despite Staurosporine, resulted in a strong reduction of cell viability in all cultures, wild type and knockout (Fig. 5.14). The intensity of the decreased viability differed slightly between the immature knockout cultures themselves and the wild type cultures. For example autophagy inhibition resulted in strong reduction of the cell viability in all cultures (wild type and knockout), but autophagy inhibitors seemed to be marginal more harmful to two clones (#69 and #38). Together, these results indicated, that the vulnerability to stress induction in wild type immature neuronal cultures and in immature knockout cultures were comparable, with minor differences between the knockout lines themselves and the wild type. The only exception was Staurosporine, to which the clones did not respond.

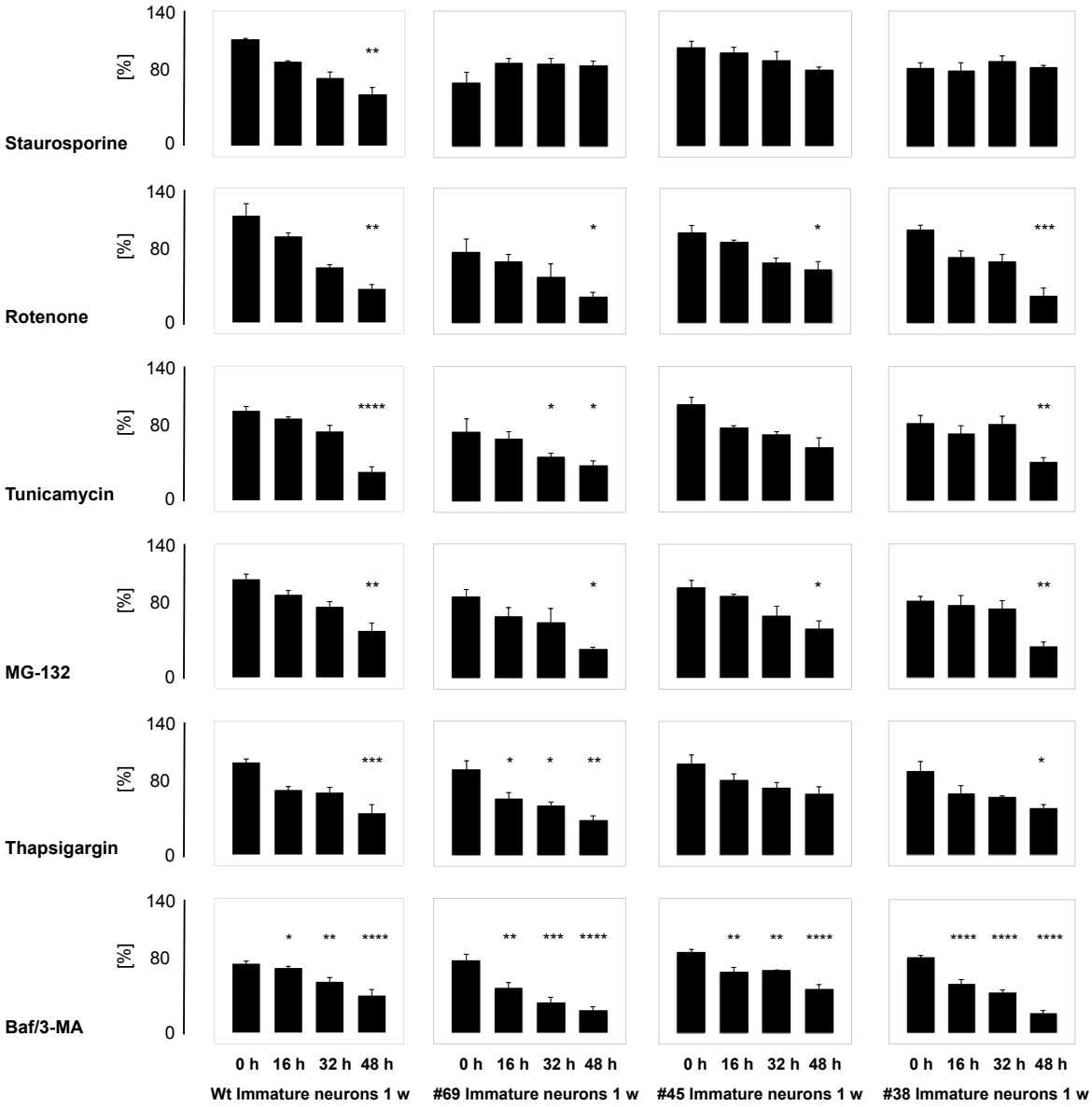

Figure 5.14: The stress induction results in comparable outcomes in wild type and Cryab knockout immature neuronal cultures. *Wild type (Wt) immature neuronal cultures and immature Cryab knockout cultures (#69, #45 and #38) were treated with the indicated stressors for up to 48 hours. The results were normalized to the respective controls. The cell viability was monitored via the PrestoBlue® assay every 16 hours. Only minimal differences between the different cultures regarding cell viability can be observed. Bar graphs show mean ± SEM; n=3 (*p < 0.05; **p < 0.01; ***p < 0.001; ****p < 0.0001). The controls are not depicted.*

Since Cryab was only slightly expressed in immature neuronal cultures and not expressed in knockout neuronal cultures, no major differences in cell viability between wild type immature and knockout immature neuronal cultures were expected. To explore, whether mature knockout cultures were less resistant against stress induction than wild type neurons, the cell viability experiments were repeated on mature neuronal knockout cultures. The cell viability of the cultures was already strongly reduced in the absence of any stressor (Data

not shown). To assess the reason for the cell deprivation, experiments in different culture media were performed. Mature neuronal cultures were cultivated in N2+ medium (NGMC medium without B27), N2+ medium with DMSO, NGMC and NGMC with DMSO for 48 hours. The viability of the cells was assessed every 24 hours by the CellTiter-Glo® assay and values obtained at 0 h were set as 100 %.

Cultivation of the mature neuronal knockout clone in N2+ medium resulted in a strong reduction of cell viability (Fig. 5.15). After 48 hours approximately 40 % of the cells in culture were dead. No reduction in cell viability was detected in wild type neuronal cultures. The addition of DMSO to the N2+ culture medium resulted in an even stronger reduction of cell viability in the knockout line. Here 50 % of the cells were not viable by the end of the experiment. No differences were observed in the wild type mature neuronal cultures. The cultivation of both, the wild type and the knockout line showed no reduction of cell viability, when cultivated in NGMC or NGMC with DMSO. Together, these experiments suggested, that mature neuronal Cryab knockout cultures were more sensitive and showed increased cell death already in media, which did not contain the protective factors of the B27 supplement. As B27 contains several antioxidants, this also indicated that the elimination of Cryab increased the susceptibility to oxidative stress.

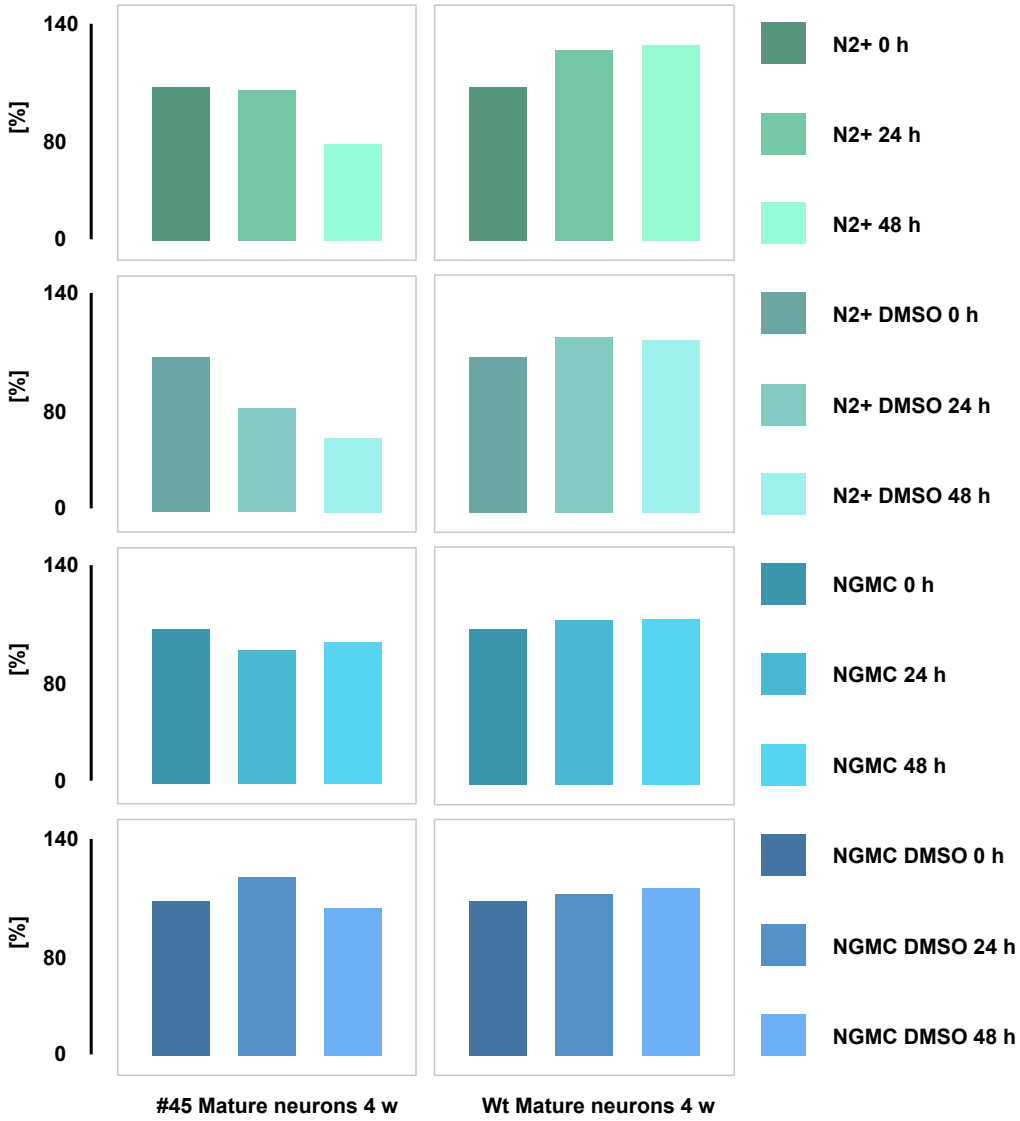

Figure 5.15: Decreased cell viability in mature neuronal cultures of the Cryab knockout lines in the absence of redox protective B27. *Wild type mature neuronal cultures and mature Cryab knockout cultures from clone #45 were cultivated in N2+ and NGMC medium with and without DMSO for 48 hours. The results were normalized to measurements of time point 0 h. The cell viability was assessed using CellTiter-Glo® assay every 24 hours. Differences between the different cultivation mediums regarding cell viability are visible. Bar graphs show mean (n=1).*

Based on these results the experimental set up was modified and all experiments looking for stress susceptibility of the Cryab knockout neurons were performed in the more protective medium containing B27 supplement. The cell viability was assessed by the CellTiter-Glo® assay.

ER stress induction had no impact on cell viability of all mature neuronal cultures (Fig.5.16). The application of Staurosporine led to a strong and significant reduction in cell viability in two of the three knockout lines. Mature neurons of clone #69 were highly affected by the presence of Staurosporine - already after 16 h a significant reduction of

viability was apparent. Wild type cultures were affected after 48 hours, whereas the cell viability of clone #38 remained stable over the course of the experiment. Inhibition of the proteasome resulted in reduced cell viability in the knockout cultures over time. Significant changes were detectable after 48 hours for clone #69 and #38. Neuronal cultures of clone #45 were also impaired. The wild type mature neurons showed only minor reductions (Fig. 5.16). Autophagy inhibition resulted in severe reduction in cell viability in all knockout lines analysed. Clone #69 and #45 displayed already after 16 hours significant decreases in cell viability. After 48 hours only ~ 20 % of mature neurons of clone #69 could be considered viable. Also cultures of clone #38 were significantly impaired at the end of the experiment (Fig. 5.16). Despite autophagy inhibition, redox stress had the most striking effect on the viability of the mature neuronal Cryab knockout cultures. Already at time point 16 h, the cell viability of cultures from clone #45 and #38 was reduced to approximately 50 %. The cell viability was reduced in all mature neuronal knockout cultures after 48 hours, with only about 30 % of surviving neurons, whereas for the wild type neuronal cultures only slight reductions were observable (Fig. 5.16). Taken together, the results indicated that, Cryab knockout rendered mature neurons more vulnerable to all stress inductions, except for ER stress induction.

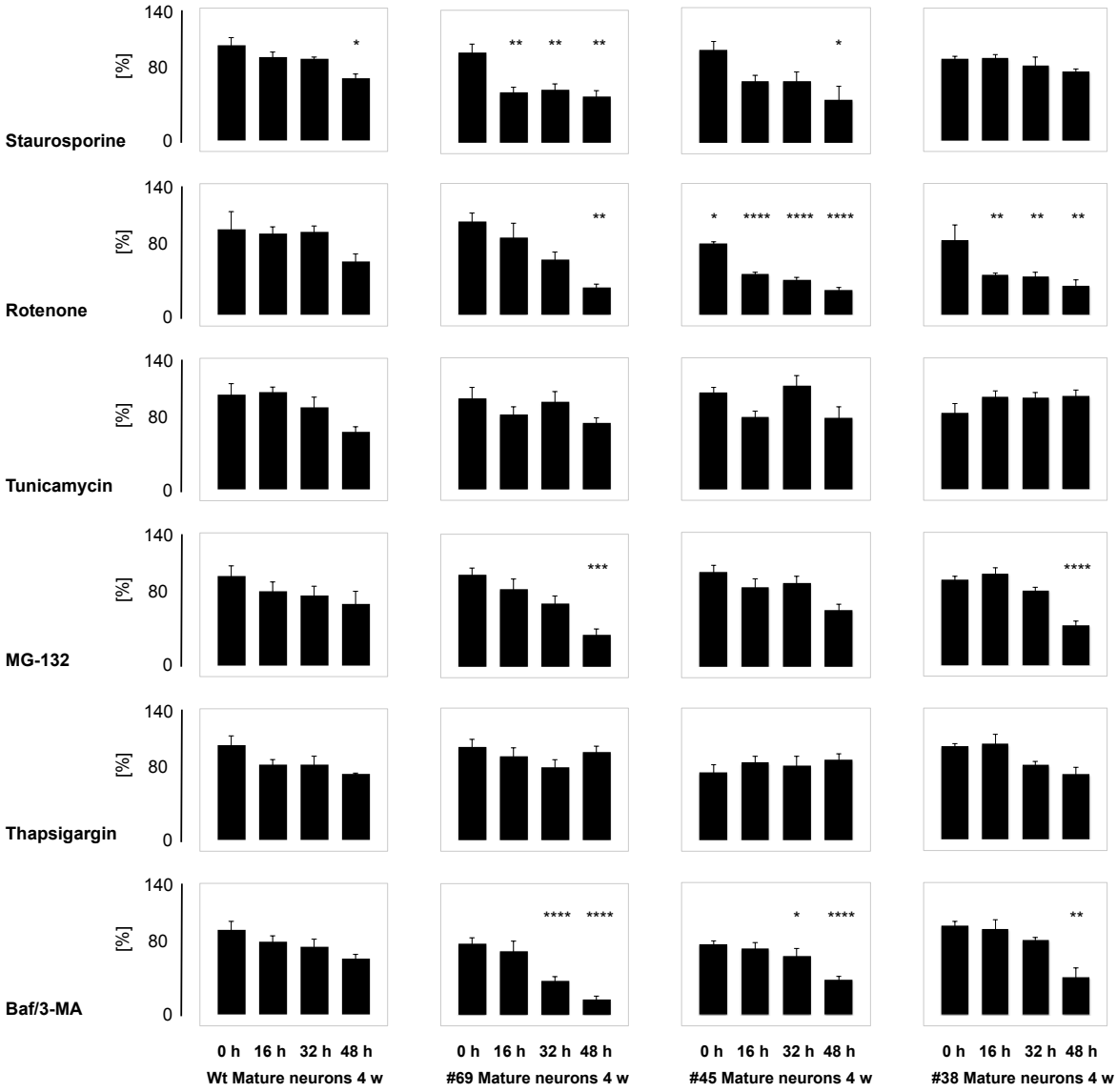

Figure 5.16: Cryab knockout renders mature neuronal cultures more vulnerable to a variety of stressors. *Mature neuronal cultures (wild type and Cryab knockout clones #69, #45 and #38) were treated with the stressors, Staurosporine, Rotenone, Tunicamycin, MG-132, Thapsigargin and Baf/3-MA for up to 48 h. The results were normalized to the respective controls. CellTiter-Glo® assay was used to explore the viability of the cells. The viability was assessed every 16 hours. In mature neuronal cultures no significant alterations regarding viability can be observed after 48 hours of exposure, whereas the knockout mature neuronal cultures are strongly affected. Especially autophagy, proteasomal and redox stress result in significant cell loss. Bar graphs display mean ± SEM; n=3 (*p < 0.05; **p < 0.01; ***p < 0.001; ****p < 0.0001). The controls are not depicted.*

5.7.3 Differences between Cryab knockout lines and wild type neuronal cultures with respect to the AKT-pathway

As an increased activity of the AKT-pathway in wild type mature neuronal cultures was observed (see chapter 5.5) and due to the high vulnerability to stress of the mature neuronal knockout cultures, it was of interest to explore, whether the activity of AKT was altered in

the knockout cultures. To this end, Western blots of immature and mature neurons of clone #69, #45 and #38 were investigated for pAKT and AKT.

The levels of phosphorylated AKT were not increased in mature neuronal cultures of the knockout clones, compared to their immature counterparts (Fig. 5.17). The quantitative data showed pAKT levels between 100 and 120 % for the knockout cultures. Summarised, I) there was no elevated activity of the AKT-pathway detectable in knockout mature neurons compared to the immature neurons and II), the measured levels of pAKT in knockout lines were lower than in the wild type mature neuronal line, indicating that the protective potential of the AKT-pathway was reduced.

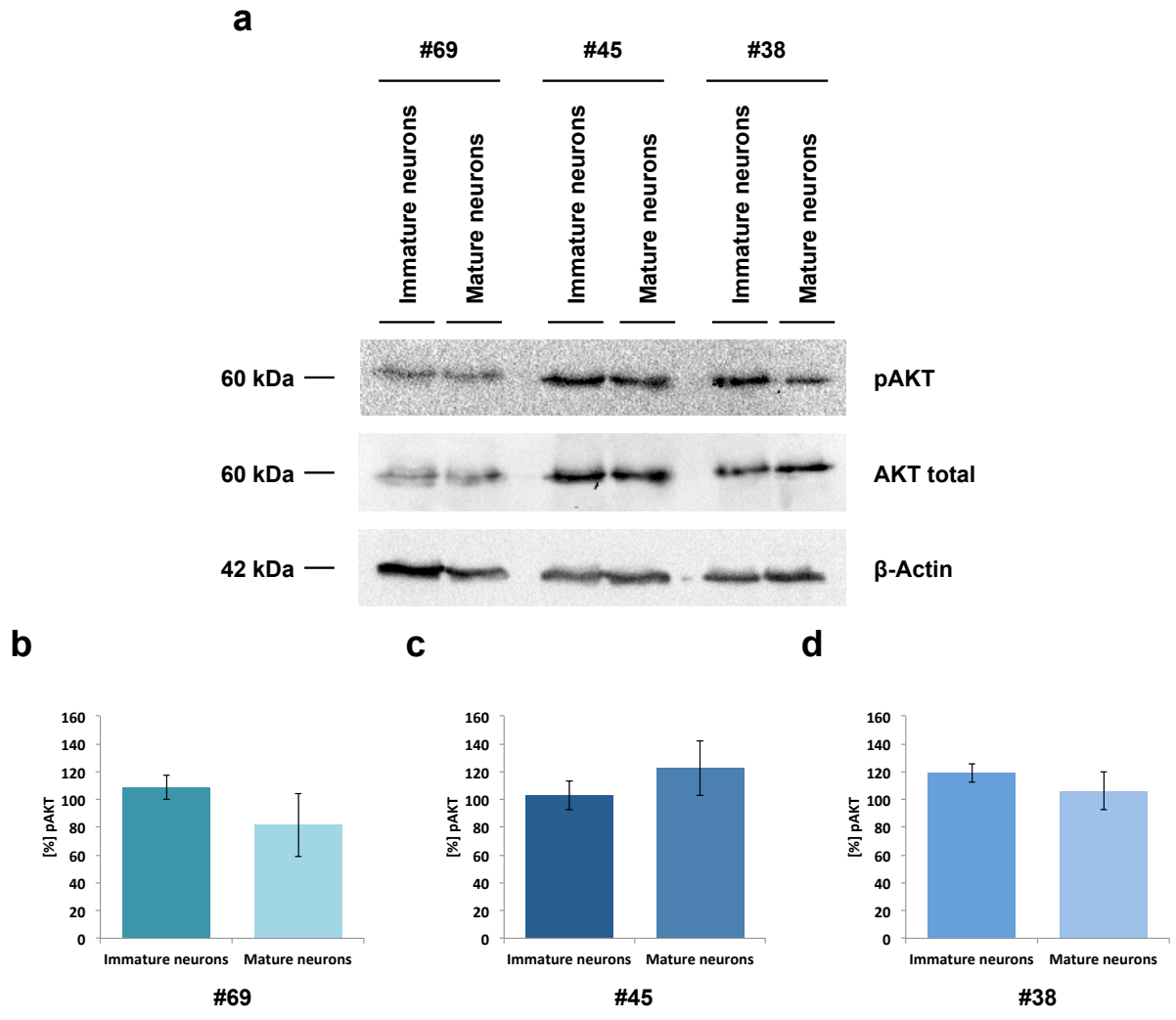

Figure 5.17: No elevated pAKT levels in mature neurons of the knockout lines. ***a:*** *Western blot analysis of AKT and its activated form, pAKT, uncovers, that there are no differences in the pAKT levels between immature and mature neuronal knockout cultures. Mature neurons were differentiated for 4 weeks.* ***b,c,d:*** *Quantity of pAKT to total AKT in immature and mature neuronal cultures of clone #69, #45 and #38. Bar graphs display mean ± SEM; (n=3).*

6 Discussion

6.1 Suitability of human induced pluripotent stem cell-derived neurons and immortalized cell lines to investigate maturation-dependent anti-apoptotic mechanisms

The characteristic of the majority of neurons is that they have to survive throughout the entire lifespan of an individual, since only in specific regions of the brain neurogenesis is observed (Eriksson et al., 1998). Thus it is consequentially that mature neurons feature mechanisms that promote their long-term survival. To investigate or to model neurodegenerative diseases immortalised cell lines have been extensively used. For example neuroblastoma cells (N2a) were used to analyse the protective effects of edaravone for Alzheimer's disease relevant symptoms (Yan et al., 2012). Another example is the neuroblastoma line SH-SY5Y that is used as a model for Parkinson disease (Lopes et al., 2010).

However, from previous studies performed in our laboratory there is evidence that immortalised cell lines are not a suitable system to model neuronal behaviour. In 2013, Mertens et al. were able to demonstrate that therapeutic relevant concentrations of nonsteroidal anti-inflammatory drugs (NSAIDs) are not able to lower the Aβ42/Aβ40 ratio in human induced pluripotent stem cell-derived neurons, while a significant reduction of the Aβ42/Aβ40 ratio is detectable in human non-neural cells, brains of transgenic mice and non-human cell lines (Mertens et al., 2013). In another study, Mertens and co-workers showed that even after 4 weeks of expression of pseudohyperphosphorylated tau in embryonic stem cell-derived neuronal cultures, neither a degeneration of the neurons, nor to the activation of caspase3 could be observed (Mertens et al., 2013). The same experiment was performed by Fath and co-workers employing PC12 cells. Here, most of the cells are degenerated, as early as 1 week of expression of pseudohyperphosphorylated tau. In those cells the caspase3 activity is increased and the cells are TUNEL-positive. Experiments with NT2-N neurons also displayed a cytotoxic effect of pseudohyperphosphorylated tau (Fath, Eidenmüller & Brandt, 2002). These results indicate that stem cell-derived mature neuronal cultures behave different when compared to immortalised cell lines.

In this study, we were interested if the neuroblastoma line SKNSH is suitable to investigate anti-apoptotic brakes in neuronal cultures. SKNSH cells were used in the same experiments as lt-NES cells and therefrom derived immature and mature neurons. The cells were then

exposed to different cellular stressors and the viability of the cells was assessed every 16 hours over a total time period of 48 hours. The cell viability assays revealed that the neuroblastoma line is much more sensitive to stress induction than the induced pluripotent stem cell-derived neuronal cultures. The cell viability of the neuroblastoma line is also more strongly reduced after the treatment with several stressors, when compared to the cell viability of the lt-NES cells. These findings were also backed by observations where caspase3 and its downstream targets are cleaved. Initial experiments aiming at assessing variances in the levels of caspase9, indicate that the protein levels of caspase9 in SKNSH cells and lt-NES cells are comparable. In contrast, significant lower levels of caspase9 could be detected in mature neuronal cultures than in the neuroblastoma line. This indicates, that proteins relevant to apoptosis are differentially regulated in the neuroblastoma cell line compared to the neuronal cultures and the progenitors and therefore might promote apoptosis in those cells.

Furthermore, the activity of the AKT-pathway is reduced in the neuroblastoma line when compared to lt-NES cells, immature and mature neurons, as shown by low levels of phosphorylated AKT in SKNSH cells. This implies that the cell survival pathways in the neuroblastoma cell line are also regulated in a different way than in the lt-NES cells, immature and mature neuronal cultures. An increase in activity of the AKT-pathway is observed in many cancers, resulting e.g. from overexpressed and constitutively active cell surface receptors or an aberrant expression of the phosphatase and tensin homolog (PTEN), which dephosphorylates phosphoinositide products of PI3K. The inhibition of the AKT-pathway in cancer cells has been shown to induce apoptosis or suppress the cell proliferation (Osaki, Oshimura & Ito, 2004). However, the present results imply that SKNSH cells do not extensively use the AKT-pathway to promote cell proliferation and to protect themselves against apoptotic stimuli.

Heat shock proteins are also expressed in another way in SKNSH cells than in the other cell populations investigated. In the neuroblastoma line, the heat shock proteins HSP70 and HSP27 are highly expressed under control conditions and are upregulated after stress induction. In the other cell populations, lt-NES cells, immature and mature neurons, only low protein levels of these heat shock proteins are observable under control conditions. Under stress conditions, the expression of HSP70 and 27 is increased in lt-NES cells and immature neurons. In mature neuronal cultures the expression especially of HSP70 is just very slightly elevated, but in mature neuronal cultures Cryab, another heat shock protein, is increased. This sHSP is also elevated in several cancers, for example in colorectal cancer

and glioblastomas (Shi et al., 2014; Goplen et al., 2010). In SKNSH cells, the expression of Cryab is only detectable after stress induction.

Together, these results indicate that the behaviour of the neuroblastoma cells regarding stress resistance is not comparable to that of the neuronal cultures and only partially comparable when comparing the stress resistance of the lt-NES cells and SKNSH cells. A variance of stress resistance of neuronal cultures and the neuroblastoma cultures could be explained by the fact that SKNSH cells were cultured as proliferating cells and were not subjected to differentiation protocols. However, in the proliferative state, they should at least be similar to the lt-NES cells, which is also not the case for all stressors used in the cell viability assays. Also the expression of heat shock proteins and the activity of the AKT-pathway differs between the neuroblastoma cultures and the lt-NES cultures. This shows that the behaviour of the SKNSH cells is neither comparable to neuronal cultures nor to the proliferating lt-NES cells. Together with the observations made by Mertens and co-workers the results of this study indicate that SKNSH cultures are a suboptimal model to investigate anti-apoptotic brakes in neuronal precursors and neurons. These findings also demonstrate that for experiments to observe protective mechanisms to overcome apoptotic stimuli, or to identify appropriate drugs to treat human diseases, the cellular model has to be chosen carefully in order to receive reliable results.

6.2 Maturation-dependent increasing stress resistance of mature neuronal cultures

As neurons arise during embryonic development and cannot be sufficiently replaced in humans, they have to persist throughout the entire life span of an individual. Since there is a lack of neurogenesis in most parts of the brain, it is tempting to speculate that neurons have elaborated strategies to protect themselves against stress and apoptosis (Eriksson et al., 1998; Kole, Annis & Deshmukh, 2013). Apoptotic pathways are commonly active in immature neurons, and are thought to ensure a precise formation of neuronal circuitries. However, in mature neurons a rapid induction of apoptosis would result in a tremendous neuronal loss over time, which is why they are thought to harbour a mechanism allowing them to overcome apoptotic stimuli. Studies on neurons of mice revealed that neurons become more resistant to different types of stress over the course of their maturation, e.g. nerve growth factor (NGF) deprivation or nerve transection (Kole, Annis & Deshmukh,

2013). To address whether human neurons also become more resistant to stress when they mature, cell viability assays under different stress conditions were performed. These experiments are necessary as not all mechanisms observed in rodents can be transferred to the human system (Mertens et al., 2013 and Weggen et al., 2001). The stressors that were chosen to evoke cellular stress include: Protein kinase stress, oxidative stress, ER stress, proteasomal stress and autophagy stress. Cell viability assays were performed on lt-NES cells, immature and mature neuronal cultures to uncover maturation-dependent changes. The viability of the cells was monitored every 16 hours and investigated over a total time period of 48 hours. The experiments reveal that the neural precursors are strongly impaired after the application of all stressors. The cell viability of immature neurons is also reduced after stress induction - but to a much lesser extent than in lt-NES cells. In contrast to this, mature neuronal cultures, differentiated for 4 and 9 weeks do not seem to be vulnerable to stress induction, since no significant reductions in cell viability was observed after 48 hours. The absence of decreased cell viability in mature neurons after treatment with cellular stressors implies that these cells have elaborated strategies to overcome apoptotic stimuli.

Investigations on neurons of rodents showed a maturation-dependent decrease of caspase3 levels (Yakovlev et al., 2001). To uncover, whether the resistance to stress of mature neurons is also reflected by reduced levels of caspase3, a decrease in its activation and of its downstream targets, Western blot analysis of caspase3 and cleaved PARP and immunocytochemical analysis of cleaved caspase3 were performed. The experiments show a reduced activation of caspase3, in mature neuronal cultures when compared to lt-NES cell cultures and immature neuronal cultures, this is suggested by the lack of cleaved PARP in neuronal cultures and the immuncytochemical analysis. However, no variances between the different populations regarding caspase3 levels were detected under control conditions. Together, these results indicate that the caspase cascade is not, or barely induced in mature neurons. Further experiments are needed to decipher the mechanisms underlying the stress resistance of mature neurons. Some strategies employed by mature neurons of rodents are known from the literature, like the downregulation of Bax and its sequestration in the cytoplasm (Polster et al., 2003).

6.3 Downregulation of pro-apoptotic proteins as mechanism to overcome apoptotic stimuli

Caspase9 is an initiator caspase, and, together with cytochrome c and Apaf-1 forms the apoptosome. Cleavage of Caspase9 results in a small and a large subunit (the large subunit contains the active site), a second cleavage step removes the N-terminal prodomain from the large subunit. The fully active caspase consists of two large and two small subunits. Activation of caspase9 leads to the activation of downstream caspases and the induction of apoptosis (Park, 2012; Clarke & Tyler, 2009). Because initial experiments did not show alterations in the protein levels of caspase3 between the different cell populations under control conditions and since caspase3 seems to be less active in mature neuronal cultures, the expression of caspase9, which is acting upstream of caspsae3 in the caspase cascade, was explored. Protein levels of caspase9 were of interest, because the knockout of caspase9 inhibits the activation of caspase3 (Kuida et al., 1998). In this context, reduced caspase9 levels were thought to result in reduced caspase3 activation.

Western blot analysis demonstrates, that caspase9 levels of the neuroblastoma line and the lt-NES cells are higher than that of the neuronal cultures, with mature neuronal cultures showing the lowest levels of caspase9. The decrease in caspase9 protein levels in mature neurons seems to be dependent on maturation time, and the reduction of caspase9 levels in mature neuronal cultures compared to immature neuronal cultures is significant for iPS cell-derived cultures

Due to the reduced amount of caspase9 in iPS cell-derived mature neuronal cultures, it is tempting to speculate that the reduced availability of caspase9 results in lower levels of activated caspase9, since the base material needed for high levels of active caspase9 is inaccessible. One can then assume that lower levels of activated caspase9 result in reduced activation of the downstream targets, since it has been shown that the knockout of caspase9 abolishes the activation of casapse3 (Kuida et al., 1998). In addition, when reduced levels of active caspase9 and downstream targets are expected, also reduced amounts of proteins protecting cells downstream of caspase9 activation against apoptosis are necessary.

Aside from the observed downregulation of caspase9 in iPS cell-derived mature neuronal cultures, a reduced expression of Apaf-1 in these cultures compared to the immature cultures was also detected by gene expression analysis (data not shown). Downregulation of Apaf-1 was detected in neurons of rodents (Yakovlev et al., 2001). Repression of Apaf-1 was also found in mature sympathetic neurons of mice. It is thought that repressing Apaf-1 renders

neurons resistant to cytochrome c (Kole, Annis & Deshmukh, 2013). Summarising, a downregulation of two components of the apoptosome is observed. Based on these findings, one might assume that the formation of the apoptosome is impaired in iPS cell-derived mature neurons.

In addition to the downregulation, several other mechanisms have been described by which the activation of caspase9 could be prevented. The phosphorylation of caspase9 through AKT inhibits its protease activity (Cardone et al., 1998). Another mechanism used to prevent caspase9 activation is the expression of a caspase9 variant, caspase9S, containing the prodomain, but missing most of the large subunit, including the catalytic site. Through binding of caspase9S to Apaf-1, the interaction of Apaf-1 and caspase9 and its activation is blocked (Seol & Billiar, 1999).

6.4 Maturation-dependent activation of the pro-survival AKT-pathway as protective mechanism

The AKT-pathway represents an important cell survival pathway. Here, the protein AKT is recruited to the plasma membrane by PIP_3 and PIP_2. This interaction causes a conformational change and allows the phosphorylation of AKT. The activated AKT dissociates from the membrane and translocates to the cytoplasm and the nucleus, where it phosphorylates downstream targets (Osaki, Oshimura & Ito, 2004; Lawlor & Alessi, 2001). Several targets of AKT are involved in the apoptosis machinery. Specifically, phosphorylation of Bad or caspase9 by AKT inhibits their pro-apoptotic capacity (Downward 1999; Cardone et al., 1998), while phosphorylation of the forkhead transcription factor sequesters it in the cytoplasm and thereby prevents the expression of pro-apoptotic genes (Brunet et al., 1999).

6.4.1 In mature neurons protective proteins that interact with the AKT-pathway are upregulated leading to a maturation-dependent elevated activity of the AKT-pathway as mechanism against stress induction

Gene expression analysis was performed to gain deeper insights into the mechanisms used by mature neurons, making them tolerant to stress induction. Data was analysed by Enrichr giving a first hint that despite other pathways the AKT-pathway might be upregulated in

mature neurons. For the 110 highest upregulated genes in mature neurons, literature was screened if there were protective/neuroprotective effects described for the respective genes. And it was of interest, if some of the proteins upregulated in mature neurons are related to one specific pathway, as indicated by Enrichr. The results show, that a variety of genes encoding for proteins that are significantly upregulated in mature neurons compared to immature neurons converge into the AKT-pathway. Proteins with protective properties regulated by the AKT-pathway and proteins stimulating the activation of the AKT-pathway are upregulated in mature neuronal cultures. Among the stimulating proteins is p62, a protein involved in autophagy. It recognises specific ubiquitinylated proteins and targets them for autophagy. During this process, p62 is also digested (Lamark et al., 2009). It has been shown, that high amounts of p62 positively regulate the function of nuclear factor (erythroid-derived 2)-like 2 (Nrf2). This is achieved by the interaction of p62 with kelch-like ECH-associated protein 1 (Keap1). Through its competitive binding to Keap1, Keap1 cannot facilitate the ubiquitinylation of Nrf2. Hereby, levels of Nrf2 increase, so that it is able to induce the transcription of proteins under a promoter containing an antioxidant response element (ARE) (Komatsu et al., 2010). Another study indicates, that p62 is binding to protein kinase Cζ (PKCζ), a negative regulator of AKT, and thereby allows the activation of AKT (Joung, Kim & Kwon, 2005). Another protective property of p62 is its upregulation after oxidative stress induction. p62 decreases the association of 14-3-3θ and PDK1, an upstream kinase of AKT, by binding to 14-3-3θ. Together this leads to a prolonged phosphorylation of AKT under stress conditions (Heo et al., 2009). In summary, these studies uncover, that upregulated p62 levels lead to competitive binding to proteins negatively influencing the cell survival, resulting in elevated levels or the release of proteins positively influencing the viability of the cell e.g. by biasing the phosphorylation of AKT. Thus, it is tempting to speculate, that the upregulated levels of p62 observed in mature neuronal cultures have the same positive impact on their cell survival. In addition, the elevated p62 levels in mature neuronal cultures might lead to increased activity of autophagy and an increased autophagic flux.

Another protein involved in the AKT-pathway is Rab31, a Rab GTPase belonging to the Ras superfamiliy, which regulates the vesicle transport from the Golgi apparatus to early and late endosomes (Chua & Tang, 2014). Two studies indicated, that the overexpression of Rab31 in cancer cells is able to decrease the number of apoptotic cells, reduce the activity of caspase3 and 7 diminishes the amount of cPARP, while the knockdown of Rab31 results in an elevated activity of caspase3 and 7, in higher levels of cPARP and in an increased

number of apoptotic cells (Sui et al., 2015 and Pan et al., 2016). Moreover, an overexpression of Rab31 leads to decreased expression of pro-apoptotic Bax and an increased expression of anti-apoptotic Bcl-2. Furthermore, the upregulation of Rab31 is able to elevate the levels of PI3K, pAKT and pErk. Based on this finding the teams around Sui and Pan conclude, that the downregulation of pro-apoptotic proteins and the upregulation of anti-apoptotic proteins are mediated via the activation of the AKT-pathway. These data suggest that the elevated expression of Rab31 observed in mature neuronal cultures may result in an activation of the AKT-pathway and thereby the regulation of proteins into an anti-apoptotic direction.

Vascular endothelial growth factor B (VEGFB) is also elevated in mature neuronal cultures compared to immature cultures, which is supported by gene expression analysis and qPCR. VEGFB is the ligand of the vascular endothelial growth factor receptor-1 (VEGFR-1), a receptor tyrosine kinase, and the co-receptor neuropilin 1 (NP-1). Binding of VEGFB to VEGFR-1 leads to the dimerization and the autophosphorylation of the receptor (Hoeben et al., 2004; Heldin, 1995; Li et al., 2008). The autophosphorylation generates binding sites for SH2-domain containing proteins, like phospholipase C gamma 1 (PLCγ1) and PI3K, which results in the activation of the extracellular signal-regulated kinase (Erk)-pathway and the AKT-pathway (Hoeben et al., 2004; Heldin, 1995; Hale et al., 2008; Ito et al., 1998). VEGFB exists in two splice variants, $VEGFB^{167}$ and $VEGFB^{186}$, which are both secreted. A 25 kDa protein is present intracellularly, whereas extracellular, in the medium, a 32 kDa protein is attested (Olofsson et al., 1996). Olofsson and co-workers observed that $VEGFB^{186}$ is covalently modified via O-linked glycosylation. VEGFB is also secreted as homodimer and as heterodimer with vascular endothelial growth factor (VEGF) (Olofsson et al., 1996). In contrast to the other VEGFs, VEGFB is not involved in the angiogenesis, or shows only minimal angiogenic activity (Poesen et al., 2008; Li et al., 2008), while the neuroprotective properties of VEGFB were reported by several studies. Sun et al. showed, that $VEGFB^{-/-}$ mice display increased size of infarct volume after cerebral ischemic injury and stronger neurological impairment when compared to the control mice (Sun et al., 2004). Another study showed, that VEGFB is able to rescue RGC5 cells from apoptosis. Here, the application of VEGFB reduces the amount of H_2O_2-induced apoptotic RGC5 cells (Li et al., 2008). VEGFB treatment under hypoxic conditions results in the downregulation of BH-3 only proteins like Bcl-2 modifying factor (Bmf), Puma, Bcl-2 associated agonist of cell death (Bad) and BH-3 interacting domain death agonist (Bid). Additionally, caspases are downregulated too (caspase2, 8, 9 and 12). A treatment with VEGFB also counteracts the

induction of cell death by serum deprivation and Bmf overexpression (Li et al., 2008). Li and his co-workers also reveal, that VEGFB is neuroprotective in vivo under ischemic conditions and in a NMDA injury model. The protection of neurons by VEGFB is mediated via VEGFR-1 (Li et al., 2008; Poesen et al., 2008). Neuroprotective potential for VEGFB was also observed in a Parkinson's disease (PD) model. While the application of VEGFB partially protects dopaminergic neurons and improved the forepaw preference of PD-model rats (Falk et al., 2011), the loss of VEGFB exacerbates the degeneration of motor neurons in an Amyotrophic lateral sclerosis (ALS) mouse model (Poesen et al., 2008). The researchers around Poensen suggest, that neurons express VEGFB under healthy conditions, to maintain neuroprotection in an autocrine manner and that VEBFB is also provided by activated astrocytes in a paracrine manner under stress conditions. The expression of VEGFB by astrocytes is controversial, as its expression in neurons, but not in astrocytes, also not under stress conditions, was identified by Li et al., 2008; Sun et al., 2004 and Xie et al., 2013, whereas Poesen and co-workers found VEGFB in neurons and also in activated astrocytes. Summarising these studies suggest, that VEGFB has neuroprotective capacities, which are mediated via binding to VEGFR-1, the activation of the AKT- and the Erk-pathway and a downregulation of pro-apoptotic proteins like Bmf. In the present study, gene expression analysis also revealed in our cultures an increase of Bmf in immature neuronal cultures compared to mature cultures (data not shown), which might be caused by the protection of VEGFB in mature neuronal cultures. However, it has to be mentioned, that the average detection signal was relatively low in both populations. Since the results regarding the expression of VEGFB in activated astrocytes are contradictory, it remains open, whether the neuroprotective effect in the brain is only mediate in an autocrine or also in a paracrine manner. Our cultures are highly enriched in neurons and the increase of VEGFB in mature neuronal cultures is observed under control conditions, so one might conclude, that the expected protective effects are of neuronal origin. Since VEGFB has low angiogenic activity, it is a potential candidate to treat or to address in neurodegenerative disorders (Poesen et al., 2008; Li et al., 2008). On the basis of these results, it can be assumed, that the increased VEGFB expression by mature neurons also leads to a protective mechanism/effects in cultures of mature human neurons.

Apart from proteins driving the activation of the AKT-pathway, also an increased expression of neuroprotective proteins, which are regulated by the AKT-pathway, was observed. These proteins, SCG2, SRXN1 and GCLM are regulated indirectly by the AKT-pathway, via AP-1 and Nrf2. SCG2 and SRXN1 are regulated by the AP-1 family to which also Jun belongs,

and not directly by AKT (Karin, Liu & Zandi, 1997). These proteins are activated by AKT-signalling, which was validated by studies inhibiting PI3K and generating loss of function mutations of AKT and PI3K (Ding et al., 2009; Li et al., 2004). This indicates, that the AKT-pathway can indirectly activate SCG2 and SRXN1. The AKT-pathway first activates members of the AP-1 family, which then induce the expression of SCG2 and SRXN1. In addition, Rhee and co-workers showed that the protein synthesis of SCG2 could be triggered by the AKT-Rab43 pathway (Rhee et al., 2016). The expression of GCLM is also regulated in an AP-1 manner, through the PI3K/AKT/AP-1-pathway (Lu et al., 2014). GCLM and SRXN1 are Nrf2 regulated, as AP-1 also Nrf2 is regulated by AKT, which is indicated by the inhibition of PI3K, which also results in the inhibition of Nrf2. In line with this the overexpression of AKT increases the activation of Nrf2 (Wang et al., 2008). Reddy and co-workers observed comparable results. They showed, that inhibition of PI3K/AKT decreases the expression of Nrf2 target genes (Reddy et al., 2015). PI3K inhibition can also lead to attenuation of the upregulation of Nrf2, which was induced by other factors (Zou et al., 2013). Aside Lu and co-workers showed, that the PI3K/AKT/Nrf2-pathway is involved in the GCLM expression (Lu et al., 2014). In summary these results reveal that, the AKT-pathway regulates the activity of Nrf2 and AP-1 and thereby also their downstream targets.

Secretogranin II (SCG2) is upregulated in mature neuronal cultures under control conditions. It was reported to be regulated by the transcription factor complex, activator protein 1 (AP-1) and to be protective against NO-induced apoptosis (Li, Hung & Porter, 2008). SCG2 represents the precursor of secretoneurin, a neuropeptide. To generate secretoneurin, SCG2 is proteolytically cleaved by the prohormone convertase 1 (PC1) (Fischer-Colbrie, Laslop & Kirchmair, 1995; Hofleher et al., 1995). Secretoneurin has protective properties; its administration is sufficient to induce the upregulation of Bcl-2 and Bcl-xl and is blocking the activation of caspase3 (Shyu et al., 2008). Apart from its regulation by the AKT-pathway, a further feature of secretoneurin is the ability to activate the AKT- and MAPK-pathway (Kirchmair, 2004; Kirchmair, 2004). Due to the upregulation of SCG2 in mature neuronal cultures and their resistance to stress one might assume that SCG2 has anti-apoptotic potential in our study as well.

The glutamate-cysteine ligase (GCL), which catalyses the rate limiting step of the glutathione biosynthesis, is composed of two subunits, GCLC, the catalytic subunit and GCLM, the modulatory subunit, (Huang, Anderson & Meister, 1993) which is increased in mature neuronal cultures. Glutathione (GSH) is a tripeptide of L-glutamate, cysteine and

glycine and is involved in the redox homeostasis. In a review by Deponte it was suggested, that the view on GSH mainly involved in antioxidant defence has now changed to a view of „compartmentalization of glutathione-dependent pathways", the involvement of glutathione in iron metabolism and redox regulation (Deponte, 2017; Toledano & Huang, 2017). Several studies pointed out that depletion of glutathione, either genetically, or via application of compounds, results in a reduced membrane potential, loss of cell viability, increased amounts of ROS and apoptosis. However, they also suggest that induction of Nrf2 and thereby its downstream targets like GCLM can counteract the observed loss of cell viability etc. including via increased glutathione levels (Giordano et al., 2006; Zou et al., 2012; Li et al., 20013). The work from Shi and co-workers revealed that this is also transferable to primary neuronal cultures. They showed that S-allyl cysteine activates Nrf2 as well as its downstream targets, GCLM, GCLC and HO-1, which results in protection of primary cortical neurons from oxygen and glucose deprivation-induced toxicity (Shi et al., 2015). Others showed that the overexpression of GCLM could result in a prolonged life of drosophila, indicating that enhancement of glutathione can extend their lifespan (Orr et al., 2005). GCLM is involved in the synthesis of glutathione and since glutathione is important for the redox defence and cell survival, the upregulation of GCLM may result in higher GSH concentrations and proper protection against redox stress in mature neuronal cultures.

Sulfiredoxin (SRXN1) is upregulated in mature neuronal cultures and involved in the AKT-pathway. Similar to SCG2 it is regulated by AP-1. SRXN1 activates c-Jun through a positive feedback loop. Besides its regulation by AP-1, SRXN1 is Nrf2 regulated (Wu et al., 2012; Kim et al., 2010; Zhou et al., 2105; Wei et al., 2008). SRXN1 is responsible for the reduction of hyperperoxidised peroxiredoxins (Prx). Prxs reduce H_2O_2 and alkyl hydroperoxides to water and alcohol. The oxidation of the catalytic centre of Prx to sulfenic acid (Cys-SOH) is reduced by glutathione or thioredoxin, but the oxidation to sulfinic acid (Cys-SO_2H) cannot be reduced by these thiols, for this reduction SRXN1 is essential. The reduction of hyperoxidised Prx requires SRXN1, the hydrolysis of ATP, Mg^{2+} and an electron donor, like glutathione or thioredoxin (Biteau, Labarre & Toledano, 2003; Chang et al., 2004). Zhang and co-workers showed, that the overexpression of SRXN1 after simulated ischaemia/reperfusion injury increases the cell viability, reduces cleavage of caspase3, caspase9 and PARP, diminishes the upregulation of Bax and reduces the release of cytochrome c from the mitochondria. Further Zhang et al. were able to show, that elevation of SRXN1 results in an increase of anti-apoptotic Bcl-2. Since they observed an increased amount of phosphorylated AKT after SRXN1 overexpression, they conclude, that the

protective effects are mediated via the activation of the AKT-pathway (Zhang et al., 2016). Other studies revealed, that inhibition or knockdown of SRXN1 results in an accumulation of reactive oxygen species (ROS) and hyperperoxydised Prxs, leading to oxidative mitochondrial damage and reduced cell viability. It is thought that the protection by SRXN1 is based on restoring the antioxidant activity of Prxs (Wu et al., 2017; Kim et al., 2016). Together, these results indicate, that the protective effects observed after SRXN1 overexpression are caused by the reduction of hyperoxidised Prxs and the activation of the AKT-pathway. It can be assumed, that the observed properties are transferable to our mature neuronal cultures.

Based on the results generated in our comparative gene expression analysis, the activity of the AKT-pathway was further investigated. Western blots of pAKT and AKT were performed. The results revealed, that pAKT levels are elevated in mature neurons when compared to SKNSH cells, lt-NES cells and immature neurons. Of special importance is the significant increase of pAKT in mature neuronal cultures compared to immature neuronal cultures. Western blot analysis also indicated, that pAKT levels elevate with on-going maturation. Since SKNSH cells, lt-NES cells and immature neurons are more susceptible for cellular stressors than mature neurons, which results in reduced cell viability in these cultures, the increased levels of pAKT in mature neuronal cultures indicate, that the AKT-pathway is more active in mature cultures.

These data suggest, that the active AKT-pathway is part of the protection machinery of mature neurons to overcome apoptotic stimuli and stress induction, via its properties mentioned above and via its known ability to phosphorylate the following targets, which were not further investigated in this study: I) Caspase9 and inhibit its protease activity (Cardone et al., 1998); II) Bad and thereby prevent the interaction with Bcl-xl (Downward, 1999); III) Bax promoting association with Bcl-2 family members (Gardai et al., 2004); IV) forkhead transcription factor resulting in interaction with 14-3-3 proteins, which hold the transcription factor in the cytoplasm and prevent the transcription of pro-apoptotic genes (Brunet et al., 1999); V) apoptosis signal-regulation kinase1 (ASK1), which prohibits the activation of p38 (Kim et al., 2001); VI) Md2m, which results in the destabilisation of p53 (Mayo & Donner, 2001) VII) the IκB kinase (IKK)α one of the two components of the IKK, which sequesters nuclear factor kappa-light-chain-enhancer of activated B cells (NF-κB) in the cytoplasm. NIK a MAP kinase kinase kinase and AKT phosphorylate IKKα, which targets it for degradation, and allows NF-κB to enter the nucleus (Ozes et al., 1999). All these phosphorylations have an anti-apoptotic effect and since pAKT levels are strongly

increased in mature neurons, it is tempting to speculate, that AKT phosphorylates downstream targets to overcome stress induction and apoptotic stimuli. The protective capacity of pAKT is also described in a study of Dewil and co-workers, who showed, that patients suffering from ALS have a lack of pAKT, resulting in the loss of motor neurons. A constitutively active AKT in SOD1 mice, an ALS model, counteracts the loss of motor neurons (Dewil et al., 2007).

Taking all the insights listed above into account, it is very likely, that the genes found to be upregulated in mature neuronal cultures converge into the AKT-pathway. Several studies, mentioned above, showed that, p62, Rab31 and VEGFB are able to activate the AKT-pathway and that the AKT-pathway regulates GCLM, SCG2 and SRXN1 indirectly. In addition, as mentioned above, SCG2 and SRXN1 seem to have the potential to stimulate the AKT-pathway. Considering that the active AKT is known to be critical for survival (Song, Ouyang & Bao, 2005) one may conclude, that p62, Rab31, VEGFB, SRXN1 and SCG2 are involved in the enhancement of pAKT and thereby in its protective potential. Since the upregulated genes in mature neurons have neuroprotective properties on their own, one can assume that these properties also come into effect in the protection of mature neurons against stress.

Despite the anti-apoptotic potential of the active AKT-pathway, the activation of AKT and its downstream target mTOR is also reasonable in terms of synaptic plasticity, for which synthesis of new proteins is required (Manning & Toker, 2017). Tang and co-workers showed that mTOR is involved in long-term potentiation (LTP) (Tang et al., 2002). It has also been shown, that the PI3K and AKT-dependent activation of mTOR is necessary for the metabotropic glutamate receptors (mGluRs)-depentent long-term depression (LTD), induced by an mGluR agonist (Hou & Klann, 2004).

6.5 Cryab as guarding protein in mature neurons

Cryab is a small heat shock protein with chaperone function, capable of forming a 24-mer oligomeric structure. This protein can transiently interact with early-unfolded proteins and stabilises them in order to allow them to change their structure to reach their active conformation. With late, aggregation-prone intermediates, Cryab forms stable and soluble complexes (Bakthisaran, Tangirala & Rao, 2015; Rajaraman et al., 2001). Apart from its chaperone function, Cryab processes also anti-apoptotic properties where it inhibits the formation of p17, the large active subunit of cleaved caspase3, via binding to the p24

intermediate. By this interaction, the autocatalytical cleavage is prevented (Kamradt, Chen & Cryns, 2001). In addition, Cryab can also bind to procaspase3 to prevent its activation (Mao et al., 2001). Through binding of Cryab to Bax and Bcl-XS it sequesters them in the cytosol, resulting in reduced cytochrome c release, less activation of caspase3 and strongly reduced cleavage of PARP (Mao et al., 2004).

6.5.1 Cryab might compensate for the attenuated common heat shock response

The heat shock response in some neurons is attenuated, for example in hippocampal neurons, not expressing the heat shock protein (HSP) HSP70 after thermal induction, due to a lack of heat shock factor 1 (HSF1). Furthermore, motor neurons do not induce HSP70 under several stress conditions, which is caused by the lack of HSF1 activation. Cortical neurons, too, show a decreased synthesis of the inducible HSP68 after heat shock. Neurons in general have a higher threshold for the induction of a heat shock response than astrocytes. It is thought, that the diminished heat shock response makes neurons more vulnerable to stress (Marcuccilli et al., 1996; Batulan et al., 2003; Nishimura et al., 1991; San Gil et al., 2017). Therefore, we were interested whether the heat shock response is also attenuated in our mature neuronal cultures and assessed protein levels by Western blot analysis for HSP70 and HSP27 were performed on SKNSH cells, lt-NES cells, immature and mature neuronal cultures. Under normal conditions, only the neuroblastoma line expresses high levels of HSP70. In the other populations significant lower levels of HSP70 are detectable. Following treatment with MG-132 the expression of HSP70 is strongly increased in all cell populations, except in mature neuronal cultures. Under normal and stress conditions HSP27 protein levels are lower than that of HSP70 in lt-NES cells, immature and mature neuronal cultures. After stress induction an increase of HSP27 is detectable but it is much weaker, than that of HSP70. Although MG-132 has been shown to be able to induce a heat shock response in motor neurons via the accumulation of HSF2 (Batulan et al., 2003), a strong induction in the mature neuronal cultures could not be detected. It might be, that the proteasomal inhibition was not sufficient to result in an accumulation of HSF2 in our cultures, but there is also evidence the induction of the heat shock response varies between different stimuli and neuronal populations (Marcuccilli et al., 1996; Batulan et al., 2003). However, the Western blot analysis also revealed, that HSP70 and HSP27 are constitutively expressed in all cultures – including mature neuronal cultures. The constitutive expression of HSP70 and HSP27 is also observed in motor neurons (Chen & Brown, 2007; Plumier et al., 1997). Those neurons also fail to induce HSP70 after stress induction as our mature neuronal

cultures (Batulan et al., 2003). It seems as if motor neurons and GABAergic neurons have a comparable behaviour concerning the heat shock response. Together, the results of the Western blot analysis show a reduced heat shock response in mature neuronal cultures. This is in line with the reduced levels of SIRT1 in mature neuronal cultures, which were identified via gene expression analysis. A study of Liu and co-workers pointed out, that the SIRT1 expression is reduced during neuronal differentiation and that this reduction concurs to the attenuated heat shock response in neurons (Liu et al., 2014). It was demonstrated, that SIRT1 deacetylates HSF1 at a residue critical for DNA-binding. The deacetylation results in a prolonged binding of HSF1 to the promoter. The downregulation of SIRT1 attenuates the heat shock response and releases HSF1 from the promoter (Westerheide et al., 2009). It is tempting to speculate, that the observed reduced levels of SIRT1 are also associated with a decreased heat shock response. Apart from the decreased expression of SIRT1, gene expression analysis identified also a small HSP (sHSP), Cryab, which is increased in mature neuronal cultures, compared to immature cultures. Stress induction with MG-132 results in a further elevation of expression of Cryab in both populations. Since the levels of the other HSPs in mature neurons are low even after stress induction, one might speculate, that Cryab could compensate for the other proteins. Cryab might compensate, as it is a general chaperone and stabilises early unfolded proteins to facilitate proper folding and binds aggregation prone intermediates and keeps them in large soluble aggregates (Bakthisaran, Tangirala & Rao, 2015; Rajaraman et al., 2001). In literature the expression of Cryab is mostly assessed in astrocytes, but it has also been detected for example in motor neurons (Batulan et al., 2003) and cortical neurons (Li et al., 2012). It is very unlikely, that the increased expression of Cryab is only related to the higher number of astrocytes in mature neuronal cultures, since astrocytes have a common heat shock response. HSP70 is expressed in astrocytes after induction (Marcuccilli et al., 1996). In addition, Taylor and co-workers showed, that astrocytes increase the expression of HSP70 and its release (Taylor et al., 2007). This cell population also expresses other HSPs, like HSP27 and HSP90 (Chopra, Chalifour & Schipper, 1995). If the increase in Cryab would only be related to increased amounts of astrocytes in these cultures, one would also expect a strong increase of the HSPs after stress induction, especially of HSP70, which is not detectable. The contribution of the astrocytic fraction to the increase of Cryab cannot be excluded, but due to the low heat shock response and a highly enriched content of neurons, the major effect should be caused by the neurons in the cultures. In follow-up experiments, the expression of Cryab in mature neurons would have to be validated by single cell PCR or immunocytochemistry stainings.

Whereby immunocytochemistry stainings were performed utilising several antibodies, including phospho-antibodies, without receiving specific signals. In addition to this, the study of Ke and co-workers indicates, that Cryab is associated with the proliferation of astrocytes and the protection from apoptosis in neurons (Ke et al., 2013).

Although the common heat shock response is reduced in our mature neuronal cultures, a higher susceptibility towards apoptotic stimuli was not observed in our mature cultures. To the contrary, they become more resistant to stress induction with on-going maturation, as supported by our observations from the cell viability assays. Furthermore, especially cell populations showing a strong heat shock response are highly affected by stress induction. Thus, it is likely, that the attenuated common heat shock response only has an effect, when also other protective mechanisms decline with aging and under pathological conditions, and that a strong heat shock response is used to compensate for other missing protective mechanism, like an activated survival pathway. As seen for tumour cell lines alone the inhibition of HSP70 results in cell death (Nylandsted et al., 2000). Thus a reduced heat shock response might not be the only reason for the altered stress tolerance observed by others (Oza et al., 2008). It might also be that the amount of heat shock proteins expressed by mature neurons under normal conditions is already sufficient to overcome the stress induction and that a further massive upregulation of HSP70 is not necessary, perhaps also because of the expression of Cryab.

6.5.2 Cryab and its role in stress resistance in mature neuronal cultures

Gene expression analysis revealed an upregulation of Cryab in mature neuronal cultures compared to immature cultures. The expression of Cryab was increased in both populations after treatment with MG-132. As Cryab is an sHSP, it is tempting to speculate, that it might compensate for the observed reduced heat shock response in mature neurons. We were, however, also interested in a possible impact of Cryab on the stress resistance of neuronal cultures. Thus, a CRISPR/Cas9 knockout line was generated and three clones used in subsequent experiments, including cell viability assays and Western blot analysis for AKT/pAKT. In cell viability assays on immature neuronal Cryab knockout cultures the wild type immature cultures and Cryab knockout cultures responded similar to stress induction, nevertheless with some differences. On default, Cryab might compensate for reduced autophagy and proteasomal degradation via its chaperone activity or via keeping aggregation prone proteins in solution (Rajaraman et al., 2001). The observation that the cell viability of immature neuronal cultures of clone #38 and #69 after exposure to MG-132 and Baf/3-MA

is more reduced when compared to wild type immature neuronal cultures, might be due to an expression of Cryab and its chaperone activity in immature wild type cultures. The reason why the immature Cryab knockout cultures are not affected by protein kinase stress remains elusive. As the expression level of Cryab was relatively low in immature cultures, no significant alterations after the knockout of Cryab were expected.

Cell viability assays performed on mature Cryab knockout cultures revealed, that they are vulnerable to redox stress, so that the experiments for the mature knockout cultures were performed in medium containing B27 supplement. The experiments showed, that the cell viability of mature knockout cultures is significantly reduced after stress induction by Baf/3-MA, MG-132, Rotenone and Staurosporine (clone #38 was not impaired by protein kinase stress) compared to the wild type mature cultures and also in part compared to the immature knockout cultures. It makes sense, that the cell viability of mature Cryab knockout cultures is significantly reduced after the exposure to stressors, which inhibit systems responsible for protein degradation, since Cryab under normal conditions can facilitate protein folding or can bind aggregation prone intermediates and maintain them as soluble aggregates (Rajaraman et al., 2001). This process might protect mature neurons from cellular damage caused by autophagy or proteasome inhibition. In Cryab knockout lines this is not possible and unfolded proteins might accumulate easier in the cell. The presence of Cryab and one functional system for protein degradation, autophagy or the proteasome seems to be sufficient to compensate for the one inhibited, but in the absence of Cryab, one of these systems alone seems to be overloaded. The reason why autophagy inhibition in mature neuronal cultures of clone #45 leads to a stronger reduction in cell viability than in their immature counterparts might be caused by the ability of immature neurons to induce the expression of HSP70 under stress conditions (see Fig. 5.12). It is quite likely, that HSP70 reduces the amount of misfolded proteins and thereby improves the conditions of the immature neurons under autophagy stress. Furthermore, the reduced cell viability of the mature knockout cultures under redox stress might be explained by the absence of Cryab, as it was shown, that the expression of Cryab elevates the glutathione level, probably not via its induction, but via its long-term storage (Mehlen et al., 1996). Additionally, the Cryab promoter contains two putative antioxidant-responsive element motives and an AP-1 like binding site. Under redox imbalance, an increase of Cryab and the two redox sensitive transcription factors Nrf2 and c-Jun (activated by JNK) is observed. In addition, an increased binding activity of the transcription factors in the promoter region of Cryab is identified (Fittipaldi et al., 2015), further indicating, that Cryab is involved in redox-

protection. Thus, it is tempting to speculate, that the glutathione levels in the knockout clones are reduced and they therefore have a decreased capacity to reduce ROS. The amount of viable cells in mature knockout cultures of clone #45 and #38 compared to the immature cultures, were also lower after the application of Rotenone. This might be caused by the attenuated expression of HSP70 in mature neuronal cultures, since HSP70 has been shown to be able to modulate the activity of glutathione-related enzymes and other antioxidant enzymes like superoxide dismutase (Gu, Hao & Wang, 2012; Guo et al., 2007). One might further speculate, that HSP70, which is almost absent in mature neurons, increases the activity of enzymes involved in redox protection in immature neurons. Apart from this, the mature knockout cultures display a higher vulnerability towards protein kinase stress and the expression of Cryab has been shown to be protective against stress induction by Staurosporine (Mehlen, Schulze-Osthoff & Arrigo, 1996; Terauchi et al., 2003). The reduced viability of the mature Cryab knockout cultures after the Staurosporine treatment might also in part be caused by the attenuated heat shock response of mature neurons, because HSP70 is able to protect cells against Staurosporine toxicity. In order to prevent apoptosis, it acts up- and downstream of caspase3 activation (Jäättelä et al., 1998; Terauchi et al., 2003). The absence of an impairment in mature neuronal knockout cultures, after the induction of ER stress indicates that Cryab is not involved directly in chaperoning secretory proteins in the ER. Although it is thought that it returns misfolded, mono-ubiquitynilated VEGF form the cytoplasm to the ER (Kase et al., 2010; Kerr & Byzova, 2010). The idea, that the protection against ER-stress is mediated by other chaperones, or by other pathways, like the unfolded protein response or the endoplasmic-reticulum-associated protein degradation, seems attractive. Summarising, the results reveal that stressors, in whose defence Cryab is directly involved, affect the mature knockout cultures. As chaperone it supports autophagy and the proteasomal system, by keeping the amount of unfolded proteins low and its ability, to store glutathione, protects against redox stress.

Apart from these specific protective properties, Cryab has also more general anti-apoptotic capacities, like preventing caspase3 maturation via binding to its intermediate p24, binding to procaspase3 to inhibit its activation, binding Bax and Bcl-XS and thereby preventing their translocation to the mitochondria, resulting in reduced cytochrome c release and decreased activation of caspase3 and cleavage of PARP (Kamradt, Chen & Cryns, 2001; Mao et al., 2001; Mao et al., 2004), which might protect the cells additionally from undergoing apoptosis.

Since the expression of Cryab is often investigated and described in astrocytes, one might argue, that the detected reduction of cell viability in mature neuronal Cryab knockout cultures might be based on the absence of Cryab in astrocytes or reduced number of astrocytes in the cultures. Since, the proteasomal degradation and autophagy are systems regulated by the respective cells themselves, it is not obvious if astrocytes have an impact on the regulation of these systems in neurons e.g via providing trophic factors or not. The vulnerability of mature neuronal knockout cultures towards redox stress might in part be based on the reduced release of glutathione by astrocytes. Astrocytes can release glutathione into the culture medium, and transient co-cultures of astrocytes and neurons have been shown to be able to increase the glutathione level in neurons compared to neurons cultured without astrocytes. It is thought, that γ-glutamyl transpeptidase generates the dipeptide CysGly from glutathione released by astrocytes, which is then processed by neurons as glutathione precursor (Dringen, Pfeiffer & Hamprecht, 1999). Nevertheless, neurons cultivated without astrocytes are able to generate glutathione (Hirrlinger, Schulz & Dringen, 2002; Dringen, Pfeiffer & Hamprecht, 1999).

Since in mature neuronal cultures the AKT-pathway is more active compared to immature cultures (compare Figure 5.11) we were interested in whether the knockout of Cryab has an impact on the activity of the pathway. Western blot analysis revealed similar pAKT levels in mature knockout cultures when compared to the immature knockout cultures. In both populations, the levels of pAKT are around 100-120 % and lower than that observed in mature neuronal wild type cultures. The reduced activity of the AKT-pathway in mature neuronal knockout cultures compared to the mature wild type cultures might influence their resistance to stress induction, as the AKT-pathway regulates the expression of many protective proteins (see chapter 5.5). Whether downstream targets of the AKT-pathway are decreased in mature neuronal knockout cultures, needs to be further investigated. The activity of the AKT-pathway might, in part, be regulated by VEGFB, which was increased in wild type mature neuronal cultures (Fig. 5.10) and the interaction between VEGFB and Cryab. It is thought, that neurons express VEGFB to protect themselves in an autocrine manner (Poesen et al., 2008). In addition, Cryab can interact with VEGF (Ghosh, Shenoy & Clark, 2007), but this is not possible in the knockout cultures. The binding of Cryab to VEGF might serve as protective backup under stress conditions, maybe comparable to the storage of glutathione. Another study showed, that VEGFA is decreased in Cryab$^{-/-}$ mice compared to the wild type mice. It is thought, that under normal conditions Cryab facilitated the folding of VEGFA in the ER and its secretion, via binding misfolded mono-

ubiquitinylated VEGFA and returning it to the ER. In the knockout misfolded VEGFA might be transported to the cytoplasm and be degraded, resulting in the decrease of VEGFA observed in the knockout mice (Kase et al., 2010; Kerr & Byzova, 2010). In addition to this, the knockdown of Cryab in cancer cells has been shown to reduce the secretion of VEGF (van de Schootbrugge et al., 2013). Apart from this, the overexpression of VEGF and exogenous VEGF have been shown to reduce the activity of caspase3 after redox stress, to increase the phosphorylation of VEGFR-2, (which can activate e.g. the AKT-pathway), to activate NF-κB and to upregulate Cryab, which is involved in the protection against ROS (Mercatelli et al., 2010). As Cryab is upregulated by VEGF and Cryab is responsible for the folding of VEGF, a positive feedback loop could be assumed. This would also make sense if Cryab stores VEGFB, because it then would induce Cryab for its own storage. Since VEGFB and VEGF/VEGFA belong to the same growth factor family, one might conclude, that the effects observed for VEGF/VEGFA are transferable to VEGFB.

Additionally, different studies suggest that the expression of Cryab is positively correlated to the activation of the AKT-pathway and the activation of ERK1/2 (Xu et al., 2013; Shi et al., 2016).

7 Abbreviations

Abbreviation	Full name
ALS	Amyotrophic lateral sclerosis
AP-1	Activator protein 1
Apaf-1	apoptotic protease activating factor 1
ARE	Antioxidant response element
ASK1	Apoptosis signal regulation kinase1
ATP	Adenosine triphosphate
Bad	Bcl-2 associated agonist of cell death
BCA	Bicinchoninic acid
Bid	BH-3 interacting domain death agonist
Bmf	Bcl-2 modifying factor
Bp	Base pair
BSA	Bovine serum albumin
cDNA	Complementary DNA
CHIR99021	CHIR
CREB	Cyclic AMP response element-binding protein
Cryab	αB-crystallin
DAPI	4,6-Diamidino-2-phenylindole, dihydrochloride
DMSO	Dimethyl sulfoxide
DNA	Deoxyribonucleic acid
ECM	Exctra cellular matrix
EDTA	Ethylenediaminetetraacetic acid
EGF	Epidermal growth factor
ER	Endoplasmic reticulum
Erk	Extracellular signal-regulated kinases
ES cell	Embryonic stem cell
FCS	Fetal calf serum
FGF2	Human fibroblast growth factor
GCL	Glutamate-cysteine ligase
GCLM	GCL modulatory subunit
GPCR	G protein coupled receptors
gRNA	Guide RNA

GSH	Glutathione
GSK-3	Glycogen synthase kinase 3
HRP	Horseradish peroxidase
HSE	Heat shock element
HSF1	Heat shock factor 1
HSP	Heat shock protein
IAPs	Inhibitor of apoptosis proteins
IGF-1	Insulin-like growth factor 1
IKK	IκB kinase
iPS cell	Induced pluripotent stem cell
Keap1	Kelch-like ECH-associated protein 1
LAMP2A	Lysosomal-associated membrane protein 2
LN	Laminin
lt hESNSCs	Long-term self-renewing rosette-type human ES cell-derived neural stem cells
LTD	Long term depression
lt-NES cell	long-term self-renewing neuroepithelial-like stem cell
LTP	Long-term potentiation
Mdm2	Mouse double minute 2 homolog
MEF	Mouse embryonic feeder
mGluR	Metabotropic glutamate receptors
mRNA	Messenger RNA
mTORC2	Mammalian target of rapamycin complex 2
NF-κB	Nuclear factor kappa-light-chain-enhancer of activated B cells
NGF	Nerve growth factor
NO	Nitric oxide
NP-1	Neuropilin 1
Nrf2	Nuclear factor (erythroid-derived 2)-like 2
$p75^{NTR}$	p75 neurotrophin receptor
pAKT	Phosphorylated AKT
PARP	poly (ADP-ribose) polymerase

PBS	Phosphate buffered saline
PCR	Polymerase chain reaction
PD	Parkinson's disease
PDK1	3-phosphoinositide-dependent protein kinase 1
PFA	Paraformaldehyde
PH domain	Pleckstin homology domain
PI3K	Phosphatidylinositol 3-kinase
PIP_2	Phosphatidylinositol(3,4)-bisphosphate
PIP_3	Phosphatidylinositol(3,4,5)-trisphosphate
PKCζ	Protein kinase Cζ
PLCγ1	Phospholipase C gamma 1
PO	Poly-l-ornithine
Prx	Peroxiredoxin
PtdIns	Phosphatidylinositols
PTEN	Phosphatase and tensin homolog
PVDF	Polyvinylidene fluoride
qPCR	Quantitative PCR
RNA	Ribonucleic acid
ROCK inhibitor	Rho-Kinase inhibitor
ROS	Reactive oxygen species
RT	Room temperature
RTK	Receptor tyrosine kinase
SCG2	Secretogranin II
SDS	Sodium dodecyl sulphate
SEM	Standard error of the mean
SH2	Src homology 2
sHSP	Small HSP
SM	Small molecule
SM-NP cell	small molecule neural precursor cell
SRXN1	Sulfiredoxin
TC	Tissue culture
TEMED	Tetramethylethylenediamine
TNF	Tumour necrosis factor

TrkA	Tropomyosin receptor kinase A
TSC2	Tuberous sclerosis complex 2
VEGF	Vascular endothelial growth factor
VEGFB	Vascular endothelial growth factor B
VEGFR-1	Vascular endothelial growth factor receptor-1
Wt	Wild type

8 Abstract

Neurons represent a highly specialised cell population of the central and peripheral nervous system, which is responsible for spreading information throughout the body. They are born during embryonic development and persist throughout the entire life span of an individual. Since during the development of the nervous system an excess of neurons is produced, some neurons undergo apoptosis to guarantee the correct number of neurons required for the formation of neuronal networks. In immature neurons cell death pathways are freely active, while in mature neurons apoptosis is highly controlled. They have developed elaborated strategies to protect themselves against stress and apoptosis. This study set out to decipher, whether mature neurons are more resistant toward stress than their immature counterparts and to elucidate which pathways and proteins promote the stress resistance. Experiments reveal that during the time course of maturation, iPS cell-derived neurons become increasingly resistant to several types of cellular stressors. This goes along with a failure to activate caspase3 and a downregulation of caspase9. Comparative gene expression analysis was performed to develop deeper insights into the different stress resistance between immature and mature neurons. In mature neurons upregulated protective genes, converging into the AKT-pathway, were identified. The elevated activity of the AKT-pathway in mature neurons was supported by Western blot analysis. Additionally, the small heat shock protein Cryab upregulated in mature neurons was of interest. Western blot analysis confirmed its expression and upregulation upon stress. Cryab was of special interest because the common heat shock response is attenuated in mature neurons. In line with this, a downregulation of Hsp70 and Hsp27 was shown. To investigate the contribution of Cryab to the stress resistance of mature neurons, Cryab knockout neural stem cells were generated using CRISPR/Cas9-mediated gene editing. The disruption of Cryab increased the susceptibility of mature neurons especially to redox- and autophagy stress. Together this points out that mature neurons are equipped with several strategies: the downregulation of pro-apoptotic proteins, the activation of a pro-survival pathway and the upregulation of protective proteins, to protect against stress.

9 Zusammenfassung

Neurone repräsentieren eine hoch spezialisierte Zellpopulation des peripheren und zentralen Nervensystems, die für die Weiterleitung von Informationen im Körper verantwortlich ist. Sie entstehen während der embryonalen Entwicklung und bestehen über die gesamte Lebenslänge eines Individuums. Da im Zuge der Entwicklung überzählige Neurone produziert werden, wird ihre Anzahl durch Apoptose verringert, um so die Anzahl an Neuronen zu generieren, die für die Formation von neuronalen Netzwerken nötig ist. In reifen Neuronen ist die Apoptose im Gegensatz zu unreifen Neuronen stark reguliert. Reife Neurone haben ausgeklügelte Strategien entwickelt, um sich selbst vor Stress und Apoptose zu schützen. Diese Studie hat sich vorgenommen, aufzuklären, ob reife Neurone stressresistenter sind als ihre unreifen Gegenspieler und welche Signalwege und Proteine diese Stressresistenz unterstützen könnten. Die Experimente zeigen, dass von iPS Zellen abgeleitete Neurone mit fortschreitender Reifung zunehmend unempfindlicher gegenüber einer Reihe von Stressoren werden. Diese Beobachtung geht einher mit der Herabregulierung von Caspase9 und der Unfähigkeit, Caspase3 zu aktivieren. Eine komparative Genexpressionsanalyse wurde durchgeführt, um weitere Einblicke in die unterschiedliche Stressresistenz von reifen und unreifen Neuronen zu erhalten. In reifen Neuronen wurden hochregulierte protektive Gene entdeckt, die in dem AKT Signalweg zusammenlaufen. Die erhöhte Aktivität des AKT Signalweges wurde durch Western-Blot-Analysen bestätigt. Zudem war das kleine Hitzeschockprotein Cryab, welches in reifen Neuronen hochreguliert ist, von Interesse. Mittels Western-Blot-Analyse wurde die Expression bestätigt, ebenso wie die weitere Hochregulierung durch Stress. Cryab war von besonderem Interesse, da die übliche Hitzeschockreaktion bei reifen Neuronen reduziert ist. Passend hierzu konnte bei ihnen eine Herabregulierung von HSP27 und HSP70 gezeigt werden. Um den Beitrag von Cryab zur Stressresistenz von reifen Neuronen zu untersuchen, wurden mittels CRISPR/Cas9 vermittelter Geneditierung neuronal Stammzellen mit einem Cryab knockout generiert. Der Knockout von Cryab führt bei reifen Neuronen zu einer höheren Anfälligkeit gegenüber Redox- und Autophagiestress. Zusammengefasst zeigen die Ergebnisse, dass reife Neurone mit einer Reihe von Strategien ausgestattet sind, um sich vor Stress zu schützen: der Herabregulierung von proapoptotischen Proteinen, der Aktivierung von Überlebenssignalwegen und der Hochregulierung von protektiven Proteinen.

10 References

Alessi, DR, Andjelkovic M, Caudwell B, Cron P, Morrice N, Cohen P, Hemmings, BA (1996) Mechanism of activation of protein kinase B by insulin and IGF-1. *EMBO J.* **15(23),** 6541–6551.

Arrigoni O, De Tullio MC. (2002). Ascorbic acid: much more than just an antioxidant. *Biochim Biophys Acta.* **1569 (1-3),** 1-9.

Bakthisaran R, Tangirala R, Rao ChM. (2015) Small heat shock proteins: Role in cellular functions and pathology. *Biochim Biophys Acta.* **1854(4),** 291-319.

Baler R, Dahl G, Voellmy R. (1993) Activation of human heat shock genes is accompanied by oligomerization, modification, and rapid translocation of heat shock transcription factor HSF1. *Mol Cell Biol.* **13(4),** 2486-96.

Barkett M, Gilmore TD. (1999) Control of apoptosis by Rel/NF-kappaB transcription factors. *Oncogene.* **18(49),** 6910-24.

Batulan Z, Shinder GA, Minotti S, He BP, Doroudchi MM, Nalbantoglu J, Strong MJ, Durham HD. (2003) High threshold for induction of the stress response in motor neurons is associated with failure to activate HSF1. *J Neurosci.* **23(13),** 5789-98.

Beere HM, Wolf BB, Cain K, Mosser DD, Mahboubi A, Kuwana T, Tailor P, Morimoto RI, Cohen GM, Green DR. (2000) Heat-shock protein 70 inhibits apoptosis by preventing recruitment of procaspase-9 to the Apaf-1 apoptosome. *Nat Cell Biol.* **2(8),** 469-75.

Ben-Shushan E, Feldman E, Reubinoff BE. (2015) Notch signaling regulates motor neuron differentiation of human embryonic stem cells. *Stem Cells.* **33(2),** 403-15.

Benn SC, Woolf CJ. (2004) Adult neuron survival strategies--slamming on the brakes. *Nat Rev Neurosci.* **(9),** 686-700.

Bethany A. Kerr and Tatiana V. Byzova (2010) αB-crystallin: a novel VEGF chaperone. Comment on Kase et al, page 3398. *Blood.* **115(16),** 3181-3183.

Biteau B, Labarre J, Toledano MB. (2003) ATP-dependent reduction of cysteine-sulphinic acid by S. cerevisiae sulphiredoxin. *Nature.* **425(6961),** 980-4.

Brunet A, Bonni A, Zigmond MJ, Lin MZ, Juo P, Hu LS, Anderson MJ, Arden KC, Blenis J, Greenberg ME. (1999) Akt promotes cell survival by phosphorylating and inhibiting a Forkhead transcription factor. *Cell.* **96(6),** 857-68.

Brunet A, Datta SR, Greenberg ME. (2001) Transcription-dependent and -independent control of neuronal survival by the PI3K-Akt signaling pathway. *Curr Opin Neurobiol.* **11(3),** 297-305.

Cardone MH, Roy N, Stennicke HR, Salvesen GS, Franke TF, Stanbridge E, Frisch S, Reed JC. (1998) Regulation of cell death protease caspase-9 by phosphorylation. *Science.* **282(5392),** 1318-21.

Chaitanya GV, Alexander JS, Babu PP. (2010) PARP-1 cleavage fragments: signatures of cell-death proteases in neurodegeneration. *Cell Communication and Signaling* **8(31).**

Chang TS, Jeong W, Woo HA, Lee SM, Park S, Rhee SG. (2004) Characterization of mammalian sulfiredoxin and its reactivation of hyperoxidized peroxiredoxin through reduction of cysteine sulfinic acid in the active site to cysteine. *J Biol Chem.* **279(49),** 50994-1001.

Charette SJ, Lavoie JN, Lambert H, Landry J. (2000) Inhibition of Daxx-mediated apoptosis by heat shock protein 27. *Mol Cell Biol.* **20(20),** 7602-12.

Chen S, Brown IR. (2007) Neuronal expression of constitutive heat shock proteins: implications for neurodegenerative diseases. *Cell Stress Chaperones.* **12(1),** 51–58.

Chen EY, Tan CM, Kou Y, Duan Q, Wang Z, Meirelles GV, Clark NR, Ma'ayan A. (2013) Enrichr: interactive and collaborative HTML5 gene list enrichment analysis tool. *BMC Bioinformatics.* **128(14)**.

Chopra VS, Chalifour LE, Schipper HM. (1995) Differential effects of cysteamine on heat shock protein induction and cytoplasmic granulation in astrocytes and glioma cells. *Brain Res Mol Brain Res.* **31(1-2),** 173-84.

Chua CE, Tang BL. (2014) Engagement of the small GTPase Rab31 protein and its effector, early endosome antigen 1, is important for trafficking of the ligand-bound epidermal growth factor receptor from the early to the late endosome. *J Biol Chem.* **289(18),**12375-89.

Clarke P, Kenneth KL (2009) Apoptosis in animal models of virus-induced diseases. *Nat Rev Micobiol.* **7(2),** 144-55.

Concannon CG, Orrenius S, Samali A. (2001) Hsp27 inhibits cytochrome c-mediated caspase activation by sequestering both pro-caspase-3 and cytochrome c. *Gene Expr.* **9(4-5),** 195-201.

Cross DA, Alessi DR, Cohen P, Andjelkovich M, Hemmings BA. (1995) Inhibition of glycogen synthase kinase-3 by insulin mediated by protein kinase B. *Nature.* **378(6559),** 785-9.

Dang TN, Arseneault M, Zarkovic N, Waeg G, Ramassamy C. (2010) Molecular regulations induced by acrolein in neuroblastoma SK-N-SH cells: relevance to Alzheimer's disease. J *Alzheimers Dis.* **21(4),** 1197-216.

Dávila D, Jiménez-Mateos EM, Mooney CM, Velasco G, Henshall DC, Prehn JH (2014) Hsp27 binding to the 3'UTR of bim mRNA prevents neuronal death during oxidative stress-induced injury: a novel cytoprotective mechanism. *Mol Biol Cell.* **25(21),** 3413-23.

De Giorgi F, Lartigue L, Bauer MK, Schubert A, Grimm S, Hanson GT, Remington SJ, Youle RJ, Ichas F. (2002) The permeability transition pore signals apoptosis by directing Bax translocation and multimerization. *FASEB J.* **16(6),** 607-9.

Degterev A, Boyce M, Yuan J. (2001) The channel of death. *J Cell Biol* **155(5),** 695-698.

Deponte M. The Incomplete Glutathione Puzzle: Just Guessing at Numbers and Figures? (2017) *Antioxid Redox Signal.* **ars.2017.7123.**

Dewil M, Lambrechts D, Sciot R, Shaw PJ, Ince PG, Robberecht W, Van den Bosch L. (2007) Vascular endothelial growth factor counteracts the loss of phospho-Akt preceding motor neurone degeneration in amyotrophic lateral sclerosis. *Neuropathol Appl Neurobiol.* **33(5),** 499-509.

Ding J, Ning B, Huang Y, Zhang D, Li J, Chen CY, Huang C. (2009) PI3K/Akt/JNK/c-Jun signaling pathway is a mediator for arsenite-induced cyclin D1 expression and cell growth in human bronchial epithelial cells. *Curr Cancer Drug Targets.* **9(4),** 500-9.

Dokladny K, Myers OB, Moseley PL. (2015) Heat shock response and autophagy--cooperation and control. *Autophagy.* **11(2),** 200-13.

Downward J. (1999) How BAD phosphorylation is good for survival. *Nat Cell Biol.* **1(2),** E33-5.

Dringen R, Pfeiffer B, Hamprecht B. (1999) Synthesis of the antioxidant glutathione in neurons: supply by astrocytes of CysGly as precursor for neuronal glutathione. *J Neurosci.* **19(2),** 562-9.

Du K, Montminy M. (1998) CREB is a regulatory target for the protein kinase Akt/PKB. J *Biol Chem.* **273(49),** 32377-9.

Dudek H, Datta SR, Franke TF, Birnbaum MJ, Yao R, Cooper GM, Segal RA, Kaplan DR, Greenberg ME. (1997) Regulation of neuronal survival by the serine-threonine protein kinase Akt. *Science.* **275(5300),** 661-5.

Eriksson PS, Perfilieva E, Björk-Eriksson T, Alborn AM, Nordborg C, Peterson DA, Gage FH. (1998) Neurogenesis in the adult human hippocampus. *Nat Med.* **4(11),** 1313-7.

Falk A, Koch P, Kesavan J, Takashima Y, Ladewig J, Alexander M, Wiskow O, Tailor J, Trotter M, Pollard S, Smith A, Brüstle O. (2012) Capture of Neuroepithelial-Like Stem Cells from Pluripotent Stem Cells Provides a Versatile System for In Vitro Production of Human Neurons. *PLoS One.* **7(1),** e29597.

Falk T, Yue X, Zhang S, McCourt AD, Yee BJ, Gonzalez RT, Sherman SJ. (2011) Vascular endothelial growth factor-B is neuroprotective in an in vivo rat model of Parkinson's disease. *Neurosci Lett.* **496(1),**43-7.

Fath T, Eidenmüller J, Brandt R. (2002) Tau-mediated cytotoxicity in a pseudohyperphosphorylation model of Alzheimer's disease. *J Neurosci.* **22(22),** 9733-41.

Fischer-Colbrie R, Laslop A, Kirchmair R. (1995) Secretogranin II: molecular properties, regulation of biosynthesis and processing to the neuropeptide secretoneurin. *Prog Neurobiol.* **46(1),** 49-70.

Fittipaldi S, Mercatelli N, Dimauro I, Jackson MJ, Paronetto MP, Caporossi D. (2015) Alpha B-crystallin induction in skeletal muscle cells under redox imbalance is mediated by a JNK-dependent regulatory mechanism. *Free Radic Biol Med.* **86,** 331-42.

Franke TF, Kaplan DR, Cantley LC, Toker A. (1997) Direct Regulation of the Akt Proto-Oncogene Product by Phosphatidylinositol-3,4-bisphosphate. *Science.* **275(5300),** 665-8.

Freyd T, Warszycki D, Mordalski S, Bojarski AJ, Sylte I, Gabrielsen M (2017) Ligand-guided homology modelling of the GABAB2 subunit of the GABAB receptor. *PLoS One.* **12(3),** e0173889.

Gardai SJ, Hildeman DA, Frankel SK, Whitlock BB, Frasch SC, Borregaard N, Marrack P, Bratton DL, Henson PM. (2004) Phosphorylation of Bax Ser184 by Akt regulates its activity and apoptosis in neutrophils. *J Biol Chem.* **279(20),** 21085-95.

Garrido C, Bruey JM, Fromentin A, Hammann A, Arrigo AP, Solary E. (1999) HSP27 inhibits cytochrome c-dependent activation of procaspase-9. *FASEB J.* **13(14),** 2061-70.

Ghosh JG, Shenoy AK Jr, Clark JI. (2007) Interactions between important regulatory proteins and human alphaB crystallin. *Biochemistry.* **46(21),** 6308-17.

Giordano G, White CC, McConnachie LA, Fernandez C, Kavanagh TJ, Costa LG. (2006) Neurotoxicity of domoic Acid in cerebellar granule neurons in a genetic model of glutathione deficiency. *Mol Pharmacol.* **70(6),** 2116-26.

Goplen D, Bougnaud S, Rajcevic U, Bøe SO, Skaftnesmo KO, Voges J, Enger PØ, Wang J, Tysnes BB, Laerum OD, Niclou S, Bjerkvig R. (2010) αB-crystallin is elevated in highly infiltrative apoptosis-resistant glioblastoma cells. *Am J Pathol.* **177(4),** 1618-28.

Gore A, Li Z, Fung HL, Young JE, Agarwal S, Antosiewicz-Bourget J, Canto I, Giorgetti A, Israel MA, Kiskinis E, Lee JH, Loh YH, Manos PD, Montserrat N, Panopoulos AD, Ruiz S, Wilbert ML, Yu J, Kirkness EF, Izpisua Belmonte JC, Rossi DJ, Thomson JA, Eggan K, Daley GQ, Goldstein LS, Zhang K. (2011) Somatic coding mutations in human induced pluripotent stem cells. *Nature.* **471(7336),** 63-7.

Gu XH, Hao Y, Wang XL. (2012) Overexpression of heat shock protein 70 and its relationship to intestine under acute heat stress in broilers: 2. Intestinal oxidative stress. *Poult Sci.* **91(4),** 790-9.

Guay J, Lambert H, Gingras-Breton G, Lavoie JN, Huot J, Landry J. (1997) Regulation of actin filament dynamics by p38 map kinase-mediated phosphorylation of heat shock protein 27. *J Cell Sci.* **110 (Pt 3),** 357-68.

Guettouche T, Boellmann F, Lane WS, Voellmy R. (2005) Analysis of phosphorylation of human heat shock factor 1 in cells experiencing a stress. *BMC Biochem.* **6:4.**

Guo S, Wharton W, Moseley P, Shi H. (2007) Heat shock protein 70 regulates cellular redox status by modulating glutathione-related enzyme activities. *Cell Stress Chaperones*. **12(3),** 245-54.

Ha JY, Kim JS, Kim SE, Son JH (2014) Simultaneous activation of mitophagy and autophagy by staurosporine protects against dopaminergic neuronal cell death. *Neurosci Lett.* **561,** 101-6.

Hale BG, Batty IH, Downes CP, Randall RE. (2008) Binding of influenza A virus NS1 protein to the inter-SH2 domain of p85 suggests a novel mechanism for phosphoinositide 3-kinase activation. *J Biol Chem.* **283(3),**1372-80.

Havasi A, Li Z, Wang Z, Martin JL, Botla V, Ruchalski K, Schwartz JH, Borkan SC. (2008) Hsp27 inhibits Bax activation and apoptosis via a phosphatidylinositol 3-kinase-dependent mechanism. *J Biol Chem.* **283(18),** 12305-13.

Heldin CH. (1995) Dimerization of cell surface receptors in signal transduction. *Cell.* **80(2),** 213-23.

Heo SR, Han AM, Kwon YK, Joung I (2009) p62 protects SH-SY5Y neuroblastoma cells against H2O2-induced injury through the PDK1/Akt pathway. *Neurosci.Lett.* **450(1),** 45-50.

Hirrlinger J, Schulz JB, Dringen R. (2002) Glutathione release from cultured brain cells: multidrug resistance protein 1 mediates the release of GSH from rat astroglial cells. *J Neurosci Res.* **69(3),** 318-26.

Hoeben A, Landuyt B, Highley MS, Wildiers H, Van Oosterom AT, De Bruijn EA. (2004) Vascular Endothelial Growth Factor and Angiogenesis. *Pharmacol Rev.* **56(4),** 549-80.

Hoflehner J, Eder U, Laslop A, Seidah NG, Fischer-Colbrie R, Winkler H. (1995) Processing of secretogranin II by prohormone convertases: importance of PC1 in generation of secretoneurin. *FEBS Lett.* **360(3),** 294-8.

Hou L, Klann E. (2004) Activation of the phosphoinositide 3-kinase-Akt-mammalian target of rapamycin signaling pathway is required for metabotropic glutamate receptor-dependent long-term depression. *J Neurosci.* **24(28),** 6352-61.

Huang CS, Anderson ME, Meister A. (1993) Amino acid sequence and function of the light subunit of rat kidney gamma-glutamylcysteine synthetase. *J Biol Chem.* **268(27),** 20578-83.

Hussein SM, Batada NN, Vuoristo S, Ching RW, Autio R, Närvä E, Ng S, Sourour M, Hämäläinen R, Olsson C, Lundin K, Mikkola M, Trokovic R, Peitz M, Brüstle O, Bazett-Jones DP, Alitalo K, Lahesmaa R, Nagy A, Otonkoski T. (2011) Copy number variation and selection during reprogramming to pluripotency. *Nature.* **471(7336),** 58-62.

Ito N1, Wernstedt C, Engström U, Claesson-Welsh L. (1998) Identification of vascular endothelial growth factor receptor-1 tyrosine phosphorylation sites and binding of SH2 domain-containing molecules. *J Biol Chem.* **273(36),** 23410-8.

Jäättelä M, Wissing D, Kokholm K, Kallunki T, Egeblad M. (1998) Hsp70 exerts its anti-apoptotic function downstream of caspase-3-like proteases. *EMBO J.* **17(21),** 6124-34.

Jäättelä M. (1999) Escaping cell death: survival proteins in cancer. *Exp Cell Res.* **248(1),** 30-43.

Jakob U, Gaestel M, Engel K, Buchner J. (1993) Small heat shock proteins are molecular chaperones. *J Biol Chem.* **268(3),** 1517-20.

Jeffrey PL, Capes-Davis A, Dunn JM, Tolhurst O, Seeto G, Hannan AJ, Lin SL (2000) CROC-4: a novel brain specific transcriptional activator of c-fos expressed from proliferation through to maturation of multiple neuronal cell types. *Mol Cell Neurosci.* **16(3),** 185-96.

Jope RS, Johnson GV. (2004). The glamour and gloom of glycogen synthase kinase-3. *Trends Biochem Sci* **29(2),** 95-102.

Joung I, Kim HJ, Kwon YK (2005) p62 modulates Akt activity via association with PKCzeta in neuronal survival and differentiation. *Biochem Biophys Res Commun.* **334(2),** 654-60.

Kamradt MC, Chen F, Cryns VL (2001) The small heat shock protein alpha B-crystallin negatively regulates cytochrome c- and caspase-8-dependent activation of caspase-3 by inhibiting its autoproteolytic maturation. *J Biol Chem.* **276(19*),*** 16059-63.

Kamradt MC, Chen F, Cryns VL. (2001) The small heat shock protein alpha B-crystallin negatively regulates cytochrome c- and caspase-8-dependent activation of caspase-3 by inhibiting its autoproteolytic maturation. *J Biol Chem.* **276(19),** 16059-63.

Karin M, Liu Zg, Zandi E. (1997) AP-1 function and regulation. *Curr Opin Cell Biol.* **9(2),** 240-6.

Kase S, He S, Sonoda S, Kitamura M, Spee C, Wawrousek E, Ryan SJ, Kannan R, Hinton DR. (2010) alphaB-crystallin regulation of angiogenesis by modulation of VEGF. *Blood.* **115(16),** 3398-406.

Ke K, Li L, Rui Y, Zheng H, Tan X, Xu W, Cao J, Xu J, Cui G, Xu G, Cao M. (2013) Increased expression of small heat shock protein αb-crystallin after intracerebral hemorrhage in adult rats. *J Mol Neurosci.* **51(1),** 159-69.

Kim AH, Khursigara G, Sun X, Franke TF, Chao MV. (2001) Akt phosphorylates and negatively regulates apoptosis signal-regulating kinase 1. *Mol Cell Biol.* **21(3),** 893-901.

Kim H, Jung Y, Shin BS, Kim H, Song H, Bae SH, Rhee SG, Jeong W. (2010) Redox regulation of lipopolysaccharide-mediated sulfiredoxin induction, which depends on both AP-1 and Nrf2. *J Biol Chem.* **285(45),** 34419-28.

Kim H, Lee GR, Kim J, Baek JY, Jo YJ, Hong SE, Kim SH, Lee J, Lee HI, Park SK, Kim HM, Lee HJ, Chang TS, Rhee SG, Lee JS, Jeong W. (2016) Sulfiredoxin inhibitor induces preferential death of cancer cells through reactive oxygen species-mediated mitochondrial damage. *Free Radic Biol Med.* **91,** 264-74.

Kirchmair R, Egger M, Walter DH, Eisterer W, Niederwanger A, Woell E, Nagl M, Pedrini M, Murayama T, Frauscher S, Hanley A, Silver M, Brodmann M, Sturm W, Fischer-Colbrie R, Losordo DW, Patsch JR, Schratzberger P. (2004) Secretoneurin, an angiogenic neuropeptide, induces postnatal vasculogenesis. *Circulation.* **110(9),**1121-7.

Kirchmair R, Gander R, Egger M, Hanley A, Silver M, Ritsch A, Murayama T, Kaneider N, Sturm W, Kearny M, Fischer-Colbrie R, Kircher B, Gaenzer H, Wiedermann CJ, Ropper AH, Losordo DW, Patsch JR, Schratzberger P (2004) The neuropeptide secretoneurin acts as a direct angiogenic cytokine in vitro and in vivo. *Circulation.* **109(6),** 777-83.

Klucken J, Shin Y, Masliah E, Hyman BT, McLean PJ. (2004) Hsp70 Reduces alpha-Synuclein Aggregation and Toxicity. *J Biol Chem.* **279(24),** 25497-502.

Koch P, Opitz T, Steinbeck JA, Ladewig J, Brüstle O (2009) A rosette-type, self-renewing human ES cell-derived neural stem cell with potential for in vitro instruction and synaptic integration. *Proc Natl Acad Sci USA* **106(9),** 3225-3230.

Koh JY, Wie MB, Gwag BJ, Sensi SL, Canzoniero LM, Demaro J, Csernansky C, Choi DW. (1995) Staurosporine-induced neuronal apoptosis. *Exp Neurol.* **135(2),** 153-9.

Kole AJ, Annis RP, Deshmukh M. (2013) Mature neurons: equipped for survival. *Cell Death Dis.* **4,** e689.

Komatsu M, Kurokawa H, Waguri S, Taguchi K, Kobayashi A, Ichimura Y, Sou YS, Ueno I, Sakamoto A, Tong KI, Kim M, Nishito Y, Iemura S, Natsume T, Ueno T, Kominami E, Motohashi H, Tanaka K, Yamamoto M (2010) The selective autophagy substrate p62 activates the stress responsive transcription factor Nrf2 through inactivation of Keap1. *Nat Cell Biol.* **12(3),** 213-23.

Kuida K, Haydar TF, Kuan CY, Gu Y, Taya C, Karasuyama H, Su MS, Rakic P, Flavell RA. (1998) Reduced apoptosis and cytochrome c-mediated caspase activation in mice lacking caspase 9. *Cell.* **94(3),** 325-37.

Lamark T, Kirkin V, Dikic I, Johansen T (2009) NBR1 and p62 as cargo receptors for selective autophagy of ubiquitinated targets. *Cell Cycle.* **8(13),** 1986-90.

Lauder A, Castellanos A, Weston K. (2001) c-Myb transcription is activated by protein kinase B (PKB) following interleukin 2 stimulation of Tcells and is required for PKB-mediated protection from apoptosis. *Mol Cell Biol.* **21(17),** 5797-805.

Lawlor MA, Alessi DR. (2001) PKB/Akt: a key mediator of cell proliferation, survival and insulin responses? *J Cell Sci*.**114(Pt 16),** 2903-10.

Lewis SE, Mannion RJ, White FA, Coggeshall RE, Beggs S, Costigan M, Martin JL, Dillmann WH, Woolf CJ. (1999) A role for HSP27 in sensory neuron survival. *J Neurosci.* **19(20),** 8945-53.

Li J, Chen H, Tang MS, Shi X, Amin S, Desai D, Costa M, Huang C. (2004) PI-3K and Akt are mediators of AP-1 induction by 5-MCDE in mouse epidermal Cl41 cells. *J Cell Biol.* **165(1),** 77-86.

Li L, Hu GK (2015) Pink1 protects cortical neurons from thapsigargin-induced oxidative stress and neuronal apoptosis. *Biosci Rep*. **35(1),** pii: e00174.

Li L, Hung AC and Porter AG (2008) Secretogranin II: a key AP-1-regulated protein that mediates neuronal differentiation and protection from nitric oxide-induced apoptosis of neuroblastoma cells. *Cell Death Differ.* **15(5),** 879-88.

Li T, Mo X, Jiang Z, He W, Lu W, Zhang H, Zhang J, Zeng L, Yang B, Xiao H, Hu Z. (2012) Study of αB-crystallin expression in Gerbil BCAO model of transient global cerebral ischemia. *Oxid Med Cell Longev*. 2012:945071.

Li Y, Zhang F, Nagai N, Tang Z, Zhang S, Scotney P, Lennartsson J, Zhu C, Qu Y, Fang C, Hua J, Matsuo O, Fong GH, Ding H, Cao Y, Becker KG, Nash A, Heldin CH, Li X. (2008) VEGF-B inhibits apoptosis via VEGFR-1-mediated suppression of the expression of BH3-only protein genes in mice and rats. *J Clin Invest.* **118(3),** 913-23.

Li Z, Dong X, Liu H, Chen X, Shi H, Fan Y, Hou D, Zhang X. (2013) Astaxanthin protects ARPE-19 cells from oxidative stress via upregulation of Nrf2-regulated phase II enzymes through activation of PI3K/Akt. *Mol Vis*. **19,** 1656-66.

Lin TK, Chen SD, Chuang YC, Lin HY, Huang CR, Chuang JH, Wang PW, Huang ST, Tiao MM, Chen JB, Liou CW. (2014). Resveratrol Partially Prevents Rotenone-Induced Neurotoxicity in Dopaminergic SH-SY5Y Cells through Induction of Heme Oxygenase-1 Dependent Autophagy. *International Journal of Molecular Sciences,* **15(1),** 1625–1646.

Liu DJ, Hammer D, Komlos D, Chen KY, Firestein BL, Liu AY. (2014) SIRT1 knockdown promotes neural differentiation and attenuates the heat shock response. *J Cell Physiol*. **229(9),** 1224-35.

Liu X, Fu B, Chen D, Hong Q, Cui J, Li J, Bai X, Chen X (2015) miR-184 and miR-150 promote renal glomerular mesangial cell aging by targeting Rab1a and Rab31. *Exp Cell Res.* **336(2),** 192-203.

Lloyd-Burton S, Roskams AJ (2012) SPARC-like 1 (SC1) is a diversely expressed and developmentally regulated matricellular protein that does not compensate for the absence of SPARC in the CNS. *J Comp Neurol.* **520(12),** 2575-90.

Lopes FM, Schröder R, da Frota ML Jr, Zanotto-Filho A, Müller CB, Pires AS, Meurer RT, Colpo GD, Gelain DP, Kapczinski F, Moreira JC, Fernandes Mda C, Klamt F. (2010) Comparison between proliferative and neuron-like SH-SY5Y cells as an in vitro model for Parkinson disease studies. *Brain Res.* 1337 (85-94).

Lu CY, Yang YC, Li CC, Liu KL, Lii CK, Chen HW. (2014) Andrographolide inhibits TNFα-induced ICAM-1 expression via suppression of NADPH oxidase activation and induction of HO-1 and GCLM expression through the PI3K/Akt/Nrf2 and PI3K/Akt/AP-1 pathways in human endothelial cells. *Biochem Pharmacol.* **91(1),** 40-50.

Lynch DK, Ellis CA, Edwards PA, Hiles ID. (1999) Integrin-linked kinase regulates phosphorylation of serine 473 of protein kinase B by an indirect mechanism. *Oncogene.* **18(56);** 8024-32.

Manning BD, Toker A. (2017) AKT/PKB Signaling: Navigating the Network. *Cell.* **169(3),** 381-405.

Mao YW, Liu JP, Xiang H, Li DW.(2004) Human alphaA- and alphaB-crystallins bind to Bax and Bcl-X(S) to sequester their translocation during staurosporine-induced apoptosis. *Cell Death Differ.* **11(5),** 512-26.

Mao YW, Xiang H, Wang J, Korsmeyer S, Reddan J, Li DW. (2001) Human bcl-2 gene attenuates the ability of rabbit lens epithelial cells against H2O2-induced apoptosis through down-regulation of the alpha B-crystallin gene. *J Biol Chem.* **276(46),** 43435-45.

Marcuccilli CJ, Mathur SK, Morimoto RI, Miller RJ. (1996) Regulatory differences in the stress response of hippocampal neurons and glial cells after heat shock. *J Neurosci.* **16(2),** 478-85.

Marr HS, Basalamah MA, Bouldin TW, Duncan AW, Edgell CJ (2000) Distribution of testican expression in human brain. *Cell Tissue Res.* **302(2),** 139-44.

Mayer MP, Bukau B. (2005) Hsp70 chaperones: Cellular functions and molecular mechanism. *Life Sciences.* **62(6),** 670-684.

Mayo LD, Donner DB. (2001) A phosphatidylinositol 3-kinase/Akt pathway promotes translocation of Mdm2 from the cytoplasm to the nucleus. *Proc Natl Acad Sci U S A.* **98(20),** 11598-603.

Mayshar Y, Ben-David U, Lavon N, Biancotti JC, Yakir B, Clark AT, Plath K, Lowry WE, Benvenisty N. (2010) Identification and classification of chromosomal aberrations in human induced pluripotent stem cells. *Cell Stem Cell*. **7(4),** 521-31.

Mehlen P, Kretz-Remy C, Préville X, Arrigo AP. (1996) Human hsp27, Drosophila hsp27 and human alphaB-crystallin expression-mediated increase in glutathione is essential for the protective activity of these proteins against TNFalpha-induced cell death. *EMBO J.* **15(11),** 2695-706.

Mehlen P, Schulze-Osthoff K, Arrigo AP. (1996) Small stress proteins as novel regulators of apoptosis. Heat shock protein 27 blocks Fas/APO-1- and staurosporine-induced cell death. J *Biol Chem.* **271(28),** 16510-4.

Mercatelli N, Dimauro I, Ciafré SA, Farace MG, Caporossi D. (2010Garrido. *Free Radic Biol Med.* **49(3),** 374-82.

Mertens J, Stüber K, Poppe D, Doerr J, Ladewig J, Brüstle O, Koch P. (2013) Embryonic stem cell-based modeling of tau pathology in human neurons. *Am J Pathol.* **182(5),** 1769-79.

Mertens J, Stüber K, Wunderlich P, Ladewig J, Kesavan JC, Vandenberghe R, Vandenbulcke M, van Damme P, Walter J, Brüstle O, Koch P. (2013) APP processing in human pluripotent stem cell-derived neurons is resistant to NSAID-based γ-secretase modulation. *Stem Cell Reports.* **1(6),** 491-8.

Mertens, Jérôme: Amyloid generation and axonal tau pathology in human pluripotent stem cell-derived neurons expressing Alzheimer's disease-associated mutant proteins, Diss., Rheinischen Friedrich-Wilhelms-Universität Bonn, 2012.

Miyashita T, Reed JC. (1995) Tumor suppressor p53 is a direct transcriptional activator of the human bax gene. *Cell.* **80(2),** 293-9.

Nishimura RN, Dwyer BE, Clegg K, Cole R, de Vellis J. (1991) Comparison of the heat shock response in cultured cortical neurons and astrocytes. *Brain Res Mol Brain Res.* **9(1-2),** 39-45.

Nylandsted J, Rohde M, Brand K, Bastholm L, Elling F, Jäättelä M. (2000) Selective depletion of heat shock protein 70 (Hsp70) activates a tumor-specific death program that is independent of caspases and bypasses Bcl-2. *Proc Natl Acad Sci U S A.* **97(14),** 7871-6.

Olofsson B, Pajusola K, von Euler G, Chilov D, Alitalo K, Eriksson U. (1996) Genomic organization of the mouse and human genes for vascular endothelial growth factor B (VEGF-B) and characterization of a second splice isoform. *J Biol Chem.* **271(32),** 19310-7.

Orr WC, Radyuk SN, Prabhudesai L, Toroser D, Benes JJ, Luchak JM, Mockett RJ, Rebrin I, Hubbard JG, Sohal RS. (2005) Overexpression of glutamate-cysteine ligase extends life span in Drosophila melanogaster. *J Biol Chem.* **280(45),** 37331-8.
Osaki M, Oshimura M, Ito H. (2004) PI3K-Akt pathway: its functions and alterations in human cancer. *Apoptosis.* **9(6),** 667-76.

Oslowski CM, Urano F. (2011) Measuring ER stress and the unfolded protein response using mammalian tissue culture system. *Methods in enzymology.* **490,** 71–92.

Oza J, Yang J, Chen KY, Liu AY. (2008) Changes in the regulation of heat shock gene expression in neuronal cell differentiation. *Cell Stress Chaperones.* **13(1),** 73-84.

Ozes ON, Mayo LD, Gustin JA, Pfeffer SR, Pfeffer LM, Donner DB. (1999) NF-kappaB activation by tumour necrosis factor requires the Akt serine-threonine kinase. *Nature.* **401(6748),** 82-5.

Pan Y, Zhang Y, Chen L, Lui Y, Feng Y,Yan J (2016) The Critical Role of Rab31 in Cell Proliferation and Apoptosis in Cancer Progression. *Mol Neurobiol.* **53(7),** 4431-7.

Park HH. (2012) Structural features of caspase-activating complexes. *Int J Mol Sci.* **(4),** 4807-18.

Plater ML, Goode D, Crabbe MJ. (1996) Effects of Site-directed Mutations on the Chaperone-like Activity of αB-Crystallin. J Biol Chem. **271(45**), 28558-66.

Plumier JC, Hopkins DA, Robertson HA, Currie RW. (1997) Constitutive expression of the 27-kDa heat shock protein (Hsp27) in sensory and motor neurons of the rat nervous system. J *Comp Neurol.* **384(3),** 409-28.

Poesen K, Lambrechts D, Van Damme P, Dhondt J, Bender F, Frank N, Bogaert E, Claes B, Heylen L, Verheyen A, Raes K, Tjwa M, Eriksson U, Shibuya M, Nuydens R, Van Den Bosch L, Meert T, D'Hooge R, Sendtner M, Robberecht W, Carmeliet P. (2008) Novel Role for Vascular Endothelial Growth Factor (VEGF) Receptor-1 and Its Ligand VEGF-B in Motor Neuron Degeneration. *J Neurosci.* **28(42),**10451-9.

Polster BM, Robertson CL, Bucci CJ, Suzuki M, Fiskum G. (2003) Postnatal brain development and neural cell differentiation modulate mitochondrial Bax and BH3 peptide-induced cytochrome c release. *Cell Death Differ.* **10(3),** 365-70.

Poppe, Daniel: Gene targeting in human pluripotent cell-derived neural stem cells for the study and treatment of neurological disorders, Diss., Rheinischen Friedrich-Wilhelms-Universität Bonn, 2015.

Poter AG and RU Jänicke (1999) Emerging roles of caspase-3 in apoptosis. *Cell Death Differ* **6,** 99-104.

Rajaraman K, Raman B, Ramakrishna T, Rao CM. (2001) Interaction of human recombinant alphaA- and alphaB-crystallins with early and late unfolding intermediates of citrate synthase on its thermal denaturation. *FEBS Lett.* **497(2-3),** 118-23.

Reddy NM, Potteti HR, Vegiraju S, Chen HJ, Tamatam CM, Reddy SP. (2015) PI3K-AKT Signaling via Nrf2 Protects against Hyperoxia-Induced Acute Lung Injury, but Promotes Inflammation Post-Injury Independent of Nrf2 in Mice. *PLoS One*. **10(6),** e0129676.

Reinhardt P, Glatza M, Hemmer K, Tsytsyura Y, Thiel CS, Höing S, Moritz S, Parga JA, Wagner L, Bruder JM, Wu G, Schmid B, Röpke A, Klingauf J, Schwamborn JC, Gasser T, Schöler HR, Sterneckert J. (2013) Derivation and Expansion Using Only Small Molecules of Human Neural Progenitors for Neurodegenerative Disease Modeling. *PLoS One.* **8(3),** e59252.

Rhee M, Lee SH, Kim JW, Ham DS, Park HS, Yang HK, Shin JY, Cho JH, Kim YB, Youn BS, Sul HS, Yoon KH. (2016) Preadipocyte factor 1 induces pancreatic ductal cell differentiation into insulin-producing cells. *Sci Rep*.**(6),** *23960.*

Richter K, Haslbeck M, Buchner J. (2010) The heat shock response: life on the verge of death. *Mol Cell.* **40(2),** 253-66.

Roszkowska M, Skupien A, Wójtowicz T, Konopka A, Gorlewicz A, Kisiel M, Bekisz M, Ruszczycki B, Dolezyczek H, Rejmak E, Knapska E, Mozrzymas JW, Wlodarczyk JA, Wilczynski GM, Dzwonek J (2016) CD44: a novel synaptic cell adhesion molecule regulating structural and functional plasticity of dendritic spines. *Mol Biol Cell*. **27(25),** 4055-4066.

Rusten TE, Stenmark H (2010) p62, an autophagy hero or culprit? *Nat Cell Biol.* **12(3),** 207-9.

San Gil R, Ooi L, Yerbury JJ, Ecroyd H. (2017) The heat shock response in neurons and astroglia and its role in neurodegenerative diseases. *Mol Neurodegener.* **12(1),** 65.

Seol DW, Billiar TR. (1999) A caspase-9 variant missing the catalytic site is an endogenous inhibitor of apoptosis. *J Biol Chem.* **274(4),** 2072-6.

Shi C, He Z, Hou N, Ni Y, Xiong L, Chen P. (2014) Alpha B-crystallin correlates with poor survival in colorectal cancer. *Int J Clin Exp Pathol.* **7(9),** 6056-63.

Shi H, Jing X, Wei X, Perez RG, Ren M, Zhang X, Lou H. (2015) S-allyl cysteine activates the Nrf2-dependent antioxidant response and protects neurons against ischemic injury in vitro and in vivo. *J Neurochem.* **133(2),** 298-308.

Shi QM, Luo J, Wu K, Yin M, Gu YR, Cheng XG. (2016) High level of αB-crystallin contributes to the progression of osteosarcoma.*Oncotarget.* **7(8),** 9007-16.

Shyu WC, Lin SZ, Chiang MF, Chen DC, Su CY, Wang HJ, Liu RS, Tsai CH, Li H (2008) Secretoneurin promotes neuroprotection and neuronal plasticity via the Jak2/Stat3 pathway in murine models of stroke. *J Clin Invest.* **118(1),** 133-48.

Singsai K, Akaravichien T, Kukongviriyapan V, Sattayasai J. (2015) Protective Effects of Streblus asper Leaf Extract on H2O2-Induced ROS in SK-N-SH Cells and MPTP-Induced Parkinson's Disease-Like Symptoms in C57BL/6 Mouse. *Evid Based Complement Alternat Med.* **2015,** 970354.

Song G, Ouyang G, Bao S. (2005) The activation of Akt/PKB signaling pathway and cell survival. *J Cell Mol Med.* **9(1),** 59-71.

Sui Y, Zheng X, Zhao D (2015) Rab31 promoted hepatocellular carcinoma (HCC) progression via inhibition of cell apoptosis induced by PI3K/AKT/Bcl-2/BAX pathway. *TumourBiol.* **36(11),** 8661-70.

Sun Y, Jin K, Childs JT, Xie L, Mao XO, Greenberg DA. (2004) Increased severity of cerebral ischemic injury in vascular endothelial growth factor-B-deficient mice. *J Cereb Blood Flow Metab*. **24(10),** 1146-52.

Sun Y, Jin K, Childs JT, Xie L, Mao XO, Greenberg DA. (2006) Vascular endothelial growth factor-B (VEGFB) stimulates neurogenesis: evidence from knockout mice and growth factor administration. *Dev Biol.* **289(2),** 329-35.

Takahashi K, Yamanaka S. (2006) Induction of pluripotent stem cells from mouse embryonic and adult fibroblast cultures by defined factors. *Cell.* **126(4),** 663-76.

Tang SJ, Reis G, Kang H, Gingras A-C, Sonenberg N, Schuman EM. (2002) A rapamycin-sensitive signaling pathway contributes to long-term synaptic plasticity in the hippocampus. *Proc Natl Acad Sci U S A*. **99(1),** 467-472.

Tarjányi O, Berta G, Harci A, Bacsa EB, Stark B, Pap M, Szeberényi J, Sétáló G Jr. (2013) The role of Src protein in the process formation of PC12 cells induced by the proteasome inhibitor MG-132. *Neurochem Int.* **63(5),** 413-22.

Taylor AR, Robinson MB, Gifondorwa DJ, Tytell M, Milligan CE. (2007) Regulation of heat shock protein 70 release in astrocytes: role of signaling kinases. *Dev Neurobiol.* **67(13),** 1815-29.

Terauchi R, Takahashi KA, Arai Y, Ikeda T, Ohashi S, Imanishi J, Mazda O, Kubo T. (2003) Hsp70 prevents nitric oxide-induced apoptosis in articular chondrocytes. *Arthritis Rheum.* **48(6),** 1562-8.

Toledano M, Huang ME (2017) The unfinished puzzle of glutathione physiological functions, an old molecule that still retains many enigmas. Antioxid Redox Signal. 10.1089/ars.2017.7230.

van de Schootbrugge C, Bussink J, Span PN, Sweep FC, Grénman R, Stegeman H, Pruijn GJ, Kaanders JH, Boelens WC. (2013) αB-crystallin stimulates VEGF secretion and tumor cell migration and correlates with enhanced distant metastasis in head and neck squamous cell carcinoma. *BMC Cancer.* **13,** 128.

Vanhaesebroeck B, Waterfield MD. (1999) Signaling by distinct classes of phosphoinositide 3-kinases. *Exp Cell Res.* **253(1),** 239-54.

Vogelbaum MA, Tong JX, Rich KM. (1998) Developmental regulation of apoptosis in dorsal root ganglion neurons. *J Neurosci.* **18(21),** 8928-35.

Wada T, Penninger JM. (2004) Mitogen-activated protein kinases in apoptosis regulation. *Oncogene.* **23(16),** 2838-49.

Wang CY, Guttridge DC, Mayo MW, Baldwin AS Jr. (1999) NF-kappaB induces expression of the Bcl-2 homologue A1/Bfl-1 to preferentially suppress chemotherapy-induced apoptosis. *Mol Cell Biol.* **19(9),** 5923-9.

Wang L, Chen Y, Sternberg P, Cai J. (2008) Essential roles of the PI3 kinase/Akt pathway in regulating Nrf2-dependent antioxidant functions in the RPE. *Invest Ophthalmol Vis Sci.* **49(4),** 1671-8.

Weggen S, Eriksen JL, Das P, Sagi SA, Wang R, Pietrzik CU, Findlay KA, Smith TE, Murphy MP, Bulter T, Kang DE, Marquez-Sterling N, Golde TE, Koo EH. (2001) A subset of NSAIDs lower amyloidogenic Abeta42 independently of cyclooxygenase activity. *Nature.* **414(6860),** 212-6.

Wei Q, Jiang H, Matthews CP, Colburn NH. (2008) Sulfiredoxin is an AP-1 target gene that is required for transformation and shows elevated expression in human skin malignancies. *Proc Natl Acad Sci U S A.* **105(50),** 19738-43.

Westerheide SD, Anckar J, Stevens SM Jr, Sistonen L, Morimoto RI. (2009) Stress-inducible regulation of heat shock factor 1 by the deacetylase SIRT1. *Science.* **323(5917),** 1063-6.

Wu CL, Yin JH, Hwang CS, Chen SD, Yang DY, Yang DI. (2012) c-Jun-dependent sulfiredoxin induction mediates BDNF protection against mitochondrial inhibition in rat cortical neurons. *Neurobiol Dis.* **46(2),** 450-62.

Wu J, Chen Y, Yu S, Li L, Zhao X, Li Q, Zhao J, Zhao Y. (2017) Neuroprotective effects of sulfiredoxin-1 during cerebral ischemia/reperfusion oxidative stress injury in rats. *Brain Res Bull.* **132,** 99-108.

Wu J, Izpisua Belmonte (2016) JC.Stem Cells: A Renaissance in Human Biology Research. *Cell.* **165(7),** 1572-1585.

Wu X, Walker J, Zhang J, Ding S, Schultz PG. (2004). Purmorphamine induces osteogenesis by activation oft he hedgehog signaling pathway. *Chem Biol.* **11(9),** 1229-38.

Xie L, Mao X, Jin K, Greenberg DA. (2013) Vascular endothelial growth factor-B expression in postischemic rat brain. *Vasc Cell.* **5:8**. doi: 10.1186/2045-824X-5-8. eCollection 2013.

Xu F1, Yu H, Liu J, Cheng L. (2013) αB crystallin regulates oxidative stress-induced apoptosis in cardiac H9c2 cells via the PI3/AKT pathway. *Mol Biol Rep*. **40(3),** 2517-26.

Yakovlev AG, Ota K, Wang G, Movsesyan V, Bao WL, Yoshihara K, Faden AI. (2001) Differential expression of apoptotic protease-activating factor-1 and caspase-3 genes and susceptibility to apoptosis during brain development and after traumatic brain injury. *J Neurosci.* **21(19),** 7439-46.

Yan Y, Gong K, Ma T, Zhang L, Zhao N, Zhang X, Tang P, Gong Y. (2012) Protective effect of edaravone against Alzheimer's disease-relevant insults in neuroblastoma N2a cells. *Neurosci Lett.* **531(2),** 160-5.

Yao CA, Ortiz-Vega S, Sun YY, Chien CT, Chuang JH, Lin Y. (2017) Association of mSin1 with mTORC2 Ras and Akt reveals a crucial domain on mSin1 involved in Akt phosphorylation. *Oncotarget.* **8(38),** 63392-63404.

Zhang J, He Z, Guo J, Li Z, Wang X, Yang C, Cui X. (2016) Sulfiredoxin-1 protects against simulated ischaemia/reperfusion injury in cardiomyocyte by inhibiting PI3K/AKT-regulated mitochondrial apoptotic pathways. *Biosci Rep.* **36(2).** pii: e00325.

Zhang JX, Wang R, Xi J, Shen L, Zhu AY, Qi Q, Wang QY, Zhang LJ, Wang FC, Lü HZ, Hu JG. (2017) Morroniside protects SK-N-SH human neuroblastoma cells against H2O2-induced damage. *Int J Mol Med.* doi: 10.3892/ijmm.2017.2882.

Zheng X, Krakowiak J, Patel N, Beyzavi A, Ezike J, Khalil AS2, Pincus D. (2016) Dynamic control of Hsf1 during heat shock by a chaperone switch and phosphorylation. *Elife.* **5.** pii: e18638.

Zhou BP, Liao Y, Xia W, Spohn B, Lee MH, Hung MC. (2001) Cytoplasmic localization of p21Cip1/WAF1 by Akt-induced phosphorylation in HER-2/neu-overexpressing cells. *Nat Cell Biol.* **3(3),** 245-52.

Zhou Y, Duan S, Zhou Y, Yu S, Wu J, Wu X, Zhao J, Zhao Y. (2015) Sulfiredoxin-1 attenuates oxidative stress via Nrf2/ARE pathway and 2-Cys Prdxs after oxygen-glucose deprivation in astrocytes. *J Mol Neurosci.* **55(4),** 941-50.

Zhu Z, Li R, Stricker R, Reiser G. (2015) Extracellular α-crystallin protects astrocytes from cell death through activation of MAPK, PI3K/Akt signalling pathway and blockade of ROS release from mitochondria. *Brain Res.* **1620,** 17-28.

Zou W, Chen C, Zhong Y, An J, Zhang X, Yu Y, Yu Z, Fu J. (2013) PI3K/Akt pathway mediates Nrf2/ARE activation in human L02 hepatocytes exposed to low-concentration HBCDs. *Environ Sci Technol.* **47(21),** 12434-40.

Zou X, Feng Z, Li Y, Wang Y, Wertz K, Weber P, Fu Y, Liu J. (2012) Stimulation of GSH synthesis to prevent oxidative stress-induced apoptosis by hydroxytyrosol in human retinal pigment epithelial cells: activation of Nrf2 and JNK-p62/SQSTM1 pathways. *J Nutr Biochem.* **23(8),** 994-1006.

11 Danksagung

Prof. Dr. Philipp Koch danke ich für die Überlassung meines Dissertationsthemas und die fachliche Beratung und Betreuung.

Ich möchte mich bei Prof. Dr. Oliver Brüstle für die Möglichkeit der Promotion an seinem Institut unter optimalen Forschungsbedingungen bedanken.

Bei Prof. Dr. Walter Witke, Prof. Dr. Pankratz und Prof. Dr. Pavel Kroupa möchte ich mich für die Bildung der Promotionskommission bedanken.

Ruven Wilkens gilt mein Dank für die Weiterverfolgung dieses spannenden Themas sowie für den anregenden Austausch.

Jonas Doerr möchte ich für die fachliche Diskussion und Beratung danken.

Mein Dank gilt auch meinen ehemaligen Arbeitskollegen, Jasmin Jatho-Gröger, Ruven Wilkens, Kevin Weynans und Bettina Bohl für die tolle Zusammenarbeit, fachlichen Diskussionen und Ihre Freundschaft, wodurch die Arbeit im Labor in positiver Erinnerung bleiben wird. Ebenfalls danke ich Ammar Jabali, Fabio Marsoner und Vira Iefremova sowie allen ehemaligen Mitgliedern der AG Koch für ein angenehmes und produktives Arbeitsklima.

Mein besonderer Dank gilt meinen Freunden und meiner Familie und hier im speziellen meinen Eltern, Gerhild Stechow-Menger und Jörg Stechow, meinen Großeltern und meiner Schwester Laura, die immer für mich da waren und ohne deren Unterstützung in jeglicher Hinsicht, ich diese Arbeit nicht mehr geschrieben hätte.

Meinem Freund Henning Heyn möchte ich für seine Geduld, seinen Zuspruch und vieles mehr danken. Mein Fels in der Brandung.